

**ENGINEERING OF PLASMID VECTORS FOR ENHANCING
AGROBACTERIUM-MEDIATED PLANT TRANSFORMATION**

TEO YUH LENG

MASTER OF SCIENCE

FACULTY OF SCIENCE

UNIVERSITI TUNKU ABDUL RAHMAN

FEBRUARY 2022

**ENGINEERING OF PLASMID VECTORS FOR ENHANCING
AGROBACTERIUM-MEDIATED PLANT TRANSFORMATION**

BY

TEO YUH LENG

A dissertation submitted to Department of Biological Science,

Faculty of Science,

Universiti Tunku Abdul Rahman,

In partial fulfilment of the requirements for the degree of

Master of Science

February 2022

ABSTRACT

ENGINEERING OF PLASMID VECTORS FOR ENHANCING AGROBACTERIUM-MEDIATED PLANT TRANSFORMATION

TEO YUH LENG

Agrobacterium-mediated transformation (AMT) is the most widely used approach for plant transformation due to its ease of application and low cost. However, only limited crop plants can be consistently transformed with high efficiency. The bottleneck of the AMT approach lies in the low-copy tumour-inducing (Ti) plasmid that limits the expression of virulence genes. Furthermore, helper plasmids that can enhance the AMT efficiency are not commercially available, thus constraining the advancement in plant transformation. This project aimed to enhance the overall plant transformation efficiency by constructing a broad host range (BHR) expression vector to express the key regulatory virulence genes of *Agrobacterium tumefaciens* and a miniaturized helper Ti plasmid to harbour the essential virulence genes. First, the BHR expression vector (pYL101C) was constructed via Golden Gate cloning, including ColE1 and pBBR1 ori, a Gm^R selectable marker, a strong constitutive integrin promoter (P_{INTc}) followed by a multiple cloning site downstream for facile gene cloning. As for the miniaturized helper Ti plasmid, plasmid pYL102 was constructed based on plasmid pCAMBIA5105, using long PCR amplification and homologous recombination. As a result, the size of pYL102

was reduced to 30.6 kb, which is a ~40% reduction of pCAMBIA5105. To test the functionality of the constructed vector system, a key virulence gene for AMT, *virG-N54D*, was cloned into pYL101C to produce pYL101C::*virG-N54D* and was electroporated into the *A. tumefaciens* C58C1 strain together with the binary vector pGWB2::*e35S-sfGFP* and pYL102 for transient plant transformation. Two days after agroinfiltration of *Nicotiana benthamiana* leaves, strong green fluorescence was observed on spots infiltrated with the positive control and test *Agrobacterium* harbouring the constructed ternary vector system, but not in the mock-infiltrated leaves. The fluorescence intensity from the test agroinfiltrated leaves was significantly higher than those of the mock-infiltrated leaves ($p < 0.01$), indicating that the constructed vector system is functional in plant transformation and can be utilized to increase transformation efficiency.

ACKNOWLEDGEMENT

Foremost, I would like to express my sincere appreciation and utmost gratitude towards my supervisor, Assoc. Prof. Dr. Wong Hann Ling and my co-supervisor, Asst. Prof. Dr. Loh Pek Chin. Without their patience, motivation and guidance, this project would be an impossible task to accomplish. I am heartily thankful for their steadfast encouragement, invaluable advice and helpful suggestions in solving hurdles and difficulties I endured during the research project and also the writing process of dissertation and journal articles. Besides, I would also like to express my deepest gratitude towards Ministry of Higher Education (MOHE) and UTAR for providing the financial support that funds this research project.

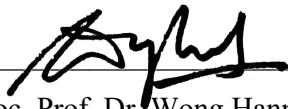
Furthermore, I would like to say a big “thank you” to my friends, the panel of judges during presentation and also laboratory officers as they provide endless support and constructive suggestions in carrying out this research project. I am also grateful to have my laboratory mates in D213B lab, especially Mr. Toh Wai Keat and Ms. Tor Xin Yen, for lending a helping hand whenever I needed and giving moral support with their encouraging words.

Last but not least, I owe my deepest gratitude and appreciation to my family members for their unconditional love, support and understanding throughout this research project. Without their support, I might not be able to make it in achieving this far.

APPROVAL SHEET

This dissertation entitled "**ENGINEERING OF PLASMID VECTORS FOR ENHANCING *AGROBACTERIUM*-MEDIATED PLANT TRANSFORMATION**" was prepared by TEO YUH LENG and submitted as partial fulfilment of the requirements for the degree of Master of Science at Universiti Tunku Abdul Rahman.

Approved by:



(Assoc. Prof. Dr. Wong Hann Ling)
Associate Professor / Supervisor
Department of Biological Science
Faculty of Science
Universiti Tunku Abdul Rahman

Date: 4 Feb 2022



(Asst. Prof. Dr. Loh Pek Chin)
Assistant Professor / Co-Supervisor
Department of Biological Science
Faculty of Science
Universiti Tunku Abdul Rahman

Date: 4 Feb 2022

FACULTY OF SCIENCE

UNIVERSITI TUNKU ABDUL RAHMAN

Date: 4th February, 2022

SUBMISSION OF DISSERTATION

It is hereby certified that **TEO YUH LENG** (ID No: **18ADM01346**) has completed this dissertation entitled “**ENGINEERING OF PLASMID VECTORS FOR ENHANCING AGROBACTERIUM-MEDIATED PLANT TRANSFORMATION**” under the supervision of Assoc. Prof. Dr. Wong Hann Ling (Supervisor) from the Department of Biological Science, Faculty of Science, Universiti Tunku Abdul Rahman, and Asst. Prof. Dr. Loh Pek Chin (Co-Supervisor) from the Department of Biological Science, Faculty of Science, Universiti Tunku Abdul Rahman.

I understand that the University will upload softcopy of my dissertation in pdf format into UTAR Institutional Repository, which may be made accessible to UTAR community and public.

Yours truly,



TEO YUH LENG

DECLARATION

I, TEO YUH LENG, hereby declare that the dissertation is based on my original work except for quotations and citations which have been duly acknowledged. I also declare that it has not been previously or concurrently submitted for any other degree at UTAR or other institutions.

A handwritten signature in black ink, appearing to read 'Teo.' with a horizontal line underneath.

Name: TEO YUH LENG

Date: 4th February, 2022

TABLE OF CONTENTS

	Page
ABSTRACT	ii
ACKNOWLEDGEMENT	iv
APPROVAL SHEET	v
SUBMISSION OF DISSERTATION	vi
DECLARATION	vii
TABLE OF CONTENTS	viii
LIST OF TABLES	xi
LIST OF FIGURES	xii
LIST OF ABBREVIATIONS	xvi
CHAPTERS	
1.0 INTRODUCTION	1
1.1 Project Background	1
1.2 Problem Statement	3
1.3 Research Objectives	4
1.4 Significance of Study	5
2.0 LITERATURE REVIEW	6
2.1 Plant Genetic Engineering	6
2.2 <i>Agrobacterium tumefaciens</i>	7
2.2.1 Host Range	8
2.2.2 Tumour-inducing (Ti) Plasmid	9
2.2.3 Virulence (<i>vir</i>) Genes	10
2.2.4 Mutant of VirG – VirG-N54D	12
2.3 <i>Agrobacterium</i> -mediated Gene Transfer in Plants' Genome	13
2.4 Plasmid as Vector	14
2.4.1 Bacterial Expression Vector	16
2.4.2 Binary Vector System	17
2.5 Type IIS Restriction Endonucleases	20
2.6 Golden Gate Cloning	21
2.7 Homologous Recombination	23
2.8 Reporter Genes	25
2.8.1 Superfolder Green Fluorescent Protein (<i>sfGFP</i>)	26
3.0 MATERIALS AND METHODS	29
3.1 Project Workflow	29
3.2 Buffers, Media, Antibiotics, Bacterial Strains and Plant Used	31
3.3 General Methodology	32
3.3.1 Agarose Gel Electrophoresis	32
3.3.2 Plasmid Extraction and Purification	33
3.3.3 Agarose Gel Purification	33

3.3.4	PCR Product Purification by Ethanol Precipitation	33
3.3.5	Measurement of DNA Concentration and Purity	34
3.3.6	DNA Amplification by Polymerase Chain Reaction	34
3.3.6.1	General PCR Amplification	35
3.3.6.2	Colony PCR Amplification for Verifying Recombinant Clones	36
3.3.7	Restriction Endonuclease (RE) Digestion	36
3.3.8	Ligation of DNA Fragments	37
3.3.9	NEBuilder® HiFi DNA Assembly Cloning	37
3.3.10	Preparation of Competent Cells	38
3.3.11	Bacterial Transformation via Electroporation	39
3.3.12	Bacterial Transformation via Heat Shock Method	39
3.3.13	DNA Sequencing	40
3.3.14	Agroinfiltration on <i>Nicotiana benthamiana</i>	40
3.4	Construction of BHR Expression Vector pYL101C	41
3.5	Construction of Plasmid pYL101C:: <i>sfGFP</i>	43
3.5.1	Molecular Cloning of <i>sfGFP</i> into pYL101C	43
3.5.2	Host Range Testing for pYL101C:: <i>sfGFP</i>	43
3.6	Construction and Functionality Test of Plasmid pYL101C:: <i>virG-N54D</i>	44
3.6.1	Total RNA Extraction from <i>Agrobacterium</i> harbouring pYL101C:: <i>virG-N54D</i>	45
3.6.2	Removal of DNA from Extracted RNA sample using DNase I	45
3.6.3	Reverse Transcription for mRNA of <i>virG-N54D</i>	46
3.7	Construction of Miniaturized Ti plasmid pYL102	47
3.7.1	Construction of pYL102-P1	47
3.7.2	Long PCR amplification of pYL102	48
3.7.3	Assembly of pYL102 Fragments and Verification of pYL102	48
3.8	<i>In planta</i> Functionality Testing using <i>N. benthamiana</i> via Agroinfiltration	49
4.0	RESULTS	51
4.1	Construction of Broad Host Range Expression Vector	51
4.1.1	PCR Amplification of Fragments for pYL101C	52
4.1.2	Verification of pYL101C	56
4.2	Molecular Cloning of pYL101C:: <i>sfGFP</i> and Host Range Testing	57
4.2.1	PCR Amplification and Cloning of <i>sfGFP</i> Reporter Gene	57
4.2.2	Host Range Testing of pYL101C:: <i>sfGFP</i>	58
4.2.3	Plasmid Stability Test for pYL101C:: <i>sfGFP</i>	61
4.3	Construction of Miniaturized Helper Ti Plasmid, pYL102	62
4.3.1	Construction of Intermediate Plasmid, pYL102-P1	62
4.3.2	Construction of pYL102 by Long PCR Amplification	66

4.4	Functionality Testing for the Constructed Plasmid System	69
4.4.1	Molecular Cloning of pYL101C:: <i>virG</i> -N54D	69
4.4.2	Reverse Transcription PCR for <i>virG</i> -N54D in <i>Agrobacterium tumefaciens</i>	69
4.4.3	Verification for <i>Agrobacterium</i> transformants harbouring the Constructed Vector System	71
4.4.4	Visualization of Green Fluorescence in Infiltrated <i>Nicotiana benthamiana</i> leaves	73
4.4.5	Statistical Analysis of Fluorescence Intensity of the <i>Agrobacterium</i> -transformed Plant Cells	75
5.0	DISCUSSION	78
5.1	Construction of Broad Host Range Expression Vector, pYL101C	78
5.2	BHR Reporter Vector, pYL101C:: <i>sfGFP</i>	81
5.3	Construction of Miniaturized Ti Plasmid, pYL102	83
5.4	Molecular Cloning of Key Virulence Gene, <i>virG</i> -N54D into pYL101C	85
5.5	Functionality of Constructed Vector System in <i>Agrobacterium</i> -mediated Plant Transformation	86
5.6	Future Prospective	87
6.0	CONCLUSION	89
	REFERENCES	91
	APPENDIX A	105
	APPENDIX B	106
	APPENDIX C	107
	APPENDIX D	108
	APPENDIX E	109
	APPENDIX F	110
	APPENDIX G	111
	APPENDIX H	112
	APPENDIX I	113
	APPENDIX J	114
	APPENDIX K	115
	APPENDIX L	116
	APPENDIX M	117
	APPENDIX N	118
	APPENDIX O	119
	APPENDIX P	120

LIST OF TABLES

Table		Page
2.1	Functions of each <i>vir</i> genes in Ti plasmid in facilitating <i>Agrobacterium</i> -mediated transformation.	11
3.1	List and formulation of buffers and media.	31
3.2	List of stocks, working concentrations and solvents of antibiotics.	31
3.3	List of bacterial strains and plant used.	32
3.4	Components of reaction mixture for PCR amplification.	35
3.5	Components for general digestion reaction.	37
3.6	Components of reaction mixture for RT-PCR.	46
A	List of primers used in this study.	105
B	List of restriction endonucleases (REs) used in this study.	103
E	Fragments sizes of plasmids after <i>EcoRI</i> digestion.	109

LIST OF FIGURES

Figure		Page
2.1	Schematic diagram of <i>Agrobacterium</i> -mediated plant transformation process.	14
2.2	Schematic diagram of the mechanism for Golden Gate cloning using type IIS restriction enzymes to assemble DNA fragments.	23
2.3	A palette of GFP-like proteins.	27
3.1	Overall workflow for the project.	30
3.2	Six fragments to be assembled into pYL101C from different sources.	42
4.1	Schematic representation of the construction of BHR expression vector, pYL101C.	52
4.2	Gel electrophoresis of P_{INTc} promoter in 1.2% agarose gel at 100 V for 40 minutes.	54
4.3	Gel electrophoresis of <i>T7</i> terminator in 1.5% agarose gel at 100 V for 40 minutes.	54
4.4	Gel electrophoresis of <i>lacI</i> operon in 1.2% agarose gel at 100 V for 40 minutes.	54
4.5	Gel electrophoresis of ColE1-Gm ^R amplicons in 1.2% agarose gel at 100 V for 40 minutes.	55
4.6	Gel electrophoresis of BHR1 oriV amplicons in 1.2% agarose gel at 100 V for 40 minutes.	55
4.7	Gel electrophoresis of MCS fragment in 3% agarose gel at 100 V for 50 minutes.	55
4.8	Gel electrophoresis of <i>KpnI</i> -digested pYL101C in 1.0% agarose gel at 100 V for 40 minutes.	56
4.9	Schematic diagram of plasmid map for the broad host range expression vector, pYL101C.	57
4.10	Schematic diagram on the construction of pYL101C:: <i>sfGFP</i> .	58
4.11	Gel electrophoresis of PCR-amplified <i>sfGFP</i> fragment after purified in 1.2% agarose at 100 V for 40 minutes.	59

4.12	Gel electrophoresis of recombinant pYL101C:: <i>sfGFP</i> after double digestion of <i>Xba</i> I and <i>Sac</i> I in 1.0% agarose gel at 100 V for 40 minutes.	59
4.13	Schematic diagram of the complete plasmid map for the 6.7 kb pYL101C:: <i>sfGFP</i> .	60
4.14	Visualization of the expressed sfGFP in various Gram-negative bacterial hosts harbouring the recombinant pYL101C:: <i>sfGFP</i> , under blue light excitation.	60
4.15	Visualization of sfGFP fluorescence in <i>E. coli</i> cells harbouring pYL101C:: <i>sfGFP</i> under blue light excitation, on both selective and non-selective culture medium at fourth passage of sub-culturing.	61
4.16	Schematic diagram of pCAMBIA5105 and the T-DNA region to be removed via <i>Mau</i> BI digestion.	63
4.17	Gel electrophoresis of intact plasmid pCAMBIA5105 and <i>Mau</i> BI-digested pCAMBIA5105 in 0.8% agarose gel at 100 V for 40 minutes.	64
4.18	Schematic diagram of the complete plasmid map for the 37.8 kb pYL102-P1.	64
4.19	Verification on pYL102-P1 using <i>Eco</i> RI digestion.	65
4.20	Schematic representation of three fragments to be assembled into pYL102 via homologous recombination.	67
4.21	Gel electrophoresis of three PCR-amplified fragments for pYL102 construction after purification, in 1% agarose gel at 100 V for 40 minutes.	67
4.22	Schematic diagram of the plasmid map for pYL102 after assembly of fragments via homologous recombination.	68
4.23	Gel electrophoresis of <i>Eco</i> RI-digested pCAMBIA5105 and pYL102 in 0.8% agarose gel at 100 V for 1 hour and 15 minutes.	68
4.24	Gel electrophoresis of <i>vir</i> G-N54D amplicons in 1% agarose gel at 100 V for 40 minutes.	70
4.25	Schematic representation of the construction of pYL101C:: <i>vir</i> G-N54D.	70
4.26	Gel electrophoresis of RT-PCR product of <i>vir</i> G-N54D in 1.0% agarose gel at 100 V for 40 minutes.	71

4.27	Gel electrophoresis of extracted plasmids from <i>A. tumefaciens</i> C58C1 harbouring the constructed vector system in 1.0% agarose gel at 100 V for 40 minutes.	72
4.28	Gel electrophoresis of colony PCR on the total extracted plasmids from <i>A. tumefaciens</i> C58C1 harbouring the constructed vector system in 1.0% agarose gel at 100 V for 40 minutes.	73
4.29	Representative image of <i>Nicotiana benthamiana</i> leaf infiltrated with various <i>Agrobacterium</i> bacterial cultures.	74
4.30	Microscopic images of <i>N. benthamiana</i> leaf disks infiltrated with <i>Agrobacterium</i> cultures under blue light excitation at magnification of 400×.	75
4.31	Average fluorescence intensity of <i>N. benthamiana</i> leaf extract infiltrated with different <i>Agrobacterium</i> culture.	76
4.32	Relative fluorescence intensity of <i>N. benthamiana</i> leaf extract infiltrated with <i>Agrobacterium</i> harbouring different plasmids under blue light excitation.	77
C1	Schematic representation on pYL101C construction using Golden Gate cloning, starting from PCR amplification to ligation.	107
C2	Schematic diagram of the six fragments to-be assembled for pYL101C after <i>AarI</i> and <i>Esp3I</i> digestion.	107
D	Flowchart of pYL102 construction via RE digestion, PCR amplification and homologous recombination.	108
E	Schematic diagrams of plasmids pCAMBIA5105, pYL102-P1 and pYL102, with <i>EcoRI</i> restriction sites labelled.	109
F	Sequence alignment of <i>lacI</i> region on the constructed pYL101C, showing 100% to the expected sequence.	110
G	Sequence alignment of <i>lacI</i> promoter and Gm ^R region on the constructed pYL101C, showing 100% to the expected sequence.	111
H	Sequence alignment of Gm ^R region on the constructed pYL101C, showing 100% to the expected sequence.	112
I	Sequence alignment of ColE1 ori region on the constructed pYL101C, showing 100% to the expected sequence.	113

J	Sequence alignment of <i>rrnB</i> terminators and <i>P_{INTc}</i> regions on the constructed pYL101C, showing 100% to the expected sequence.	114
K	Sequence alignment of <i>T7</i> terminators and <i>oriV</i> regions on the constructed pYL101C, showing 100% to the expected sequence.	115
L	Sequence alignment of <i>pBBR1 rep</i> and <i>lacI</i> regions on the constructed pYL101C, showing 100% to the expected sequence.	116
M	Sequence alignment of <i>virG-N54D gene</i> on the recombinant pYL101C:: <i>virG-N54D</i> , showing 100% to the expected sequence.	117
N	Sequence alignment of <i>sfGFP gene</i> on the recombinant pYL101C:: <i>sfGFP</i> , showing 100% to the expected sequence.	118
O	Schematic diagram of plasmid map for the recombinant pYL101C:: <i>virG-N54D</i> .	119
P	Schematic diagram of plasmid map for the binary vector pGWB2:: <i>e35S-sfGFP</i> .	120

LIST OF ABBREVIATIONS

×g	Time gravity
°C	Degree Celsius
μM	Micromolar
BHR	Broad host range
bp	Base pair
CaCl ₂	Calcium chloride
cDNA	Complement DNA
DNA	Deoxyribonucleic acid
dNTP	Deoxynucleoside triphosphate
EDTA	Ethylenediaminetetraacetic acid
GFP	Green fluorescent protein
GUS	B-glucuronidase
IPTG	Isopropyl β-d-1-thiogalactopyranoside
kb	Kilobase
L	Liter
LB	Left Border
M	Molar
MCS	Multiple cloning site
MES	2-(N-morpholino) ethanesulfonic acid
Mg ²⁺	Magnesium ion
MgCl ₂	Magnesium chloride
mRNA	Messenger DNA
NaCl	Sodium chloride
OD ₆₀₀	Optical density measured at 600 nm
Ori	Origin of replication
PCR	Polymerase chain reaction
pmol	Picomole
RB	Right Border
RE	Restriction endonuclease
RNA	Ribonucleic acid
Rpm	Revolution per minute
RT	Reverse transcriptase

RT-PCR	Reverse transcription PCR
sfGFP	Superfolder green fluorescent protein
sp.	Species
T4SS	Type IV Secretion System
T-DNA	Transferred DNA
Ti	Tumour-inducing
UV	Ultraviolet
V	Volt
<i>vir</i>	Virulence

CHAPTER 1

INTRODUCTION

1.1 Project Background

In 2011, the United Nations estimated that the world population of 7.7 billion would spike up by two billion in 30 years and may reach the peak of 11 billion in 2100. However, the findings from a new study suggested that the global population was expected to peak at 9.7 billion at 2064 and experience a decline to 8.79 billion in 2100 (Vollset *et al.*, 2020). Famine and malnutrition have become a global issue and to fulfil the second Sustainable Development Goal of “Zero Hunger and Improved Nutrition”, major transformation in food security and nutrition systems is inevitable (International Service for the Acquisition of the Agri-biotech Application, 2021). However, the escalating growth of human population and the worldwide climate change have caused adverse effects on sustainable food supply. The discovery of genes with desired phenotypic traits and incorporating them in major crop plants has become one of the priorities for plant biologists as it allows the process of gene transfer to be manipulated at a more fundamental level with shorter time (Phillips, 2008). Plant transformation is one of the vital tools in plant biotechnology and *Agrobacterium*-mediated transformation is the widely used method due to its non-destructive approach and cost effectiveness.

Agrobacterium tumefaciens is a soil-borne phytopathogen that is well-known for causing the neoplastic crown gall disease in most of the

dicotyledonous plants (Tomlinson and Fuqua, 2009). This disease, which is characterized by the growth of tumour at subterranean-to-aerial transition zone of the infected plant, is induced by the presence a tumour-inducing (Ti) plasmid within the virulent *A. tumefaciens* (Christie and Gordon, 2014). During the infection of plants by *Agrobacterium*, a fragment of DNA is transferred from the Ti plasmid of the bacterium into the plant genome. This ability of inter-kingdom gene transfer makes *Agrobacterium* a versatile tool for various research, especially in plant genetic manipulation. The molecular basis of this transformation is the transfer and integration of T-DNA from Ti plasmid into plant nuclear genome which requires various virulence proteins encoded by the virulence (*vir*) genes residing on the plasmid. These virulence proteins form an archetypal type IV secretion system (T4SS), that is responsible for the translocation of the T-DNA from the bacterium to the plant cell (Christie, Whitaker and González-Rivera, 2014).

To facilitate *Agrobacterium*-mediated transformation, scientists developed the binary vector system, in which two functionally complementing plasmids separately carrying the T-DNA and virulence gene clusters, that not only produced a higher plant transformation efficacy, but also made genetic manipulation easier (Mohammadhassan, Kashefi and Delcheg, 2014). Vast efforts have been channeled to develop versatile and efficient binary vectors with the ultimate aim to enhance the efficiency of *Agrobacterium*-mediated transformation on recalcitrant crops (Hoekema *et al.*, 1983; Komari *et al.*, 2007; Anand *et al.*, 2018).

1.2 Problem Statement

In the past decades, various attempts were conducted to improve the transformation efficiency not only in dicots, but also in monocots. Although *Agrobacterium*-mediated transformation is relatively easy to perform, its low transformation rate in recalcitrant plants is still a major limitation for plant biologists. Despite the continuous efforts in improving the transformation efficiency in recalcitrant crops such as rice, maize and soybean, the number of crops that can be transformed and its transformation efficiency remain low (Sah *et al.*, 2014; Zhi *et al.*, 2015; Li *et al.*, 2017). A key contributing factor that led to predicament is the unsolved challenges imposed by the Ti plasmid. The narrow or limited bacterial host range of Ti plasmid forbade the manipulation of the plasmid in *Escherichia coli*, which is the workhorse of molecular biology. The low copy number of the large Ti plasmid has led to low expression of virulence gene. Furthermore, the current binary vector systems do not meet the expectation for high transformation rate. To-date, helper plasmids that can enhance the *Agrobacterium*-mediated transformation rate are not commercially available, thus constraining the advancement in *Agrobacterium*-mediated plant transformation.

1.3 Research Objectives

In this study, the general objective is to construct a vector system for transformation, comprising of two plasmid vectors, which separately express the key regulatory virulence gene, *virG-N54D* and structural virulence genes, respectively, for enhancing *Agrobacterium*-mediated plant transformation efficiency. These vectors would complement functions of commonly used binary vectors, which carries the transgene, and thus facilitating plant transformation. The four specific objectives to be achieved in this study are listed as follows:

- i. To construct an *Agrobacterium*-based broad host range (BHR) expression vector to be utilized in *Agrobacterium*-mediated transformation.
- ii. To construct a miniaturized helper tumour-inducing (Ti) plasmid for expressing structural virulence genes for *Agrobacterium*-mediated transformation.
- iii. To clone and express the key regulatory virulence gene, *virG-N54D* from the constructed BHR expression vector for assisting *Agrobacterium*-mediated transformation.
- iv. To assess the functionality of the constructed vector system *in planta* via *Agrobacterium*-mediated transient transformation of *Nicotiana benthamiana*

1.4 Significance of Study

The constructed bacterial expression vector with the broad host range ori is expected to be functional in a wide range of Gram-negative bacteria, therefore the vector can be used in multitudinous purposes in molecular biology, such as heterologous gene expression in various species, elucidation of molecular mechanism of pathogenicity and facilitation of easy genetic manipulation. Besides, by expressing the key regulatory virulence gene, *virG-N54D*, the helper plasmid may be used to eliminate the bottleneck of low virulence gene expression in *Agrobacterium*-mediated plant transformation. Furthermore, the miniaturized helper Ti plasmid would provide for easy manipulation of the virulence genes such as gene up-regulation or gene silencing, thereby opening an opportunity for enhancing *Agrobacterium*-mediated plant transformation efficacy.

CHAPTER 2

LITERATURE REVIEW

2.1 Plant Genetic Engineering

For years, many scientists have put effort into improving the crop yield to sustain the growing population on Earth (Gelvin, 2003; Ziemienowicz, 2013; Anjanappa and Gruissem, 2021). Discovery of genes with desired phenotypic traits and incorporating them into crop plants have always been the one of the focus for plant biologists. Recently, numerous commercially important crop species, such as soybean, maize, cotton, wheat and rice are routinely transformed by various biotechnological approaches. Transformation methods have been divided into three groups: (i) by means of biological vectors like virus- or *Agrobacterium*-mediated transformation; (ii) by transferring DNA directly through electroporation and particle bombardment (Keshavareddy, Kumar and Ramu, 2018); and (iii) via non-biological vector system, such as liposome fusion (Özyiğit, 2012). Although plant transformation serves as a core research tool for transgenic plant development, many challenges still need to be overcome in transforming economically important crop species, as well as forest species for lumber, paper and pulp industries. Among all the transformation methods used, *Agrobacterium*-mediated transformation is the most widely used due to its relatively non-destructive and cost-effectiveness (Gelvin, 2003; Komari, Ishida and Hiei, 2004; Anjanappa and Gruissem, 2021).

2.2 *Agrobacterium tumefaciens*

Agrobacterium tumefaciens is a well-known plant pathogen that causes tumour formation at crown of a plant. It belongs to the Proteobacteria phylum and classified under Alpha-proteobacteria and the genus of *Agrobacterium* (UniProt, 2020). Most of the Alphaproteobacteria species harbour large plasmids with the size ranging from 100 kilobases to approximately 2 megabases and these replicons are usually responsible for essential cell functions such as cell physiology, pathogenesis and symbiosis. *A. tumefaciens* is a Gram-negative, rod-shaped soil-borne bacterium and it is the one of the well-known organisms that is capable of inter-kingdom gene transfer (Pitzschke and Hirt, 2010).

The molecular basis of the transformation is due to the activities of the tumour-inducing (Ti) plasmid found within the virulent strains. A region delimited by 25 bases of border sequences, which is also known as the transferred DNA (T-DNA) region, is nicked off from the Ti plasmid and transferred into plant cell. The T-DNA strand is then integrated into host genome and being expressed to co-opt the host into manufacturing essential factors for the bacterium to survive and propagate (McCullen and Binns, 2006). The transport of T-DNA into plant cell is achieved by a molecular machinery resembling to a bacterial conjugal transfer system, known as type IV secretion system (T4SS), which depends on direct contact between the *Agrobacterium* and plant cells (Christie, Whitaker and González-Rivera, 2013). The *Agrobacterium*'s ability as a natural genetic engineer has been widely exploited for introducing genes of agronomic interest into desired crops for commercial purpose (Gelvin, 2003; Murai, 2013; Nester, 2015; Hwang, Yu and Lai, 2017).

2.2.1 Host Range

The *Agrobacterium* Ti plasmid serves as a crucial pathogenicity factor that allows inter-kingdom gene transfer. The virulence genes and T-DNA oncogenes of the bacterium are known to play pivotal roles in determining the host range. In addition, plant factors such as genetic factors, tissue types and the physiological status of the plant species influence the efficiency of transformation and tumour formation. An early review published by De Cleene and De Ley (1976) reported that *Agrobacterium* was capable of infecting 93 families of gymnosperms and dicotyledonous plants, based on the observation on the appearance of crown galls or hairy roots. Other studies have later shown that *Agrobacterium* could infect a significantly wider range of plants including monocotyledons with no signs of infection symptom (Otten, Burr and Szegedi, 2008).

The host range of some certain strain of *A. tumefaciens* is strain-specific. It was observed that strains with genetic difference in Ti plasmid exhibited distinctive host range with high host specificity and narrow host range. Multiple factors, including Ti plasmid, chromosomally encoded genes and variations of plant host genera, may determine the outcome of the interaction between this soil pathogen and its potential host (Knauf, Panagopoulos and Nester, 1982). A Ti plasmid from a broad host range strain may render the *Agrobacterium* to have a wider range of potential hosts, thereby the host range-related genes may reside on the Ti plasmid (Loper and Kado, 1979). A study showed that the host range of *A. tumefaciens* LBA649 was not extended by the *vir* region of a wide-host-range Ti plasmid. Instead, the oncogenes in T-DNA region, namely *cyt* gene, in the LBA649 strain was shown to play a crucial role for determining the host

range and thus responsible for its limited plant host range (Hoekema *et al.*, 1984). Recent studies suggest that phytohormones produced by the enzymes coded by these oncogenes may increase the susceptibility of plant cells to infection and T-DNA integration by *Agrobacterium* (Gohlke and Deeken, 2014).

2.2.2 Tumour-inducing (Ti) Plasmid

As mentioned previously, Ti plasmids cause crown gall diseases to those infected plants and also induce the production of various sugar phosphate and amino acid derivatives, known as opines. This large plasmid harbours the genes for opine synthesis and also for the corresponding opine catabolism. Therefore, Ti plasmids were traditionally classified by opine type, designated as octopine- and nopaline-type. Ti plasmid is pivotal in *Agrobacterium* as it codes for conjugative transfer, virulence, opine utilization, plasmid replication and maintenance and sensory perception of exogenous signals (Christie and Gordon, 2014).

The T-DNA region generally constitutes less than 10% of the Ti plasmid and some plasmids have multiple T-DNA regions. The translocation of T-DNA regions from the plasmid into plant cells is mainly due to the activity of the virulence genes carried on the same Ti plasmid (Gelvin, 2003). T-DNA regions are delimited by T-DNA border sequences, of which the length is about 25 bases of nucleotides with high homologous in sequence. These sequences act as target for the respective virulence proteins, which are the border-specific endonucleases that nick off the T-DNA strand from the plasmid (Gelvin, 2003; Christie and Gordon, 2014). To achieve the translocation of T-DNA, virulence

genes resided on Ti plasmid were expressed upon the induction of plant phenolic compounds and a cascade activation pathway is initiated from *virA* to *virG* and then to the remaining virulence genes (Christie and Gordon, 2014).

2.2.3 Virulence (*vir*) Gene

For plant transformation, *Agrobacterium* requires two major components: T-DNA strand and *vir* genes which resided on the tumour-inducing (Ti) plasmid. There are about 10 operons found within the *vir* region. Although the induction of *vir* gene cluster is dependent on the external factor such as plant exudates, attachment to host plant cells by the bacterium is a necessary and it is mediated by chromosomally encoded genes (Gelvin, 2003; Pitzschke and Hirt, 2010; Christie and Gordon, 2014; Hwang, Yu and Lai, 2017). As this transformation process is tedious and energy-demanding, the virulence gene expression must be under careful regulation (Pitzschke and Hirt, 2010).

The *virA* and *virG* genes are activated by plant factors such as phenolic compounds upon wounding. These genes are constitutively expressed at basal level and upon induction, the expression level increases and encodes a two-component phospho-relay system, which in turns activates the transcription of the remaining *vir* genes. Each of the expressed *vir* proteins perform their respective duties in *Agrobacterium*-mediated transformation and their respective roles are listed in Table 2.1 (Mohammadhassan, Kashefi and Delcheh, 2014).

Table 2.1: Functions of each *vir* genes in Ti plasmid in facilitating *Agrobacterium*-mediated transformation (Özyiğit, 2012).

<i>Vir</i> Gene / Operon	Roles played
<i>A</i>	Sensors for phenolic substances, activated upon the induction and express VirA protein to phosphorylate VirG protein
<i>G</i>	Activated by plant phenolic compounds and VirG protein is expressed to bind to each <i>vir</i> box of other <i>vir</i> gene operon
<i>B (B1 to B11)</i>	Transcribed upon the activation by phosphorylated VirG protein and involves in building up type IV secretion system (T4SS) by synthesizing T-pilus and forming a pore across the bacterial membrane
<i>C1</i>	Presumably drives the “overexpression of binding protein to enhance T-DNA transfer
<i>D1 & D2</i>	Expressed upon VirG protein activation and aid in processing T-DNA strands by cleaving it off from Ti plasmid at the border sequences for the transfer of Vir proteins and T-DNA strand
<i>D4</i>	Protein expressed serves as a coupling factor in directing the VirD2-T-DNA strand to the T4SS apparatus at the membrane
<i>D2, D5, E2, E3 & F</i>	Proteins expressed are suggested to be involved in T-DNA-cytoplasmic trafficking, nuclear targeting, protection from nucleolytic degradation and T-DNA integration into host genome
<i>H</i>	Presumably involved in the host range specificity of bacterial strain

2.2.4 Mutant of VirG – VirG-N54D

It is known that VirA protein interacts with the phenolic inducer at the initial step and undergoes auto-phosphorylation in the C-terminal cytoplasmic domain. Subsequently, the phosphate group is transferred to the transcriptional regulator, VirG and together these proteins constitute a phenol-activated signalling pathway (Lee *et al.*, 1992). Evidences from studies showed that *virA* and *virG* are required for the induction of other *vir* genes (Krishnamohan, Balaji and Veluthambi, 2001; Pitzschke and Hirt, 2010). This induction process is optimal under an acidic growth condition in the presence of monosaccharides and the sugar-binding protein, ChvE (Chen and Winans, 1991). VirA serves as a trans-membrane sensor kinase and undergoes auto-phosphorylation at its conserved His-474 residue upon the sensing plant signal molecules, such as acetosyringone. Subsequently, the phosphate group is transferred to the conserved Asp-52 residue of the VirG. The C-terminal domain of phosphorylated VirG binds to the *vir* box upstream of all *vir* operons and this binding presumably leads the binding of the RNA polymerase to the promoter, thereby resulting in an increased transcription of the *vir* genes (Jung *et al.*, 2004).

Previously, constitutively active mutants of VirG with the mutations N54, I77 and I106 were isolated and only VirG-N54D and VirGI77V/D52E were not responsive towards acetosyringone induction. This phenomenon is attributed to the additional negative charge of N54D in the active site mimics the phosphoryl group in the active wild-type VirG. The mutant showed stronger DNA binding affinity than the wild-type VirG and its phosphorylation presumably been achieved by accepting the phosphate group from other donors *in vivo* such as acetyl phosphate, carbomoyl phosphate and phosphoramidate (Gao *et al.*, 2006).

Van der Fits *et al.* (2000) demonstrated that the use of this constitutively active mutant of VirG (VirG-N54D) in *A. tumefaciens* strain LBA4404 had resulted in an efficient T-DNA transfer to a wide range of plant species, thereby giving rise to high transformation frequencies of various plant species.

2.3 *Agrobacterium*-mediated Gene Transfer in Plants' Genome

The *Agrobacterium*-mediated gene transfer into plant cells is achieved through several steps: recognition, virulence gene expression, host cell attachment, targeting of virulence factors and T-DNA strand into the host cell and lastly chromosomal T-DNA integration.

The T-DNA transfer kickstarts with the bacterium recognition of plant derived compounds such as acetosyringone. In the first stage, VirA and VirG act together as a two-component sensory-signal regulatory system. VirA undergoes auto-phosphorylation upon phenolic signal perception and subsequently phosphorylates and turns VirG into its active form, which activates and increases the transcriptional level of other virulence genes by interacting with the *vir*-box promoter. The phosphorylated VirG also activates its own expression by binding at the distal promoter for *virG* transcription (Subramoni *et al.*, 2014). The induced expression of *virB*, *virD4*, and *virE* genes into proteins has made up the T4SS system, which in turn facilitates the transfer and transport of T-DNA strand from the bacterium into plant nucleus (Gelvin, 2003). The next step involved the excision of the T-DNA and the translocation of the T-DNA across the bacterium membrane into the plant cells together with the produced substrates into the plant nucleus. The final stage is the integration of T-DNA into host nuclear genome

so that it can be expressed together with other host genes. The complete pathway of the *Agrobacterium*-mediated plant transformation is illustrated in Figure 2.1.

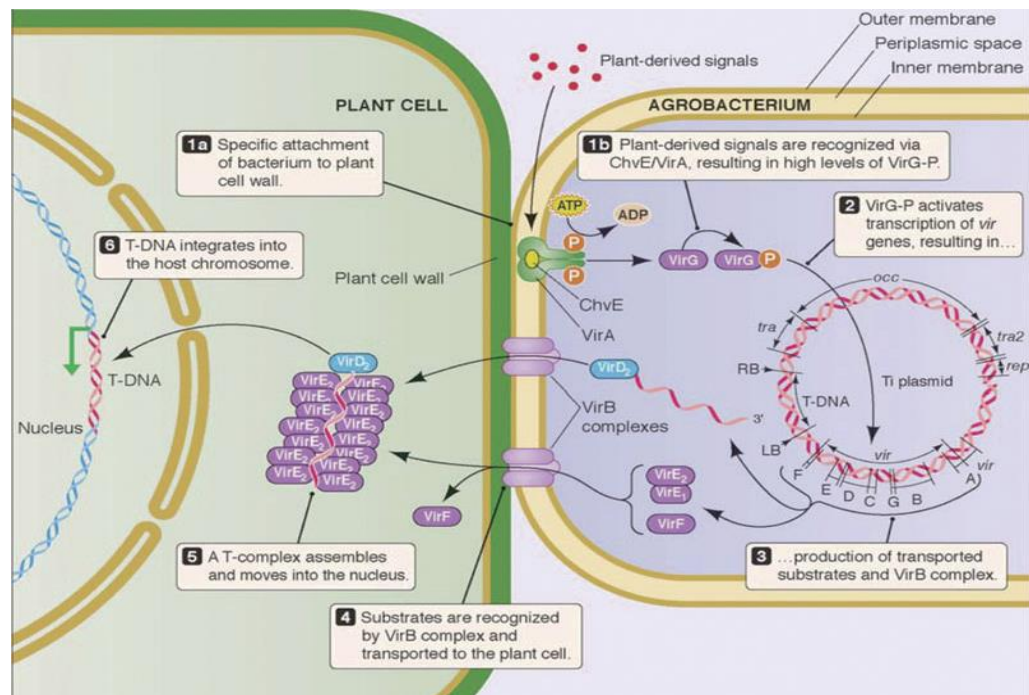


Figure 2.1: Schematic diagram of *Agrobacterium*-mediated plant transformation process. (1) Induction by plant derived signals and activation of VirA/VirG; (2 & 3) Activation and expression of other *vir* genes by phosphorylated VirG; (4) Construction of type IV secretion system across bacterial membrane into plant cell; (5) Expressed virulence proteins processed T-DNA strand and transport it into plant cell; and (6) Integration of T-DNA into host genome in nucleus (van Baarlen and Slezen, 2009).

2.4 Plasmid as Vector

To be a qualified vector, ideally a DNA molecule must be able to replicate and stably maintained in the host cells. The DNA molecule should be small, thereby causing less metabolic burden to the host and less prone to degradation during plasmid purification process to ease genetic manipulation (Brown, 2006).

A plasmid is a non-essential extrachromosomal double-stranded deoxyribonucleic acid, which is mostly circular and replicates autonomously as a stable component of the cells' genomes. Naturally occurring plasmids exist in various sizes and copy numbers. Most of the plasmids are being inherited with high fidelity despite their non-essentiality. The characteristics of being extrachromosomal and stable inheritance of plasmids making it one of the most popular choice of vector in molecular biology (Novick, 1987; Nora *et al.*, 2018). As a cloning vector, it carries foreign DNA molecules and exhibits the following four vital features: (i) able to replicate themselves and the DNA insert independently; (ii) contain different unique restriction endonuclease cutting sites; (iii) carry suitable and compatible selectable marker to distinguish host cells containing the vector from those which do not contain vector within; and (iv) relatively easy to be recovered from the transformed cells.

A few criteria need to be considered when researchers are looking for a suitable plasmid vector for cloning purpose. The insert size of DNA molecules cannot be relatively too large as it could restrict the plasmid replication and cause plasmid instability. A high copy number plasmid is preferable to generate more cloned DNA and thus increase the productivity of the recombinant proteins (Son *et al.*, 2016). In some cases, plasmids with low copy number are chosen as the recombinant protein product is toxic to the host. Plasmid incompatibility, selectable marker and multiple cloning sites also should be considered as they play important roles in cloning process (Preston and Casali, 2003) such as allowing facile gene insertion and maintain multiple plasmids within one cell.

2.4.1 Bacterial Expression Vector

Expression vectors serve as vehicles for foreign DNA to be expressed in bacterial system. These expression vectors consist of similar features as a cloning vector but they also contain regulatory elements such as enhancers and promoters to facilitate gene transcription. The promoter and termination sequences must be present on the vector to regulate the gene expression. In some vectors, a ribosomal binding site is located upstream to the start codon to facilitate efficient translation of the desired genes. Expression vectors are divided into the regulated system and constitutive system. In the constitutive system, the promoter is unregulated and allows continuous gene transcription. The regulated system is grouped into induced and repression systems and *lac* promoter, *trp* promoter and *tac* promoter are among the commonly used regulatory promoters (Terpe, 2006; Rosano and Ceccarelli, 2014). Reporter genes and epitope tags are included to facilitate detection and purification of the recombinant products expressed by the cells.

As compared to other expression systems, the bacterial expression system is preferred by researchers in producing recombinant products because bacterial cells are easier to culture, fast growing and able to give rise to higher yield of recombinant proteins. However, some eukaryotic proteins do not fold properly in a prokaryote due to the lack of post-translational modifications, rendering the recombinant proteins non-functional. In some cases, the produced products are toxic to the host cells, leading to low yield of production. Therefore, the nature of the recombinant protein needs to be considered in the selection of suitable expression system (Brondyk, 2009).

2.4.2 Binary Vector System

As mentioned previously, the key components in *Agrobacterium*-mediated transformation are the T-DNA region and the virulence gene cluster. Studies have shown that removal of genes within T-DNA region does not hinder the T-DNA transfer of *Agrobacterium* but it does prevent the tumour formation (Hellens, Mullineaux and Klee, 2000). It was also found that *vir* genes resided on a separate replicon from T-DNA did not affect their roles in the translocation of T-DNA (Komori *et al.*, 2007). In the beginning, efforts to introduce desired genes into T-DNA region for plant transformation involved cumbersome genetic manipulations due to the large size and low copy number of Ti plasmid. Besides, Ti plasmid is difficult to isolate and manipulate *in vitro* and does not replicate in *E. coli*. Tedious and complex genetic manipulations were simplified by binary vector system (Lee and Gelvin, 2008).

This binary vector strategy was developed in 1983 to separate the T-DNA region and virulence genes into two independent plasmids. In this system, a helper *vir* plasmid is a disarmed Ti plasmid within *Agrobacterium* cell whereas T-DNA region consisting gene(s) to be transferred is provided on another plasmid, commonly known as binary vector (Hellens, Mullineaux and Klee, 2000). This binary vector constitutes of T-DNA and the vector backbone. The T-DNA segment is delimited by the right border (RB) and left border (LB) and contains multiple cloning sites, selectable marker genes for plants, reporter genes and genes of interest. As for the vector backbone, it usually contains origin of replication for *E. coli* and *A. tumefaciens*, bacterial selectable marker genes and some may have a function for the mobilization of plasmid between the host and other accessory components (Komori *et al.*, 2007). In general, *in vitro*

manipulation of genes is performed in *E. coli*, thus binary vectors are designed to be able to replicate in both *E. coli* and *Agrobacterium* (Hellens, Mullineaux and Klee, 2000). In the early 1990s, a superbinary vector with additional virulence genes was developed to improve the transformation efficiency in recalcitrant plants, such as rice, maize and oil palm (Komori *et al.*, 2007; Fuad *et al.*, 2008). In some cases, the plasmid size of the superbinary vector was too large for further manipulation, thus the utilization of other plasmid co-integration has come into play in giving rise to a co-integrated superbinary vector to be coupled with an intrinsic disarmed Ti plasmid in *Agrobacterium* cell, easing the genetic manipulation and transformation of the bacterial host (Komori *et al.*, 2007).

However, extra care must be taken in matching binary vectors with specific *vir* helper *Agrobacterium* strains due to the potential conflict in antibiotic selection as the plasmid could not be stably maintained within the cell. In the current trend, the binary vector approach has included various choices for selectable markers and promoters, rendering high degree of flexibility in improving the vector. Alterations can be easily made on the binary vectors for applications, such as in gene activation tagging, gene knocking-out, promoter and enhancer trapping, transposon mutagenesis (Hellens, Mullineaux and Klee, 2000). Although the binary vector system is versatile and useful in various aspects, drawbacks do exist as non-T-DNA regions might be inserted into the plants' genome, thus decreasing the transformation frequency and event quality. Furthermore, multiple genes insertion might take place due to numerous copies of binary vector within a cell. To mitigate these problems, a binary vector with

low copy number could be the solution for enhancing the quality of plant transformation (Lee and Gelvin, 2008).

In the recent years, continuous efforts have been made to improve the binary vector system to enhance transformation rate in wide range of plant hosts. The binary vector that consists of T-DNA region has always been the priority for researchers to develop and improve as they play pivotal roles by consisting specific gene insert in T-DNA region for plant transformation, for example introducing desired drug resistance into host plants (Komari *et al.*, 1996; Torisky *et al.*, 1997; Lee and Gelvin, 2008; Murai, 2013). Besides, the flexible Gateway cloning system is also adapted into the construction and development of versatile binary vector to permit facile cloning of gene(s)-of-interest into T-DNA region apart from the conventional restriction-ligation reaction (Xu and Li, 2008; Dalal *et al.*, 2015; Leclercq *et al.*, 2015). Reduction in the plasmid size of the binary vector has resulted in an enhancement of transformation frequencies (Lee *et al.*, 2012). Few studies focus on the development of versatile Ti plasmid, except for disarming the plasmid by removing the oncogenes from it or weakening its virulence in causing tumour (Fraley *et al.*, 1986; Simpson *et al.*, 1986; Kiyokawa *et al.*, 2009). Recently, researchers have come up with an improved vector system known as the ternary vector system. In this system, smaller accessory plasmids with enhanced vector stability, improved bacterial selectable marker and *vir* genes, are used. These accessory plasmids are introduced *in trans* with the T-DNA binary vectors to give rise to a versatile ternary vector system, which in turn increased the transformation frequency in plants (Anand *et al.*, 2018).

2.5 Type IIS Restriction Endonucleases

Restriction endonucleases (REs) are widely found in various prokaryotes such as bacteria and archaea with the principal function to protect their host genomes against viral infections. RE belongs to the restriction-modification (RM) systems which comprise the activities of an endonuclease and a methyltransferase (Wilson *et al.*, 2012; Loenen *et al.*, 2014). Endonucleases cleave foreign DNA in response to defined recognition sites, whereas modification enzymes make modification at the recognition sequence in host DNA sequence, thus protecting it from the attack by the endonucleases. RM systems were classified into three types according to their subunit composition, cofactor requirement and mode of actions. Among these, type II restriction enzymes have become the focus, as they are the “work horses” of modern molecular biology for DNA analysis and gene cloning (Pingoud, Wilson and Wende, 2014).

More than 3000 type REs have been discovered and they can be categorized into eight groups. The orthodox type II REs are homodimers that recognize short, usually palindromic, sequences of four to eight bases and cleave the DNA within or in close proximity to the recognition site in the presence of cofactor Mg^{2+} . Upon the binding of endonuclease at the recognition sequence, 15 to 20 hydrogen bonds are formed between the dimeric RE and the bases of the recognition sites. The recognition process triggers large conformational changes in the enzyme and the DNA strand, leading to the activation of the catalytic centers and subsequently DNA strand cleavage. The DNA cleavage results in DNA fragments with a 3'-OH and 5'-phosphate (Wilson *et al.*, 2012; Loenen *et al.*, 2014).

Other type II restriction enzymes recognize palindromic sequences differently from the orthodox REs as they have to interact with two copies of target sequence before cleaving. Type IIS REs recognize asymmetric recognition sequence and cleave the DNA strand at a defined distance, typically few base pairs away from recognition sites. Researchers have discovered few hundreds of type IIS enzymes and to date they were characterized as monomers (Pingoud and Jeltsch, 2001) and this has been turned into an indispensable tool in molecular cloning at present, especially in characterizing genomes, sequencing genes and assembling DNA.

2.6 Golden Gate Cloning

Expression of heterologous gene requires high-throughput, efficient and accurate cloning methods and traditional DNA cloning has been ubiquitously used to clone gene(s) of interest into desired vectors by digesting the desired DNA fragments and a recipient vector with restriction enzymes and subsequently ligating them using DNA ligase. This approach only allows one to two fragments to be ligated into a vector in a single step and does not work well for simultaneous assembly of multiple fragments in a vector (Marillonnet and Grütznér, 2020). Researchers have put in efforts in developing methods that allow the assembly of multiple fragments of DNA in a single cloning step. At present, technologies based on site-specific recombination systems are being widely adopted in molecular cloning, such as Gateway system (Invitrogen) and Creator cloning system (Clontech). Although these cloning methods allow seamless and facile assembly of any desired sequence, they still pose few

limitations to overcome. One of the disadvantages is the recombination site sequences are left in the end-product and become non-essential sequence, thereby increases the product's size. Besides, although these recombination-based cloning systems are usually commercially available, they could represent a high cost when researchers are to work with large gene sets (Engler, Kandzia and Marillonnet, 2008).

The Golden Gate cloning approach is developed based on the use of type IIS RE for assembling multiple fragments (Engler, Kandzia and Marillonnet, 2008). The Golden Gate approach is simple to carry out using a restriction-ligation reaction in a thermal cycler as the reagents are readily available in most of the molecular biology laboratories (Marillonnet and Grützner, 2020). As mentioned in Section 2.5, the cleavage site of type IIS restriction enzymes are outside of their recognition sites. A researcher may design the cloning experiment in such a way that after restriction digestion and ligation, the resultant ligated product does not contain the RE recognition sequences, thus facilitating seamless fusion of DNA fragments. Using Golden Gate cloning approach, depending on construct design, the construct can be designed in such a way that original RE recognition sites are absent after ligation and the ligated product cannot be re-cleaved. However, the construct can also be designed to allow the RE recognition sites to be retained after RE digestion and ligation, where the construct can be re-cleaved. Having a non-recleavable sites after ligation facilitates the RE digestion and ligation to be carried out simultaneously and this results in high cloning efficiency, as the desired products are increased with the increasing incubation time. Furthermore, type IIS RE allows the overhangs of the digested fragments to be in a combination of any four

nucleotides, thereby multiple compatible DNA fragments can be simultaneously assembled in pre-defined linear order (Engler and Marillonnet, 2014). In short, Golden Gate cloning approach has been developed to solve the limitations of traditional RE digestion-ligation cloning approach. It also facilitates gene shuffling and assembly of DNA fragments easily.

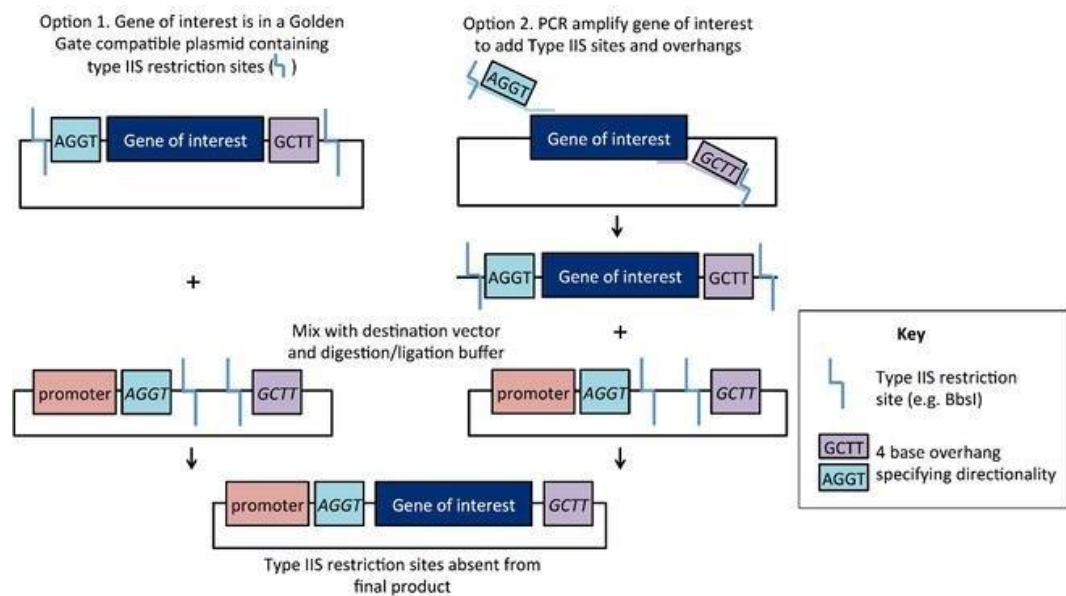


Figure 2.2: Schematic diagram of the mechanism for Golden Gate cloning using type IIS restriction enzymes to assemble DNA fragments (Gearing, 2015).

2.7 Homologous Recombination

The process of homologous genetic recombination is crucial for genetic diversity and genomic integrity. Homologous recombination allows genetic information to be exchanged between two similar molecules of single-stranded or double-stranded nucleic acids and it is widely used for repairing harmful breaks in DNA strands (National Human Genome Research Institute, 2014). One of the well-

known recombination in prokaryotes is the RecBCD pathway which constitutes two main components, RecA protein and RecBCD enzyme. The former involves in annealing of homolog DNA sequences and also branch migration, whereas the latter, also known as exonuclease V, is composed of three different polypeptides and are responsible for DNA unwinding and nuclease activity (Smith, 1987). This ability has been exploited by molecular biologists to be utilized for DNA cloning and now becomes an indispensable tool as compared to the traditional molecular cloning methods which produce linear vectors and inserts that are joined by DNA ligase.

This recombination-based cloning system offers the advantages of simplicity, flexibility and efficiency in direct cloning and subcloning, for instance a chosen DNA sequence can be cloned from a complex mixture without prior isolation (Zhang *et al.*, 2000). This approach does not require DNA ligase and restriction enzymes, as DNA fragments are to be assembled based on the flanking 15-60 bp long sequences that are homologous to the ends of the linearized vector generated by PCR amplification. The cloning reaction can take place *in vitro* by the enzymatic reactions of recombination between the inserts and the vector. Although the cloning approach by homologous recombination offers remarkable advantages over the conventional cloning method, it has not gained favour in a wider community of molecular biologists and relevant publications are scarce, probably due to the cost of the kit involved (Jacobus and Gross, 2015).

Recombineering is the homologous recombination mediated by phage-based recombination systems that include the RecE pathway and the Red pathway of λ phage. The former pathway involves two proteins of RecE and

RecT, whereas the latter is mediated by its Exo and Beta proteins. This technology enables linearized donor DNA to be targeted to circular recipient DNA using homologous sequences and it has been applied in modifying bacterial artificial chromosomes (BACs) due to its large size that hinders precise manipulation to introduce specific changes in DNA (Ellis *et al.*, 2001; Sawitzke *et al.*, 2007). As time passes, recombineering technology has evolved into a powerful tool in studying genetic functions and also contributing in genetic engineering (Narayanan *et al.*, 2009; Narayanan and Chen, 2011).

2.8 Reporter Genes

In molecular biology, researchers often utilize reporter genes to gain insight into vital processes in living organisms, such as growth regulation, differentiation, pathogenesis and carcinogenesis. These reporter genes encode proteins such enzymes and fluorescent molecules that can be measured swiftly and sensitively and assayed when they are being fused to regulatory region of a gene under study in bacteria, cell culture, animal tissues or plants (Lewis *et al.*, 1998; Li *et al.*, 2018). Reporter genes are generally used to study the strength of promoters, the efficiency of gene delivery system and translation initiation signals, to understand the intracellular fate of a gene product and also protein-protein interaction (Debnath, Prasad and Bisen, 2010).

2.8.1 Superfolder Green Fluorescent Protein (*sfGFP*)

In cell biology, fluorescent proteins serve as a versatile tool for allowing direct localization of target intracellular protein, measuring gene expression indirectly, studying protein-protein interactions or oligomeric states and acting as biosensors for cellular signalling (Scott *et al.*, 2018). A wild-type green fluorescent protein was discovered and first isolated from the jellyfish *Aequorea victoria* by Osamu Shimomura of Princeton University during his research on luminescence molecule, aequorin (Zou, 2014). This protein constitutes of 238 amino acids of which the amino acids at position 65th to 67th are responsible for the emission of visible green fluorescent light when exposed to the light spectrum ranged from blue to ultraviolet. GFP is a chromophore that can be formed spontaneously and does not require any additional co-factor, substrate or enzymatic activity except for the presence of oxygen during maturation. This unique feature allows the protein to be taken directly from *A. victoria* and being expressed in any other organism. GFP is non-toxic and could be fused to another protein without affecting its normal function, making it a better choice over those conventional fluorescent dyes (Goodsell, 2014). Researchers use GFP as a marker protein in various experimental studies for monitoring dynamic physiological processes, visualizing localization of proteins and detecting transgenic expression *in vivo* and other vast array of biochemical processes (Patrick, 2014).

When the full sequence of GFP was established, various versions of GFP were engineered through mutagenesis with the purpose to enhance its physical and biochemical properties such as fluorescence intensity and photostability of the protein. Some mutagenesis is designed to shift the major excitation peak,

improve the folding process of the protein and enhance the stability of protein structure (Patrick, 2014). For example, as the nucleotide and amino acid sequence are well understood, enhanced GFP (eGFP) was engineered by introducing mutations of F64L and S65T, that led to improved folding and spectral characteristics (Arpino, Rizkallah and Jones, 2012). GFP was also made to fluoresce with different colours by modifying the chromophore and gave rise to blue, cyan, yellow, red and others fluorescent proteins as shown in Figure 2.3.

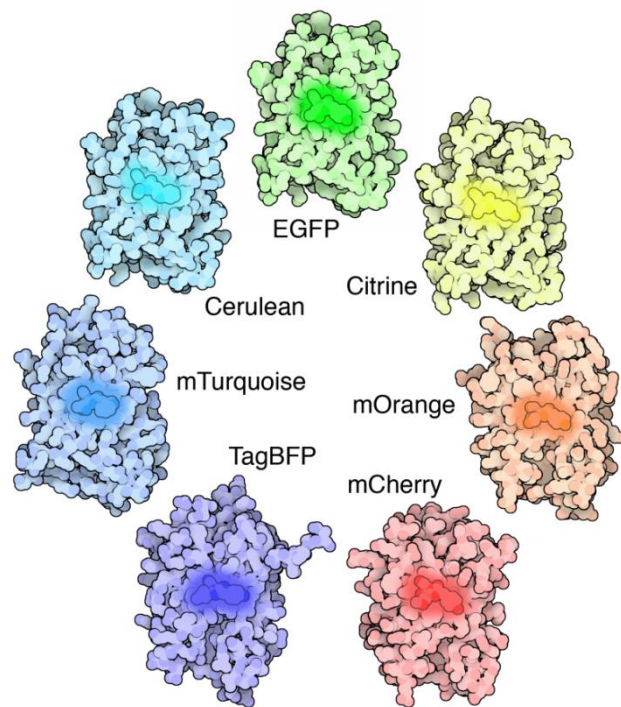


Figure 2.3: A palette of GFP-like proteins. Modifications were introduced into the amino acid code and chromophore to give rise to these monomeric marker proteins in vast array of applications (Goodsell, 2014).

Studies revealed that wild-type GFP folded poorly when GFP was being expressed in *E. coli*. Other variants of GFP with better folding properties are developed but when they were employed in protein fusion tagging, it was observed that the fused protein has reduced the folding yield and the

fluorescence intensity of these GFPs. Despite the efforts in enhancing the folding of GFP expressed alone, other variants did fold well and showed bright fluorescent only when the protein was expressed alone or when the protein was fused to well-folded proteins. To cope with this issue, a robustly folded version of GFP was developed by Pédelacq *et al.* (2006) and named this new construct as superfolder GFP (sfGFP).

Superfolder GFP is a novel GFP variant specially designed for *in vivo* high-throughput screening of protein expression levels with increased thermal stability and ability to retain its fluorescence intensity when fused to poorly folding proteins. The fluorescence of sfGFP is directly proportional to the total expression of the fusion protein, regardless the folding status or solubility of the fusion partner, turning sfGFP a strong reporter for investigating the expression of fusion protein. This fluorescent protein incorporates the red shift mutation S65T, the folding mutation F64L and six additional mutations to enhance its folding, S30R, Y39N, N105T, Y145F, I171V and A206V (Cotlet *et al.*, 2006). These mutations make the folding of GFP resistant to random mutation of which such mutation usually reduces the folding yield of GFP (Pédelacq *et al.*, 2006). With the improved properties of sfGFP, this GFP variant is the most widely used reporter gene in the studies of subcellular localization of periplasmic protein (Dinh and Bernhardt, 2011), development of biosensors, protein-protein interaction studies (Pédelacq and Cabantous, 2019) and fluorescence microscopy (Cotlet *et al.*, 2006).

CHAPTER 3

MATERIALS AND METHODS

This research project constitutes of three major parts: (i) construction of plasmid pYL101C, a constitutive, broad host range expression vector; (ii) construction of plasmid pYL102, a miniaturized Ti plasmid; and (iii) functionality test for both helper plasmids in *Agrobacterium*-mediated plant transformation.

3.1 Project Workflow

The general workflow for this project is illustrated in Figure 3.1. In brief, the project began with the construction of the first plasmid, pYL101C. Fragments with desired features were separately PCR-amplified and ligated to produce the recombinant expression vector, pYL101C. Once plasmid pYL101C was constructed, the *sfGFP* reporter gene was cloned in and the recombinant plasmid, pYL101C::*sfGFP* was tested for the functionality of the gene expression cassette and also the vector's host range across few Gram-negative bacteria. The construction of plasmid pYL102 started with the removal on T-DNA region on pCAMBIA5105, giving rise to an intermediate product, pYL102-P1 and subsequently followed by homologous recombination of long fragments, which were PCR-amplified from pYL102-P1. Simultaneously, key virulence gene, *virG*-N54D, was PCR-amplified and cloned into pYL101C, generating pYL101C::*virG*-N54D. Once both plasmids' constructions were completed,

they were tested as a whole plasmid system *in planta* to evaluate their effect on enhancing *Agrobacterium*-mediated plant transformation.

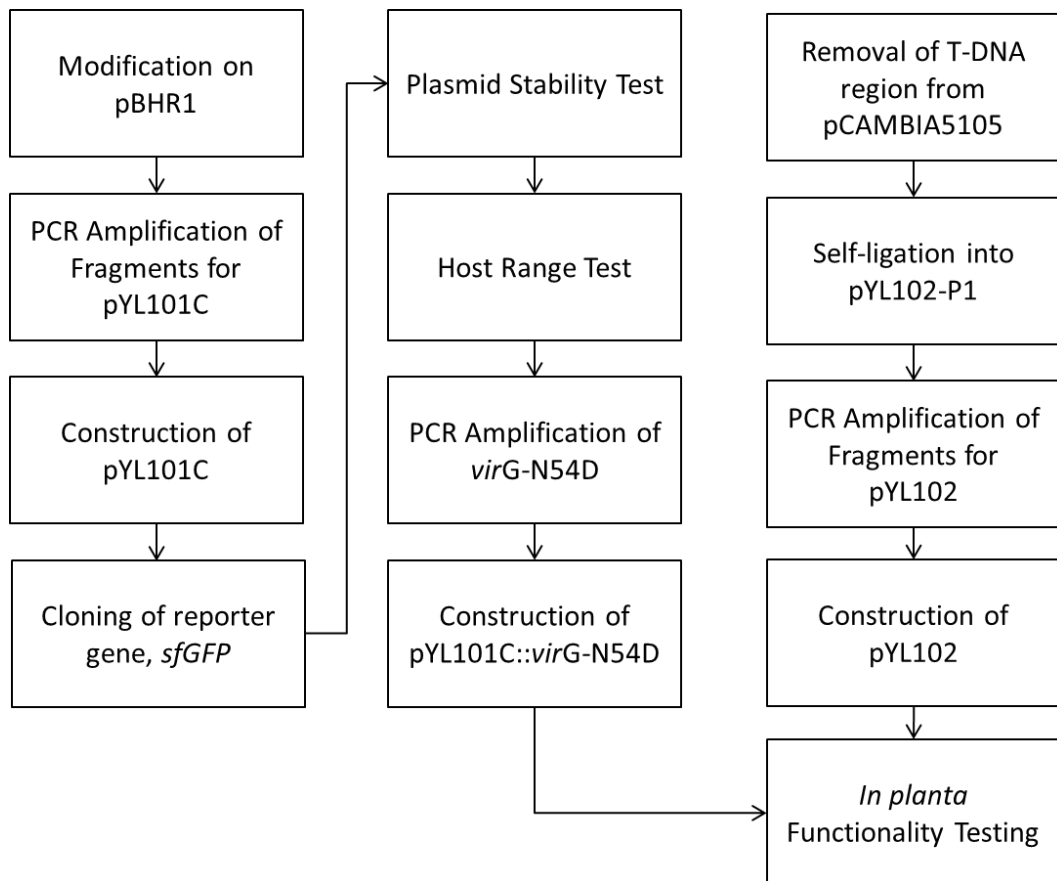


Figure 3.1: Overall workflow for the project.

3.2 Buffers, Media, Antibiotics, Bacterial Strains and Plant Used

The formulation for buffers and media used in this project were listed as in Table 3.1. All the buffers and media were topped up to the final volume of 1 L and then were autoclaved. The list of antibiotics and their working concentration was summarized in Table 3.2 and the antibiotic stock solutions were sterilized by filtration through 0.45 µm membrane. Table 3.3 shows the list of bacterial strains and plant model used in the study.

Table 3.1: List and formulation of buffers and media.

Buffer / Medium	Composition
10× TBE Buffer	54 g/L Tris-Base 27.5 g/L Boric Acid 20 mL/L 0.5 M EDTA (pH 8.0)
Agroinfiltration (AI) Buffer (pH 5.6)	10 mM MES 10 mM Magnesium Chloride (MgCl ₂) 150 µM acetosyringone (added after autoclaving)
TE Buffer	10 mM Tris-HCl (pH 8.0) 1 mM EDTA (pH 8.0)
2×YT Broth	16 g/L Tryptone 10 g/L Yeast Extract 5 g/L Sodium Chloride (NaCl)
2×YT Agar	16 g/L Tryptone 10 g/L Yeast Extract 5 g/L Sodium Chloride (NaCl) 15 g/L Agar

Table 3.2: List of stocks, working concentrations and solvents of antibiotics.

Antibiotics	Solvent	Stock concentration (mg/mL)	Working concentration (µg/mL)
Ampicillin	Distilled water	100	100
Chloramphenicol	Absolute ethanol	30	30
Gentamycin	Distilled water	50	50
Hygromycin	Distilled water	50	50
Kanamycin	Distilled water	50	50
Rifampicin	Dimethylsulfoxide	25	25
Spectinomycin	Distilled water	100	100
Streptomycin	Distilled water	50	50

Table 3.3: List of bacterial strains and plant used.

Bacterial Strain / Plant Model	Genotype / Description	Source/ Reference
<i>E. coli</i> TOP10	F ⁻ mcrA Δ (mrr-hsdRMS-mcrBC) ϕ 80lacZ Δ M15 Δ lacX74 recA1 araD139 Δ (ara-leu)7697 galU galK λ ⁻ rpsL(StrR) endA1 nupG	Invitrogen
<i>A. tumefaciens</i> C58	Wild type Nopaline type <i>A. tumefaciens</i>	ATCC 33970
<i>A. tumefaciens</i> C58C1	Plasmidless C58 derivative, Rif ^R	Koncz and Schell, 1986
<i>A. tumefaciens</i> LBA4404	Ach5 chromosomal background, Rif ^R	Hoekema <i>et al.</i> , 1983
<i>A. tumefaciens</i> GV3101	C58C1 Rif ^R pMP90 (pTiC58 Δ T-DNA) Gm ^R	Koncz and Schell, 1986
<i>Pantoea ananatis</i>	Isolated rice pathogen	Toh <i>et al.</i> , 2020
<i>Pantoea dispersa</i>	Isolated rice pathogen	Toh <i>et al.</i> , 2020
<i>Klebsiella pneumoniae</i>	A common Gram-negative human pathogen used in research and diagnostic	ATCC 13883
<i>Bacillus subtilis</i> 168	<i>trpC2</i>	Loh <i>et al.</i> , 2007
<i>Nicotiana benthamiana</i>	Used extensively as a model organism in research, especially plant-pathogen interactions	Wong <i>et al.</i> , 2007

3.3 General Methodology

The molecular cloning techniques and protocols mentioned in this section were performed routinely throughout the project.

3.3.1 Agarose Gel Electrophoresis

Agarose gel electrophoresis was used to separate and visualize DNA fragments for analysis. The concentration (w/v) of agarose gel varies according to the length (number of base pairs) of DNA fragments to be electrophoresed. Agarose gel with concentration of 0.8% to 1.0% was used for electrophoresing DNA samples with larger size, such as plasmid DNA, genomic DNA and long PCR

products and higher concentration was used for smaller DNA fragments. The electrophoresis was carried out at 100 V in 0.5× TBE buffer for 30 to 45 minutes, depending on the size of gel casted. The electrophoresed agarose gel was then post-stained with FloroSafe DNA Stain (1st Base, Singapore) and viewed under UV illumination using Bio-Rad Gel Imager (Bio-Rad, USA).

3.3.2 Plasmid Extraction and Purification

FavorPrep™ Plasmid Extraction Mini Kit (Favorgen Biotech Corporation, Taiwan) was used in extracting and purifying DNA plasmids from bacterial cells. The procedure of extraction was carried out according to the manufacturer's established protocol.

3.3.3 Agarose Gel Purification

FavorPrep™ GEL/ PCR Purification Kit (Favorgen Biotech Corporation, Taiwan) was used for the extraction of DNA fragments from agarose gel after electrophoresis. The purification was performed according the manufacturer's protocol.

3.3.4 PCR Product Purification by Ethanol Precipitation

A volume of 40 µL of 3 M sodium acetate was added to 200 µL of PCR products and subsequently an equal volume of ice-cold absolute isopropanol was added into the solution and kept at -80°C for 30 minutes. The mixture was then

centrifuged at 15000 rpm, 4°C for 25 minutes and the supernatant was discarded. The pellet was then washed with an equal volume of ice-cold 70% ethanol and the centrifugation step was repeated. The supernatant was discarded and the pellet was subjected to vacuum drying to remove the residual ethanol. A volume of 20 to 50 µL of pre-warmed elution buffer was used to dissolve the DNA pellet for subsequent work (OpenWetWare, 2007).

3.3.5 Measurement of DNA Concentration and Purity

After the DNA samples were obtained and purified, their concentration (ng/µL) and purity ($A_{280/260}$) were measured using NanoDrop 2000 UV-Vis Spectrophotometer (Thermo Fisher Scientific, USA).

3.3.6 DNA Amplification by Polymerase Chain Reaction

In this research, polymerase chain reaction (PCR) was extensively used for vector construction. General PCR amplification was used to amplify DNA fragments for cloning purpose whereas colony PCR amplification was adopted to verify putative recombinant clones. The components needed for the reaction mixture in both general and colony PCR amplification were listed in Table 3.4.

Table 3.4: Components of reaction mixture for PCR amplification.

General PCR Amplification		
Reagents	Volume Needed (in μL)	Final Concentration
5 \times Q5 Reaction Buffer	2.0	1 \times
10 mM 1st Base dNTP mix	0.1	100 μM
10 μM Forward Primer	0.2	0.2 μM
10 μM Reverse Primer	0.2	0.2 μM
Q5 High Fidelity DNA Polymerase	0.1	0.02 U/ μL
DNA Template	1.0	\sim 5.0 ng/ μL
Sterile Distilled Water	6.4	
Total	10.0	

Colony PCR Amplification		
Reagents	Volume Needed (in μL)	Final Concentration
10 \times Homemade <i>Taq</i> polymerase buffer	1.0	1 \times
10 mM 1st Base dNTP mix	0.1	100 μM
25 mM Magnesium sulphate (MgSO_4)	0.6	1.5 mM
10 μM Forward Primer	0.2	0.2 μM
10 μM Reverse Primer	0.2	0.2 μM
Homemade <i>Taq</i> DNA polymerase	0.2	0.2 U/ μL
Sterile Distilled Water	7.7	
Total	10.0	

3.3.6.1 General PCR Amplification

The reaction mixture was prepared based on Table 3.4. All the reagents and the mixture were kept cold prior to the amplification. DNA templates were added in last step and the PCR reaction mixture was gently mixed and subjected to a quick spin. A non-template control was included to ensure that the PCR reaction mixture was free from contamination. All the reaction mixtures were then subjected to standard thermocycling condition with slight alterations depending on the expected length of PCR products: 98°C for 30 seconds; followed by 30 cycles of 98°C for 5 seconds, 55°C to 60°C for 10 seconds and then 72°C for 60 seconds per 1 kb of amplicons; and subsequently 72°C for about 2 to 3 minutes as final extension prior to the holding temperature of 12°C. Agarose gel

electrophoresis was carried out to analyse the PCR products in reference to DNA ladder as mentioned in Section 3.3.1.

3.3.6.2 Colony PCR Amplification for Verifying Recombinant Clones

The reaction mixture for colony PCR was prepared accordingly based on Table 3.4. Single colonies from a transformant plate were picked using a sterilized toothpick and resuspended in the reaction mixture. The reaction mixtures were subjected to a quick spin prior to the amplification. A negative control was included and the amplification was carried out under the thermocycling conditions as followed: 95°C for 10 minutes; followed by 30 cycles of 95°C for 15 seconds, 55°C to 60°C for 15 seconds and then 72°C for 60 seconds per 1 kb of amplicons; and subsequently 72°C for about 2 to 3 minutes as final extension prior to the holding temperature of 12°C. The analysis of PCR products was performed using agarose gel electrophoresis as in Section 3.3.1 with the reference to DNA ladder.

3.3.7 Restriction Endonuclease (RE) Digestion

The RE digestions of DNA fragments were performed by incubating the reaction mixture at 37°C at various incubation time depending on the types of REs used. The components required for the digestion reaction were listed in Table 3.5.

Table 3.5: Components for general digestion reaction.

Reagents	Volume (in μL)
DNA Sample	1.0 (~1 $\mu\text{g}/\mu\text{L}$)
10 \times Reaction Buffer	2.0
Sterile Distilled Water	16.8
Restriction Enzyme	0.2 (5 U/ μL)
Total	20.0

3.3.8 Ligation of DNA Fragments

After RE digestion, DNA fragments were purified by ethanol precipitation as in Section 3.3.4. The purified DNA fragments were then put into a tube in their respective ratios. Two microliters of 10 \times T₄ DNA Ligase Buffer and one microliter of T₄ DNA Ligase were added to the tube and the mixture was topped up the final volume of 20 μL with nuclease-free water. The mixture was gently mixed by pipetting and incubated at 16 $^{\circ}\text{C}$ for at least 16 hours (New England Biolabs, 2020).

3.3.9 NEBuilder[®] HiFi DNA Assembly Cloning

DNA fragments flanked with respective homologous sequences were simultaneously assembled using NEBuilder[®] HiFi DNA Assembly Cloning Kit (New England Biolabs, USA). The cloning reaction was performed in a 20 μL volumes containing about 0.2 pmols of total DNA fragments, 10 μL of NEBuilder[®] HiFi DNA Assembly Master Mix and topped up to 20 μL by sterile distilled water. The reaction mixture was then incubated at 50 $^{\circ}\text{C}$ for 15 minutes before being transformed into chemically competent *E. coli* cells.

3.3.10 Preparation of Competent Cells

A single colony of *E. coli* TOP10 was inoculated into 5 mL of 2×YT broth supplemented with 100 µg/mL of streptomycin and incubated in a shaker incubator at 220 rpm, 37°C for overnight. In the case of *A. tumefaciens*, the bacterial suspension was cultured in 5 mL of 2×YT broth supplemented with 25 µg/mL at 28°C for 2 days.

To prepare electrocompetent cells, 500 µL of overnight bacterial culture was inoculated in 50 mL of 2×YT broth together with the respective antibiotics. The culture was then agitated at 220 rpm for about 2 to 3 hours with the initial value of OD₆₀₀ less than 0.1. When the OD₆₀₀ value achieved the reading within the range of 0.4 to 0.6, the culture was centrifuged at 3500 ×g, 4°C for 15 minutes. All the subsequent procedures were performed under cold condition. After centrifugation, the supernatant was discarded and 50 mL of ice-cold 10% glycerol (equal volume) was added to resuspend the pellet. The bacterial suspension was then centrifuged again and the protocol was repeated with 25 mL of ice-cold 10% glycerol (half volume) to resuspend the cell pellet. Centrifugation and pellet resuspension were repeated with 5 mL of ice-cold 10% glycerol (one-tenth volume). The resuspension was centrifuged again and the supernatant was discarded. The leftover cell pellet was resuspended with 600 µL of ice-cold 10% glycerol and the competent cells were aliquoted in 12 chilled microcentrifuge tubes, each containing 50 µL and they were kept at -80°C for future use.

As for chemically competent cells, the preparation procedure was similar until the step of the first centrifugation. After the supernatant was discarded, 1

to 1.5 mL of ice-cold calcium chloride (CaCl₂) solution was added and the pellet was resuspended and incubated on ice for an hour. The competent cells were ready for transformation process after an hour incubation.

3.3.11 Bacterial Transformation via Electroporation

An amount of 1 µL of plasmid DNA was added to 50 µL electrocompetent cells and the reaction mixture was incubated on ice for five minutes. After incubation, the reaction mixture was transferred into electroporation cuvette (Bio-Rad, USA) and electric current of 2.5 V was applied via MicroPulser Electroporator (Bio-Rad, USA). A volume of 500 µL pre-warmed 2×YT broth was added into the cells and the resuspension was incubated at optimum temperature, 220 rpm for an hour. The culture was centrifuged at 8000 rpm for two minutes and the pellet was resuspended with 200 µL supernatant. Fifty microliters of the resuspension was plated onto 2×YT agar plates supplemented with respective antibiotics.

3.3.12 Bacterial Transformation via Heat Shock Method

Plasmids or ligated products were added into *E. coli* competent cells prepared in Section 3.3.9.1 and the reaction mixture was incubated in ice for 40 minutes. The tube was tapped gently at every 10-minute interval and the reaction mixture was subjected to transient heat shock at 42°C for 90 seconds. The reaction tube was immediately placed in ice after the heat shock for five minutes. A volume of 500 µL 2×YT broth was added into the reaction mixture and the culture was then incubated at 37°C with agitation of 220 rpm for an hour. After the incubation,

the culture suspension was subjected to centrifugation at 8000 rpm for two minutes and the pellet was resuspended with 200 μ L of supernatant. A volume of 50 μ L transformed cells were then plated onto 2 \times YT agar plates supplemented with respective antibiotics.

3.3.13 DNA Sequencing

The constructed plasmids and amplified DNA fragments were outsourced to Apical Scientific Sdn. Bhd. for DNA sequencing. The sequencing result were aligned with the expected sequences using Basic Alignment Search Tool (BLAST), which uses a heuristic approach that approximates the Smith-Waterman algorithm and is available on the National Centre for Biotechnology Information website (<https://blast.ncbi.nlm.nih.gov/Blast.cgi>).

3.3.14 Agroinfiltration on *Nicotiana benthamiana*

A. tumefaciens harbouring desired plasmids were cultured in 2 \times YT broth supplemented with appropriate antibiotics and incubated at 28°C for 2 days. A total of 2 mL of bacterial culture was then added to a fresh 20 mL 2 \times YT broth and cultured at 28°C with agitation of 220 rpm until its OD₆₀₀ value reached approximately 0.8. The bacterial culture was harvested and subjected to centrifugation at 3000 \times g for 10 minutes at room temperature. After centrifugation, the supernatant was discarded, and the cell pellet was re-suspended with equal volume of Agroinfiltration (AI) buffer. The bacterial suspension was then centrifuged at 3000 \times g for another 10 minutes at room

temperature for washing purpose. The supernatant was discarded and the pellet was re-suspended with AI buffer to achieve the OD₆₀₀ value of about 0.8. The bacterial suspension was incubated at 22°C in dark condition for two hours prior to the infiltration. The first, second and third fully expanded leaves of 6-week old *N. benthamiana* were chosen and their dorsal sides were infiltrated with desired bacterial suspension using 1 mL needleless syringe. The infiltrated plants were kept in plant growth chamber at 22°C under 16 hours/ 8 hours of light/ dark cycle until further analysis (Toh, 2017).

3.4 Construction of BHR Expression Vector pYL101C

Construction of the broad host range expression vector, pYL101C began with PCR amplification of six different fragments, as illustrated in Figure 3.1, consisting key features such as a strong constitutive *P_{INTc}*-driven gene expression cassette, a Gm^R selectable marker, a ColE1 origin of replication and a pBBR1 origin of replication. Six different pairs of primer (Appendix A) were used to amplify the key features as described in Section 3.3.6.1. Fragment A (ColE1 replicon and Gm^R) was PCR-amplified with primer pair F-ColE1 and R-rnbTer using annealing temperature of 58°C whereas Fragment B (broad-host-range pBBR1 replicon) was amplified with primer pair F-oriV and R-oriV using annealing temperature of 60°C. Simultaneously, Fragment C (*P_{INTc}*) and Fragment D (*T7* terminator) were separately PCR-amplified using primer pairs F-pINTc with R-pINTc and F-T7ter with R-T7ter, respectively, at their respective annealing temperature of 50°C and 60°C. Fragment D (*lacI* gene) was PCR-amplified using primer pair F-lacI and R-lacI which annealed at 61°C. As

for the multiple cloning site (MCS), two long oligonucleotides, F-MCS and R-MCS were used for overlap PCR to give rise to the polylinker sequence.

All the PCR products were electrophoresed for analysis in reference to the 100 bp and 1 kb DNA ladders as described in Section 3.3.1 and measured for their respective concentrations and purities. Subsequently, they were subjected to purification prior to RE digestion of *AarI* and *Esp3I* as mentioned in Section 3.3.7. Digested product of six fragments were then purified and ligated as described in Section 3.3.8. Ligated product was used to transform *E. coli* TOP10 competent cells via heat shock as in Section 3.3.12. Transformants were plated onto 2×YT agar supplemented with 50 µg/mL gentamycin and incubated at 37°C for overnight. Putative clones were screened by colony PCR and positive clones were sent out for DNA sequence verification.

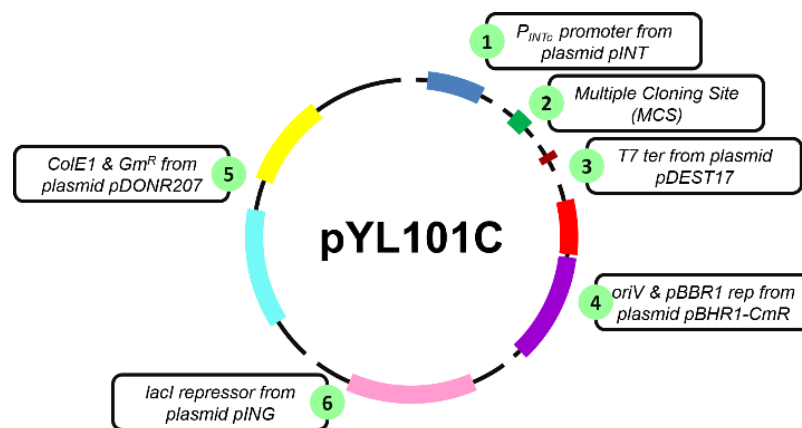


Figure 3.2: Six fragments to be assembled into pYL101C from different sources.

3.5 Construction of Plasmid pYL101C::*sfGFP*

3.5.1 Molecular Cloning of *sfGFP* into pYL101C

The superfolder green fluorescence (*sfGFP*) reporter gene was PCR-amplified using primer pair F-*sfGFP* and R-*sfGFP* (Appendix A) as described in Section 3.3.6.1 with the annealing temperature of 58°C. The *sfGFP* amplicons were electrophoresed and subsequently purified as described in Section 3.3.4 prior to cloning into pYL101C. The purified *sfGFP* fragments and pYL101C were double digested with *Bsa*I and *Sal*II, and *Not*I and *Sal*II, respectively, as described in Section 3.3.7. Digested fragments were subjected to DNA ligation (Section 3.3.8) and ligated product was used to transform *E. coli* TOP10 competent cells as described in Section 3.3.12. Transformants were plated onto 2×YT agar supplemented with 50 µg/mL gentamycin and incubated at 37°C for overnight. Putative transformants were selected after viewing under blue light (470nm) using Invitrogen S37102 Safe Imager 2.0 Blue Light Transilluminator (Thermo Fisher Scientific, USA) and the recombinant plasmid pYL101C::*sfGFP* was extracted from the colonies as described in Section 3.3.2. Subsequently, the plasmid was subjected to DNA concentration and purity measurement (Section 3.3.5) prior to restriction enzyme analysis using *Xba*I and *Sac*I (Section 3.3.7).

3.5.2 Plasmid Stability and Host Range Testing for pYL101C::*sfGFP*

Electrocompetent *E. coli* cells were transformed using the recombinant pYL101C::*sfGFP* and positive transformants showing strong green fluorescence were selected and sub-cultured onto both selective (2×YT agar supplemented with 50 µg/mL gentamycin) and non-selective media (2×YT agar with no

antibiotic) for four consecutive passages (adapted from Anand *et al.*, 2018). For bacterial host range testing, plasmid pYL101C::*sfGFP* was first used to transform *A. tumefaciens* strain C58 and LBA4404, and subsequently extended the test to *P. ananatis*, *P. dispersa*, *K. pneumonia* and *B. subtilis* 168 via electroporation as described in Section 3.3.11. Transformants of these Gram-negative bacteria were plated onto 2×YT agar supplemented with 50 µg/mL gentamycin. Transformants of *Agrobacterium* and *Pantoea* were incubated at 28°C for two days whereas *Klebsiella* transformants were incubated at 37°C for overnight. Putative clones were screened with blue light illumination (470 nm).

3.6 Construction and Functionality Test of Plasmid pYL101C::*virG*-N54D

Key regulatory gene for *Agrobacterium*-mediated transformation, *virG*-N54D, was PCR-amplified using primer pair F-*virG* and R-*virG* (Appendix A) using the annealing temperature of 60°C as described in Section 3.3.6.1. The *virG*-N54D amplicons were electrophoresed and subsequently purified as mentioned in Section 3.3.4. The purified fragments were then measured for its concentration and purity and then being double digested using *BsaI* and *SalI* for cloning purpose. Plasmid pYL101C was linearized by double digestion with *NotI* and *SalI* and both fragments were ligated as described in Section 3.3.8.

The ligated product was used to transform *E. coli* TOP10 competent cells via heat shock transformation (Section 3.3.12) and transformants were selected on 2×YT agar supplemented with 50 µg/mL gentamycin. Colony PCR was carried

out to eliminate non-transformants (Section 3.3.6.2) and the putative clones were sent out for DNA sequencing.

3.6.1 Total RNA Extraction from *Agrobacterium* harbouring pYL101C::*virG*-N54D

Once the sequence was verified, plasmid pYL101C::*virG*-N54D was extracted from *E. coli* cells and was then electroporated into *A. tumefaciens* C58C1. Three millilitres of bacterial culture in 2×YT broth was prepared for the positive transformant of *A. tumefaciens* C58C1 harbouring pYL101C::*virG*-N54D and the plasmidless *A. tumefaciens* C58C1, respectively, and incubated at 28°C with agitation of 220 rpm for two days. The bacterial cultures were subjected to total RNA extraction using TRIzol™ Reagent. The total RNA isolation from the bacterial cell was carried out according to the manufacturer's established protocol.

3.6.2 Removal of DNA from Extracted RNA sample using DNase I

Extracted RNA samples from *A. tumefaciens* C58C1 and *A. tumefaciens* C58C1 harbouring pYL101C::*virG*-N54D were subjected to DNase I digestion to remove residual DNA. A volume of 10 µL reaction mixture consisting of 1 U of DNase I (Thermo Fisher Scientific, USA), 1× Reaction Buffer with MgCl₂, about 1 µg of RNA sample and sterile distilled water was prepared and incubated at 37°C for 30 minutes. To stop the DNase I activity, 1 µL of 50 mM EDTA was added into the reaction mixture and incubated at 65°C for 10 minutes.

3.6.3 Reverse Transcription for mRNA of *virG-N54D*

DNase I-treated RNA samples were used as template for cDNA synthesis and PCR amplification of the desired gene, *virG-N54D*. The components required for RT-PCR (New England Biolabs, USA), including the non-template control and no-RT negative control, are listed in Table 3.6.

Table 3.6: Components of reaction mixture for RT-PCR.

Non-Template Control		
Reagents	Volume Needed (in μL)	Final Concentration
2 \times <i>OneTaq</i> One-Step Reaction Mix	5.0	1 \times
25 \times <i>OneTaq</i> One-Step Enzyme Mix	0.4	1 \times
10 μM Forward Primer (F- <i>virG-N54D</i>)	0.4	0.4 μM
10 μM Reverse Primer (R- <i>virG-N54D</i>)	0.4	0.4 μM
Nuclease-free Water	3.8	
Total	10.0	

Standard RT-PCR		
Reagents	Volume Needed (in μL)	Final Concentration
2 \times <i>OneTaq</i> One-Step Reaction Mix	5.0	1 \times
25 \times <i>OneTaq</i> One-Step Enzyme Mix	0.4	1 \times
10 μM Forward Primer (F- <i>virG-N54D</i>)	0.4	0.4 μM
10 μM Reverse Primer (R- <i>virG-N54D</i>)	0.4	0.4 μM
Total RNA	1.0	$\sim 1\mu\text{g}/\mu\text{L}$
Nuclease-free Water	2.8	
Total	10.0	

No-RT Negative Control		
Reagents	Volume Needed (in μL)	Final Concentration
2 \times <i>OneTaq</i> One-Step Reaction Mix	5.0	1 \times
10 μM Forward Primer (F- <i>virG-N54D</i>)	0.4	0.4 μM
10 μM Reverse Primer (R- <i>virG-N54D</i>)	0.4	0.4 μM
TaKaRa PrimeSTAR GXL Polymerase	0.2	0.25 U
Total RNA	1.0	$\sim 1\mu\text{g}/\mu\text{L}$
Nuclease-free Water	3.0	
Total	10.0	

Reaction mixtures for RT-PCR, including the non-template control and no-RT negative control, were prepared based on Table 3.6. RNA templates were added in last step and the PCR reaction mixture was gently mixed and subjected

to a quick spin in order to allow all the liquid to be slid down from the wall of tube. The reverse transcription of RNA into cDNA transcript took place at 48°C for 30 minutes and was followed by standard thermocycling conditions for amplification: initial denaturation at 94°C for one minute; followed by 40 cycles of 94°C for 15 seconds, 60°C for 30 seconds and then 68°C for 60 seconds per 1 kb of amplicons; subsequently 68°C for five minutes as final extension prior to the holding temperature of 4°C. Agarose gel electrophoresis was carried out to analyse the PCR products in reference to DNA ladder as mentioned in Section 3.3.1.

3.7 Construction of Miniaturized Ti plasmid pYL102

The miniaturized Ti plasmid pYL102 was constructed by using pCAMBIA5105 as template. Plasmid pYL102-P1 was developed as intermediate product after RE digestion on pCAMBIA5105 and was subsequently served as backbone template for long PCR amplification in order to generate three fragments. Plasmid pYL102 was constructed by assembled these three fragments and verified by restriction enzyme analysis.

3.7.1 Construction of pYL102-P1

Binary vector pCAMBIA5105 was subjected to *Mau*BI RE digestion in order to remove its T-DNA region. The reaction was carried out as mentioned in Section 3.3.7 and incubated for one to two hours. Digested products were subsequently purified and subjected to self-ligation as described in Section 3.3.8, generating

the intermediate product, pYL102-P1. The ligated product was digested with *Sbf*I to cleave intact pCAMBIA5105 prior to the transformation into *E. coli* TOP10 competent cells as mentioned in Section 3.3.12. Transformants were plated on 2×YT agar supplemented with 50 µg/mL kanamycin and 100 µg/mL spectinomycin and incubated at 37°C for overnight. The resultant plasmid, pYL102-P1 was verified by extracting the plasmid (Section 3.3.2) from putative transformants and digesting it with *Eco*RI (Section 3.3.7).

3.7.2 Long PCR Amplification of pYL102

The intermediate construct pYL102-P1 served as template DNA for pYL102 by PCR amplification. Three fragments, designated as Fragment I, Fragment II and Fragment III, were amplified using primer pairs F-102-F1 with R-102-F1, F-102-F2 with R-102-F2 and F-102-F3 with R-102-F3 (Appendix A), respectively, as described in Section 3.3.6.1. Fragment I and II were amplified using two-step PCR protocol in which the annealing step was omitted, whereas Fragment III was amplified by three-step PCR using annealing temperature of 58°C. PCR amplicons of three fragments were subjected to agarose gel electrophoresis (Section 3.3.1) for preliminary verification prior to assembly.

3.7.3 Assembly of pYL102 Fragments and Verification of pYL102

Three fragments of pYL102 were purified as described in Section 3.3.4 and assembled using the NEBuilder® HiFi DNA Assembly Cloning Kit as described in Section 3.3.9. The assembled DNA molecules were used to transform *E. coli*

TOP10 competent cells via heat shock transformation (Section 3.3.12). Transformants were plated on 2×YT agar plate supplemented with 100 µg/mL spectinomycin and incubated at 37°C for overnight. Putative clones were tested for kanamycin susceptibility by performing replica plating on 2×YT agar plate supplemented with 50 µg/mL kanamycin. The selected colony was first inoculated using a sterile toothpick onto a 2×YT agar plate supplemented with 50 µg/mL spectinomycin and subsequently the same toothpick was used to inoculate onto a 2×YT agar plate supplemented with 50 µg/mL kanamycin. Plasmids were extracted from positive clones that are susceptible to kanamycin and were then subjected to restriction digestion analysis using *EcoRI*. The digested products were electrophoresed and the band pattern was compared with those of *EcoRI*-digested pCAMBIA5105.

3.8 *In planta* Functionality Testing using *N. benthamiana* via Agroinfiltration

To test the functionality of the constructed vector system, *A. tumefaciens* strain C58C1 was transformed with different combinations of vectors. The bacterial culture was prepared as electrocompetent cells (Section 3.3.11) and the constructed pYL101C::*virG*-N54D and pYL102 were electroporated together with a plant reporter vector, pGWB2::*e35S-sfGFP*, which confers resistance to kanamycin and hygromycin. The following plasmid combinations were also separately electroporated into *A. tumefaciens* C58C1 electrocompetent cells (Section 3.3.11) for vector functionality evaluation: pYL101C::*virG*-N54D with pYL102; pYL101C::*virG*-N54D with pGWB2::*e35S-sfGFP*; and pYL102 with

pGWB2::*e35S-sfGFP*. In addition, *A. tumefaciens* GV3101::pMP90 was transformed with pGWB2::*e35S-sfGFP* to serve as a positive control in agroinfiltration, whereas plasmidless *A. tumefaciens* C58C1 acted as a negative control in agroinfiltration. Prior to the agroinfiltration, these *Agrobacterium* transformants were verified by plasmid extraction and colony PCR. Six different *Agrobacterium* suspensions harbouring different plasmid combinations were then infiltrated into *N. benthamiana* leaves, as described in 3.3.14. The infiltrated spots were excised from the leaves at 48-hour post-infiltration by using a 13 mm cork borer. The excised leaf disks were viewed under blue light at magnification of 400× using Olympus BX41 Fluorescence Microscope (Olympus, Japan). The excised leaf disks were then subjected to homogenization with the addition of 1 mL of sterile distilled water. The homogenized leaf extracts were then centrifuged to obtain the supernatant which would be used subsequently for quantification of relative fluorescence intensity. A total of 200 µL supernatant of each leaf extract was loaded into 96 well-plate and the fluorescence intensity was determined with excitation at 475 nm and emission at 509 nm using FLUOstar Omega Microplate Reader (BMG LABTECH, Germany).

CHAPTER 4

RESULTS

The ultimate aim of this project was to develop a BHR expression vector for expressing key regulatory virulence gene, *virG-N54D*, and a miniaturized helper tumour-inducing (Ti) plasmid, pYL102, in order to be used as an alternative vector system in *Agrobacterium*-mediated plant transformation. In this chapter, Section 4.1 describes the results obtained for constructing broad host range expression vector, pYL101C with constitutive expression system. Section 4.2 describes the results obtained for construction of recombinant reporter vector, pYL101C::*sfGFP* and its host range test. The result for construction of a miniaturized helper Ti plasmid, pYL102 is elaborated in Section 4.3 whereas Section 4.4 describes the outcome of the *in planta* functionality test on the constructed plasmid system.

4.1 Construction of Broad Host Range Expression Vector

The construction of BHR expression vector pYL101C involved PCR amplification, restriction endonuclease digestion and DNA ligation of six fragments consisting key features. Golden Gate cloning approach was used in assembling these fragments to generate pYL101C.

4.1.1 PCR Amplification of Fragments for pYL101C

Five fragments, namely P_{INTc} promoter, *lacI* operon, T7 transcriptional terminator, BHR1 replicon and ColE1 replicon together with Gm^R selectable marker, were separately amplified from their plasmid templates of pING, pDEST17, pBHR1-CmR and pDONR207, respectively. Plasmid pBHR1-CmR was derived from plasmid pBHR1 with the removal of *aph(3')-Ia* gene which confers resistance to kanamycin via *SbfI* digestion. Figure 4.1 illustrates the fragments to be PCR-amplified and how they were assembled to give rise to pYL101C.

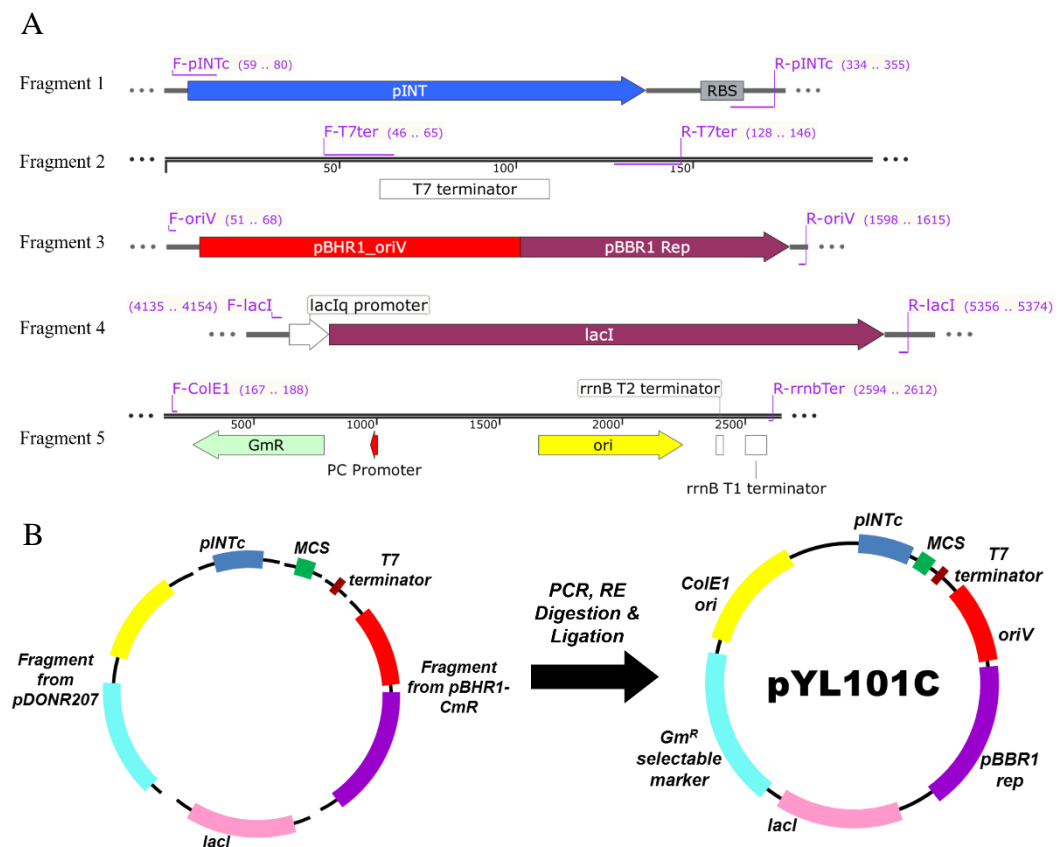


Figure 4.1: Schematic representation of the construction of BHR expression vector, pYL101C. (A) Schematic diagram of fragments to be assembled into pYL101C via Golden Gate Cloning. (B) Strategy in constructing pYL101C.

Two long oligonucleotides, namely F-MCS and R-MCS, were used in overlapping PCR in order to generate fragment of multiple cloning site (MCS). All PCR-amplified fragments were either flanked by *AarI* or *Esp3I* recognition and restriction sites. Gel electrophoresis was performed for preliminary screening of PCR amplicons prior to Golden Gate cloning. Figure 4.2 shows image of gel electrophoresis for P_{INTc} promoter PCR amplicons with the size of ~300 bp, indicating the strong constitutive integron promoter with the length of 320 bp was successfully amplified. Figure 4.3 shows image of gel electrophoresis for *T7* terminator PCR amplicons and a band with the size of ~125 bp was observed, indicating the transcriptional terminator of 127 bp was obtained. Figures 4.4 and 4.5 depict the images of gel electrophoresis for *lacI* amplicon and ColE1-Gm^R amplicon, respectively. A band with the size of ~1300 bp was observed for *lacI* amplicons, indicating that the regulatory operon fragment was successfully amplified. As for ColE1-Gm^R fragment, a band size of ~2500 bp was observed, signifying the high-copy-number replicon and the selectable marker with the length of 2479 bp were obtained. Figure 4.6 shows image of gel electrophoresis for pBHR1 oriV fragment with the size of ~1500 bp, indicating that the BHR replicon with length of 1599 bp was successfully amplified. Figure 4.7 depicts the image of gel electrophoresis for MCS fragment with the size of ~75 bp, signifying the MCS fragment consisting restriction sites for *NotI*, *XbaI*, *Sall*, *SpeI* and *PmeI*, with the length of 76 bp was successfully constructed.

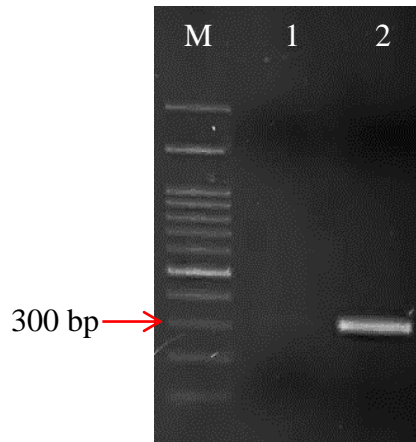


Figure 4.2: Gel electrophoresis of *P_{INTc}* promoter in 1.2% agarose gel at 100 V for 40 minutes. Lane M represents the 100 bp DNA ladder (GeneDireX, USA) whereas Lanes 1 and 2 represent PCR negative control and *P_{INTc}* amplicons, respectively.

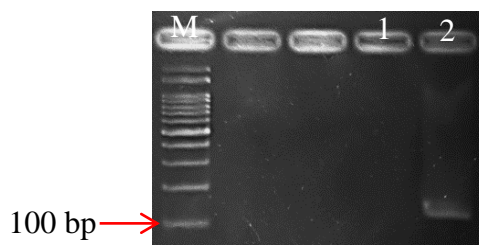


Figure 4.3: Gel electrophoresis of *T7* terminator in 1.5% agarose gel at 100 V for 40 minutes. Lane M represents the 100 bp DNA ladder (Thermo Fisher Scientific, USA) whereas Lanes 1 and 2 represent PCR negative control and *T7* fragment, respectively.

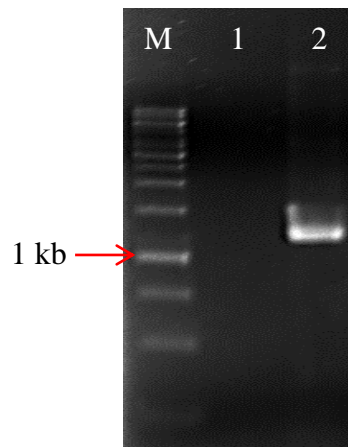


Figure 4.4: Gel electrophoresis of *lacI* operon in 1.2% agarose gel at 100 V for 40 minutes. Lane M represents the 1 kb DNA ladder (Thermo Fisher Scientific, USA) whereas Lanes 1 and 2 represent PCR negative control and *lacI* fragment, respectively.

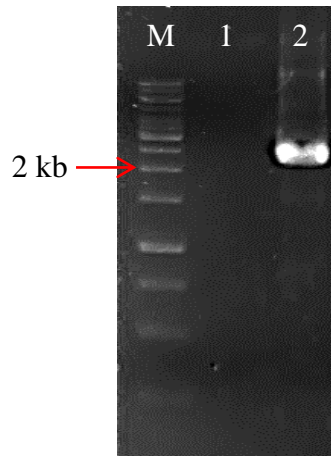


Figure 4.5: Gel electrophoresis of ColE1-Gm^R amplicons in 1.2% agarose gel at 100 V for 40 minutes. Lane M represents the 1 kb DNA ladder (Thermo Fisher Scientific, USA) whereas Lanes 1 and 2 represent PCR negative control and ColE1-Gm^R fragment, respectively.

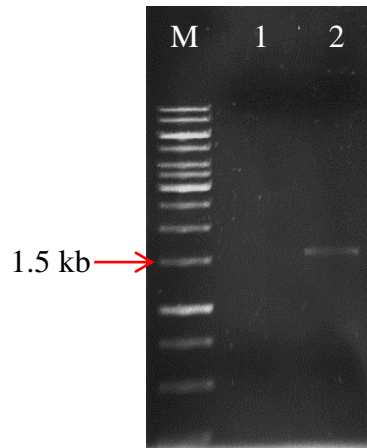


Figure 4.6: Gel electrophoresis of BHR1 oriV amplicons in 1.2% agarose gel at 100 V for 40 minutes. Lane M represents the 1 kb DNA ladder (Thermo Fisher Scientific, USA) whereas Lanes 1 and 2 represent PCR negative control and oriV fragment, respectively.

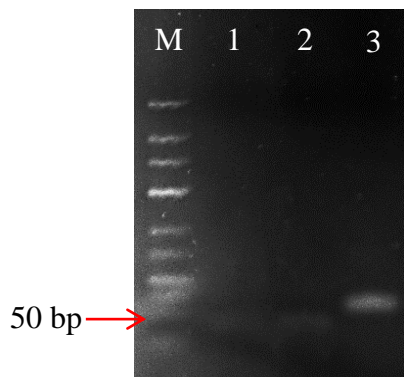


Figure 4.7: Gel electrophoresis of MCS fragment in 3% agarose gel at 100 V for 50 minutes. Lane M represents 50 bp DNA ladder whereas Lanes 1, 2 and 3 represent PCR negative controls with only forward and reverse primers, and MCS fragment, respectively.

4.1.2 Verification of pYL101C

The constructed pYL101C was then verified by colony PCR and subsequently *Kpn*I digestion as *Kpn*I is a unique cutter for pYL101C. A single band of ~6 kb was observed in two putative plasmids extracted from positive clones, indicating the 5958-bp BHR expression vector was successfully constructed, as shown in Figures 4.8 and 4.9, respectively. The plasmid was subsequently sent out for sequencing and the result showed 100% identity to the expected sequence.

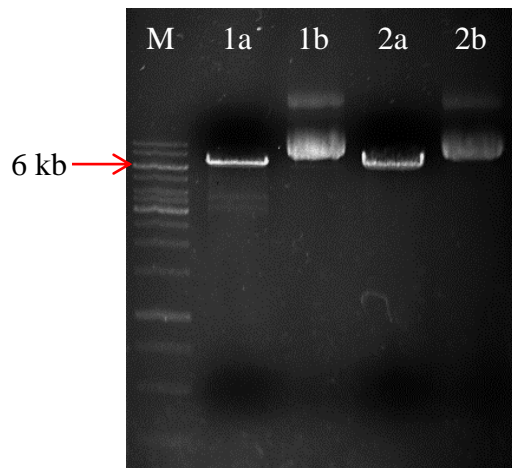


Figure 4.8: Gel electrophoresis of *Kpn*I-digested pYL101C in 1.0% agarose gel at 100 V for 40 minutes. Lane M represents the 1 kb DNA ladder (Thermo Fisher Scientific, USA). Lanes 1a and 1b represent the *Kpn*I-digested and undigested pYL101C from Clone 1, respectively whereas Lanes 2a and 2b represent the *Kpn*I-digested and undigested pYL101C from Clone 2, respectively.

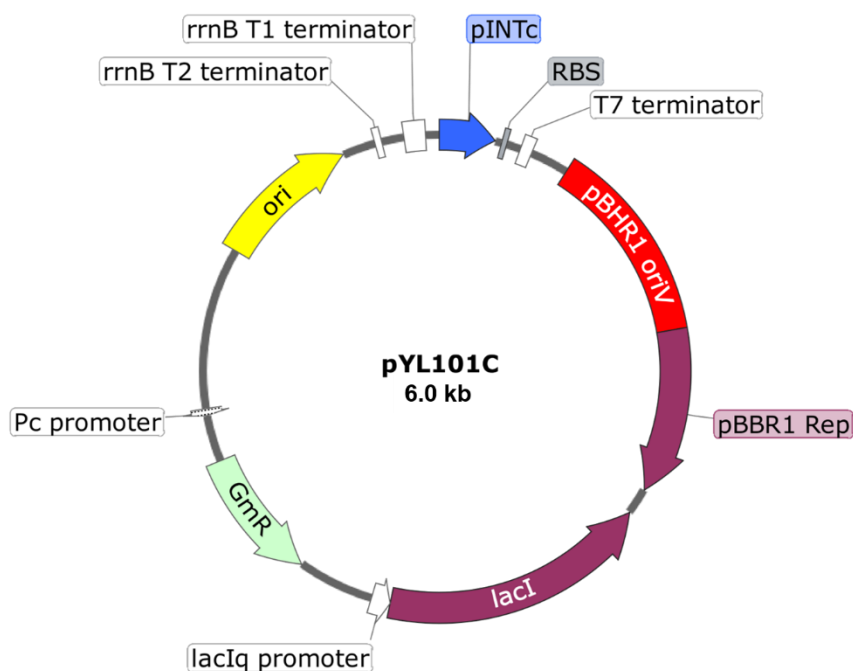


Figure 4.9: Schematic diagram of plasmid map for the broad host range expression vector, pYL101C.

4.2 Molecular Cloning of pYL101C::*sfGFP* and Host Range Testing

4.2.1 PCR Amplification and Cloning of *sfGFP* Reporter Gene

The superfolder green fluorescence protein (*sfGFP*) gene was amplified from plasmid pE35S-*sfGFP* using conventional PCR approach. Figure 4.10 illustrates the strategy of the molecular cloning of *sfGFP* gene into the constructed expression vector, pYL101C. The PCR amplicons with the length of 752 bp were flanked with *Bsa*I and *Sal*I recognition and restriction sites at the 5' - and 3' - end, respectively. Figure 4.11 shows the image of gel electrophoresis for the purified *sfGFP* fragments prior to the cloning. A single band with the size of approximately 750 bp was observed in the electrophoresed agarose gel. The resultant plasmid, pYL101C::*sfGFP* was preliminarily screened by colony PCR and subsequently subjected to *Xba*I and *Sac*I double digestion for verification

and gave rise to two fragments with the size of 5873 bp and 808 bp, respectively (Figure 4.12).

4.2.2 Host Range Testing of pYL101C::sfGFP

Recombinant plasmid, pYL101C::sfGFP, as depicted in Figure 4.13, was used to transform numerous Gram-negative bacteria, namely *E.coli*, *A. tumefaciens*, *K. pneumoniae* and *Pantoea* sp. via electroporation. Positive transformants with strong green fluorescence emission under blue light were obtained for all the tested bacteria, except for *B. subtilis* 168. No colony was observed to grow when the Gram-positive *B. subtilis* 168 was transformed with pYL101C::sfGFP. Figure 4.14 shows visualization of the green fluorescence for each Gram-negative bacterium harbouring pYL101C::sfGFP under the excitation of blue light at 470 nm.

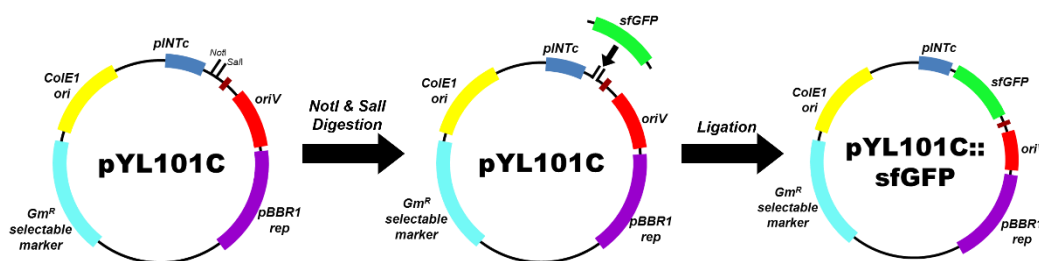


Figure 4.10: Schematic diagram on the construction of pYL101C::sfGFP. The linearized pYL101C was ligated to the *BsaI-Sall*-double digested *sfGFP* fragments to give rise to recombinant pYL101C::sfGFP.

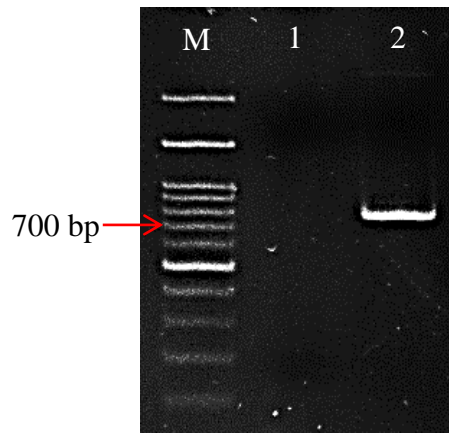


Figure 4.11: Gel electrophoresis of PCR-amplified *sfGFP* fragment after purified in 1.2% agarose at 100 V for 40 minutes. Lane M represents the 100 bp DNA ladder (GeneDireX, USA) whereas Lanes 1 and 2 represent PCR negative control and purified *sfGFP* fragments, respectively.

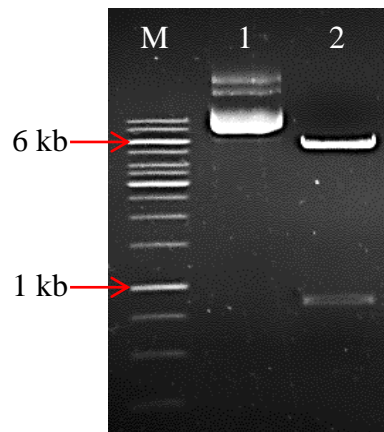


Figure 4.12: Gel electrophoresis of recombinant pYL101C::*sfGFP* after double digestion of *Xba*I and *Sac*I in 1.0% agarose gel at 100 V for 40 minutes. Lane M represents the 1 kb DNA ladder (Vivantis, Malaysia) whereas Lanes 1 and 2 represent undigested and digested pYL101C::*sfGFP*, respectively.

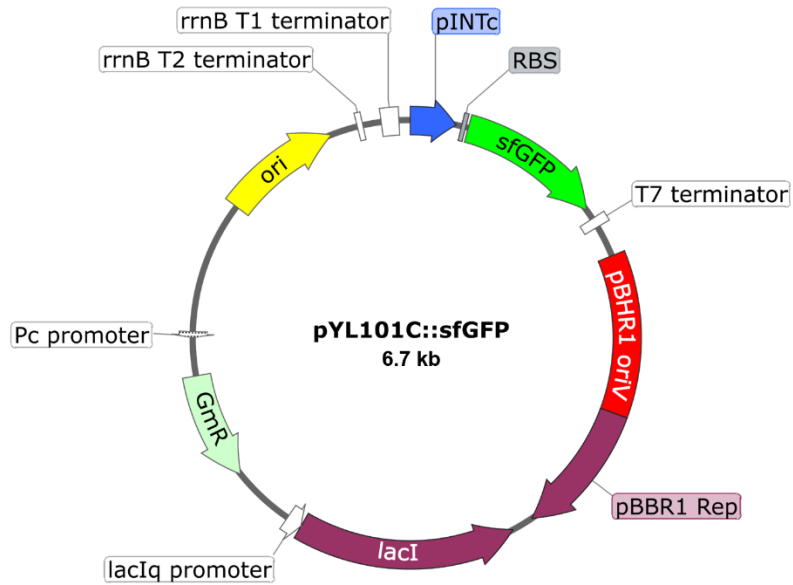


Figure 4.13: Schematic diagram of the complete plasmid map for the 6.7 kb pYL101C::sfGFP.

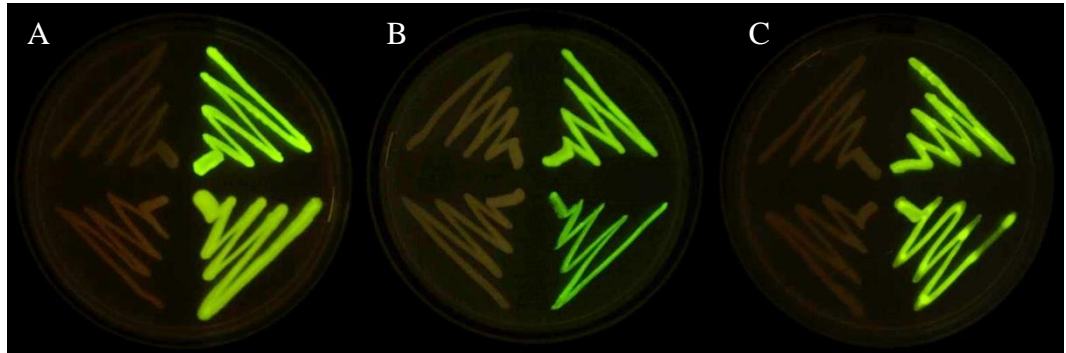


Figure 4.14: Visualization of the expressed sfGFP in various Gram-negative bacterial hosts harbouring the recombinant pYL101C::sfGFP, under blue light excitation. The plate image shows the visualization of sfGFP fluorescence of the bacteria transformed with pYL101C empty vector (left) and pYL101C::sfGFP (right), including (A) *E. coli* TOP10 strain (top), *K. pneumoniae* (bottom), (B) *A. tumefaciens* C58 strain (top), *A. tumefaciens* LBA4404 (bottom), (C) *P. ananatis* (top) and *P. dispersa* (bottom).

4.2.3 Plasmid Stability Test for pYL101C::sfGFP

Plasmid pYL101C::sfGFP was used in order to test the stability of the constructed expression vector. Competent *E. coli* cells were transformed with pYL101C::sfGFP and positive clones were selected for non-selective subculturing for four passages. Strong green fluorescence was observed under blue light excitation in all of the transformants at each passage, indicating that plasmid pYL101C::sfGFP was present and functional in the host cell. Figure 4.15 shows the visualization of sfGFP fluorescence in *E. coli* transformants at the fourth passage on both selective and non-selective 2×YT agar.

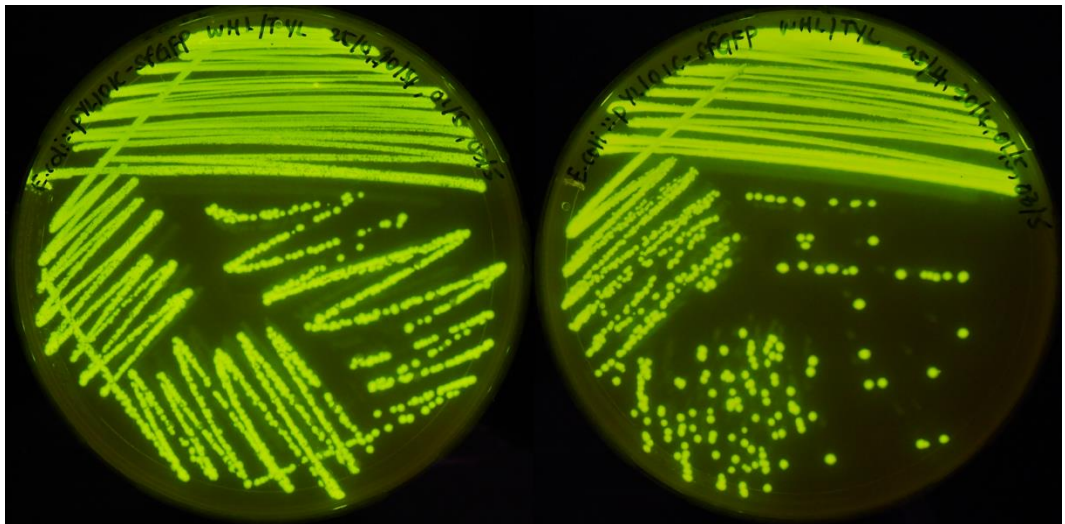


Figure 4.15: Visualization of sfGFP fluorescence in *E. coli* cells harbouring pYL101C::sfGFP under blue light excitation, on both selective and non-selective culture medium at fourth passage of sub-culturing. *E. coli* cells harbouring pYL101C::sfGFP were streaked on 2×YT agar without addition of antibiotic (*left*) and 2×YT agar supplemented with 50 µg/mL gentamycin (*right*).

4.3 Construction of Miniaturized Helper Ti Plasmid, pYL102

Plasmid pCAMBIA5105 was used as template for the construction of pYL102. To reduce the size of the helper Ti plasmid, non-essential regions for the transformation process were removed by plasmid restriction digestion and self-ligation approaches, followed by a multiple DNA fragments assembly cloning approach to generate a final product, pYL102. First, pCAMBIA5105 was subjected to RE digestion in order to remove the T-DNA region and Left Border (LB) sequence. The digested product was then allowed for self-ligation to give rise to intermediate construct, pYL102-P1. The resultant pYL102-P1 was verified by restriction enzyme analysis. Subsequently, plasmid pYL102-P1 served as PCR template to amplify three long fragments to generate pYL102.

4.3.1 Construction of Intermediate Plasmid, pYL102-P1

Plasmid pCAMBIA5105 was first extracted from its host cell and its DNA concentration and purity were determined. About one microgram of plasmid pCAMBIA5105 was subjected to *Mau*BI digestion to generate two fragments with the lengths of ~37.8 kb (Fragment A) and ~11.9 kb (Fragment B), respectively as illustrated in Figure 4.16. The ~37.8 kb fragment was self-ligated to give rise to pYL102-P1. Figure 4.17 shows the gel electrophoresis image of *Mau*BI-digested pCAMBIA5105, showing two digested fragments with their respective sizes (Appendix B). After the self-ligation, the resultant plasmid was subjected to *Sbf*I digestion to remove intact pCAMBIA5105 (T-DNA region was not removed by *Mau*BI digestion and the plasmid was self-ligated) prior to transformation into competent *E. coli* cells.

The intermediate plasmid, pYL102-P1, as shown in Figure 4.18, was verified by *EcoRI* digestion and the band pattern was compared to that of *EcoRI*-digested pCAMBIA5105 (Figure 4.19). An intact pCAMBIA5105 would generate 11 fragments upon the *EcoRI* digestion whereas pYL102-P1 would generate 10 fragments after the digestion. Both plasmids generated nine fragments with the same lengths, ranging from 412 bp to 7284 bp (Table 2). The remaining fragments of *EcoRI*-digested pCAMBIA5105 were ~10.1 kb and ~16.4 kb whereas the 10th fragment of pYL102-P1 were ~14.8 kb in length. In Figure 4.19 B, 10 bands and 9 bands were observed in the electrophoresed agarose gel for digested pCAMBIA5105 and pYL102-P1, respectively. This is due to the sizes of the two fragments, 1419 bp and 1398 bp, were too similar to be separated by standard agarose gel electrophoresis.

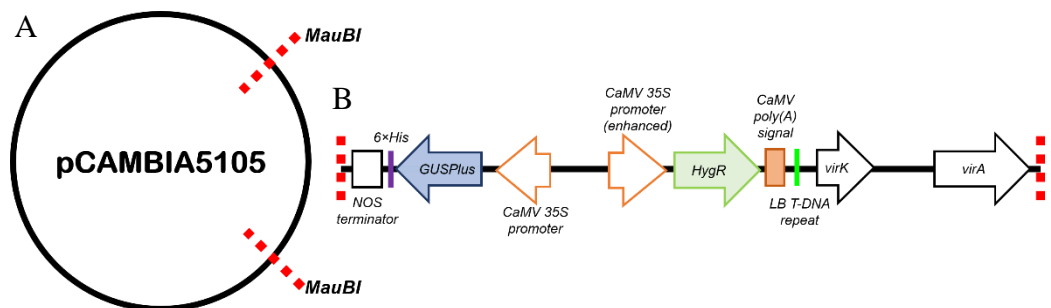


Figure 4.16: Schematic diagram of pCAMBIA5105 and the T-DNA region to be removed via *MauBI* digestion.

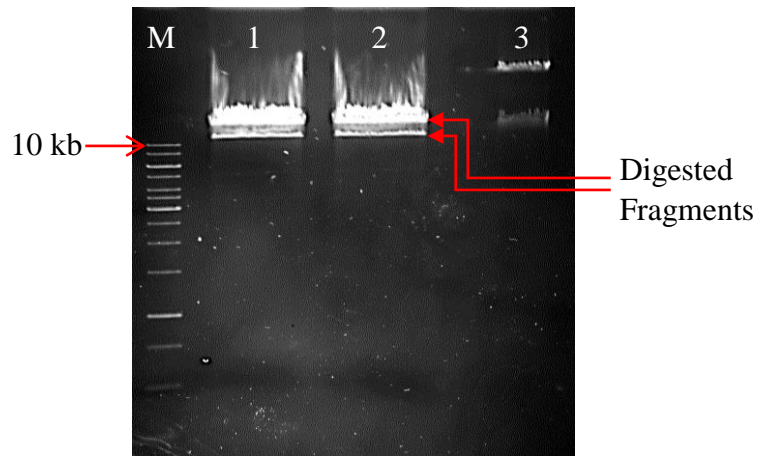


Figure 4.17: Gel electrophoresis of intact plasmid pCAMBIA5105 and *MauBI*-digested pCAMBIA5105 in 0.8% agarose gel at 100 V for 40 minutes. Lane M represents the 1 kb DNA ladder (Vivantis, Malaysia) whereas both Lanes 1 and 2 represent *MauBI*-digested pCAMBIA5105 and Lane 3 represents the undigested pCAMBIA5105, respectively.

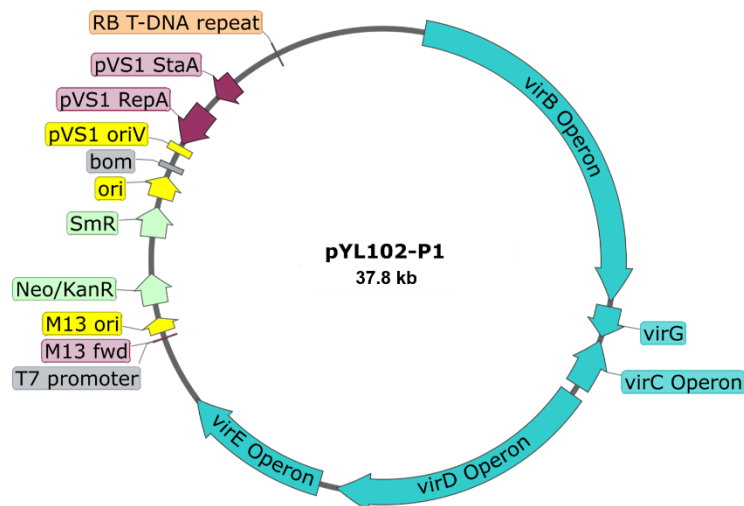


Figure 4.18: Schematic diagram of the complete plasmid map for the 37.8 kb pYL102-P1.

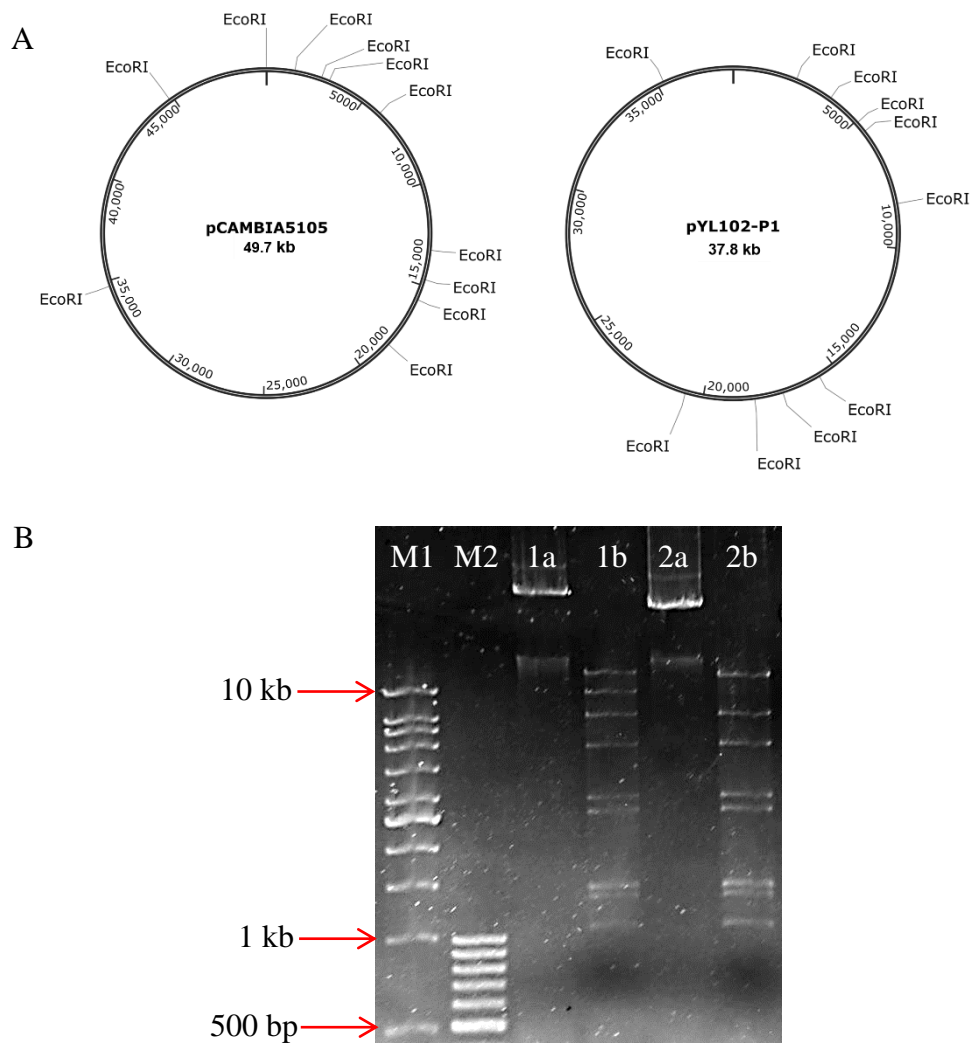


Figure 4.19: Verification on pYL102-P1 using *EcoRI* digestion. (A) Schematic diagram of plasmid maps for pCAMBIA5105 and pYL102-P1, with *EcoRI* restriction sites. (B) Gel electrophoresis of *EcoRI*-digested pCAMBIA5105 and pYL102-P1 in 0.8% agarose gel at 100 V for 1 hour and 15 minutes. Lane M1 represents the 1 kb DNA ladder (Vivantis, Malaysia) and Lane M2 represents the 100 bp DNA ladder (Thermo Fisher Scientific, USA). Lanes 1a and 1b represent undigested pCAMBIA5105 and *EcoRI*-digested pCAMBIA5105, respectively, whereas Lanes 2a and 2b represent undigested pYL102-P1 and *EcoRI*-digested pYL102-P1.

4.3.2 Construction of pYL102 by Long PCR Amplification

The verified pYL102-P1 was used as template for the construction of the final product, pYL102 and three fragments were amplified by long PCR amplification. Fragment I contains *virB* operon with the length of 12.705 kb. Fragment II contains *virC*, *virD* and *virE* operons with the length of 13.125 kb whereas pVS1 replicon, ColE1 origin of replication and the *aadA* gene (Sm^R) reside in Fragment III with the length of 5.184 kb, as shown in Figure 4.20, respectively. Figure 4.21 shows the electrophoresis of amplicons for preliminary verification prior to the assembly via homologous recombination.

The three long amplified fragments were assembled via homologous recombination and gave rise to pYL102 (Figure 4.22). For preliminary screening, replica plating was carried out to eliminate kanamycin resistance clones. Plasmids were extracted from putative clones and subjected to *EcoRI* digestion for comparison in reference to the intermediate product, pYL102-P1. Upon the digestion of *EcoRI*, pYL102 would generate nine fragments and seven of them were identical to those in the digested pCAMBIA5105, ranging from 412 bp to 2884 bp. The remaining two fragments have the lengths of 6.315 kb and 12.832 kb, which were different from the 4952 bp-, 7284 bp-, 10.103 kb- and 14.576 kb-fragments in pCAMBIA5105, as shown in Figure 4.23.

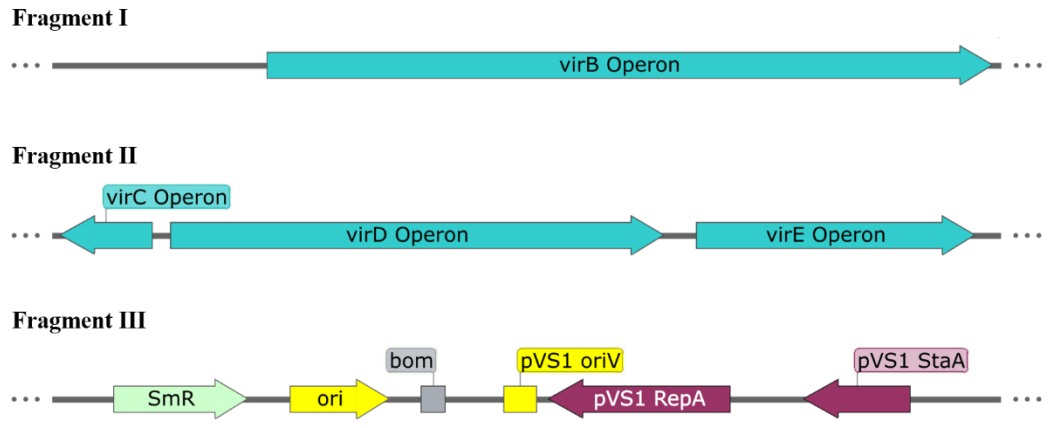


Figure 4.20: Schematic representation of three fragments to be assembled into pYL102 via homologous recombination.

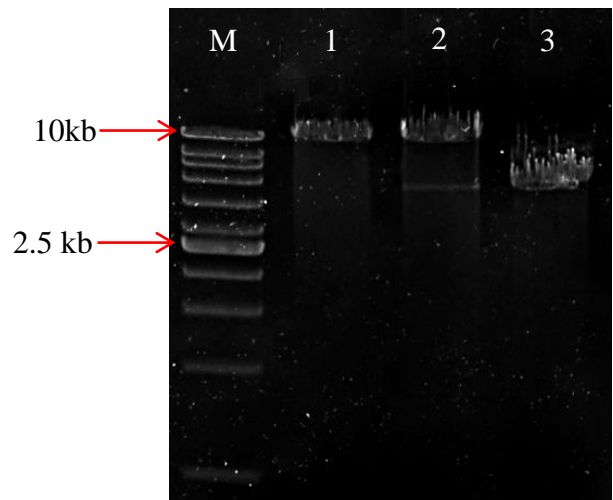


Figure 4.21: Gel electrophoresis of three PCR-amplified fragments for pYL102 construction after purification, in 1% agarose gel at 100 V for 40 minutes. Lane M represents the 1 kb DNA ladder (Vivantis, Malaysia) whereas Lanes 1, 2 and 3 represent Fragments I, II and III respectively.

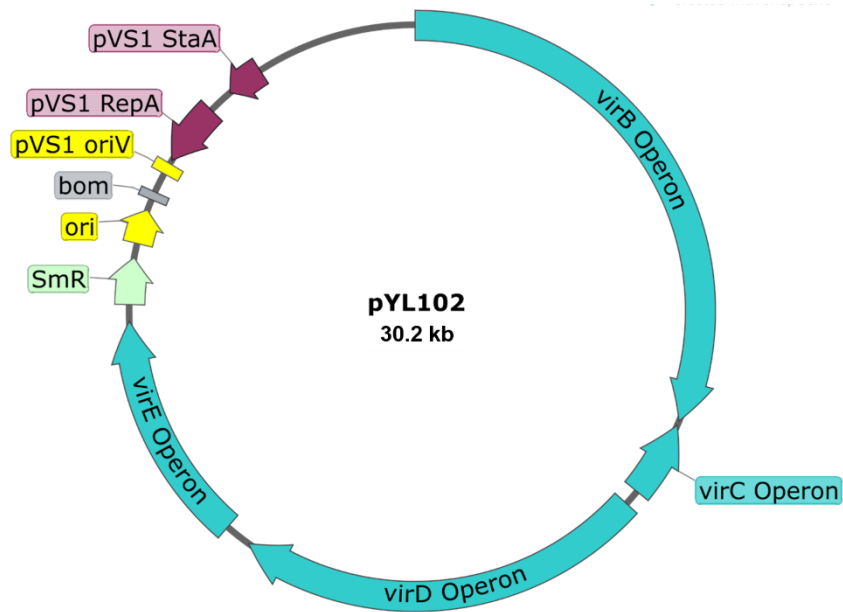


Figure 4.22: Schematic diagram of the plasmid map for pYL102 after assembly of fragments via homologous recombination.

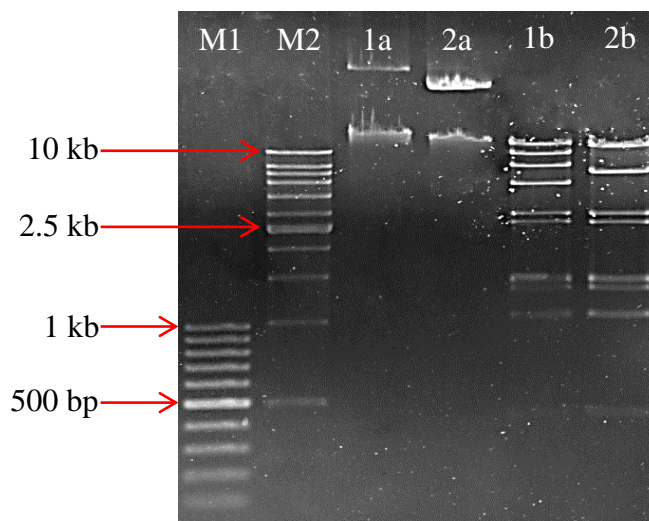


Figure 4.23: Gel electrophoresis of *EcoRI*-digested pCAMBIA5105 and pYL102 in 0.8% agarose gel at 100 V for 1 hour and 15 minutes. Lane M1 represents the 100 bp DNA ladder (Thermo Fisher Scientific, USA) and Lane M2 represents the 1 kb DNA ladder (Vivantis, Malaysia). Lanes 1a and 1b represent undigested and *EcoRI*-digested pCAMBIA5105, respectively, whereas Lanes 2a and 2b represent undigested and *EcoRI*-digested pYL102-P1, respectively.

4.4 Functionality Testing for the Constructed Plasmid System

To verify the functionality of the constructed pYL102, the complementary pYL101C::*virG*-N54D was constructed and both plasmids were tested as a whole system in model plant, *Nicotiana benthamiana*. The expression of *virG*-N54D gene in *A. tumefaciens* was verified by RT-PCR prior to the co-transformation with pYL102 and a plant-based expression vector, pGWB2.

4.4.1 Molecular Cloning of pYL101C::*virG*-N54D

The key virulence gene for *Agrobacterium*-mediated transformation, *virG*-N54D, was PCR-amplified from its template and cloned into the BHR expression vector, pYL101C. The *virG*-N54D was electrophoresed for verification prior to the cloning. As shown in Figure 4.24, a single band with the length of ~900 bp was observed, indicating the *virG*-N54D with the length of 896 bp was successfully amplified. Figure 4.25 illustrates the strategy adopted to construct pYL101C::*virG*-N54D. The resultant pYL101C::*virG*-N54D was preliminarily screened by colony PCR and subsequently sent for sequencing. The sequencing result showed 100% identity to the expected sequence.

4.4.2 Reverse Transcription PCR for *virG*-N54D in *Agrobacterium tumefaciens*

Recombinant pYL101C::*sfGFP* was electroporated into competent *A. tumefaciens* cells. Positive transformants which were resistant to gentamycin were cultured and total RNA was extracted from the cells. Primers F-*virG* and

R-col-virG were used in RT-PCR for the expressed mRNA of *virG*-N54D gene. Figure 4.26 shows the gel electrophoresis of the complementary DNA (cDNA) that was amplified from the extracted RNA from *A. tumefaciens* C58C1 empty cells and *A. tumefaciens* C58C1 cells harbouring pYL101C::*virG*-N54D, respectively. There was no band observed for both negative control and non-template control reactions. A single band was observed from the RT-PCR reaction using the total RNA extract from *A. tumefaciens* C58C1 cells harbouring pYL101C::*virG*-N54D in the electrophoresed agarose gel with the band size of ~300 bp, indicating that *virG*-N54D was expressed in *Agrobacterium* cells.

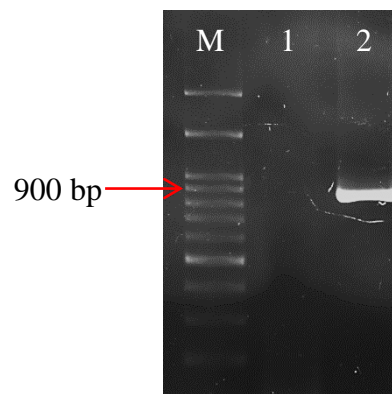


Figure 4.24: Gel electrophoresis of *virG*-N54D amplicons in 1% agarose gel at 100 V for 40 minutes. Lane M represents the 100 bp DNA ladder (GeneDireX, USA) whereas Lanes 1 and 2 represent PCR negative control and *virG*-N54D fragment, respectively.

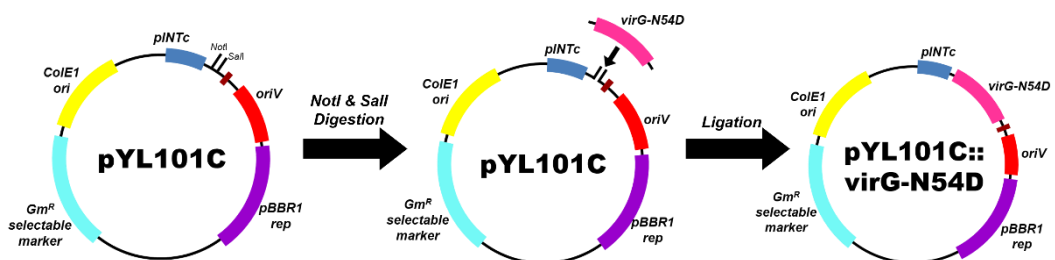


Figure 4.25: Schematic representation of the construction of pYL101C::*virG*-N54D. The *virG*-N54D fragment was double digested with *BsaI* and *SalI* and ligated to the digested pYL101C, giving rise to recombinant pYL101C::*virG*-N54D.

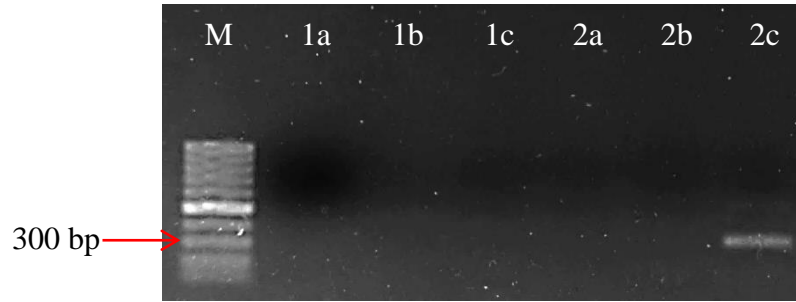


Figure 4.26: Gel electrophoresis of RT-PCR product of *virG-N54D* in 1.0% agarose gel at 100 V for 40 minutes. Lane M represents the 100 bp DNA ladder (GeneDireX, USA). Lanes 1 used total RNA extract from *A. tumefaciens* C58C1 as template whereas Lanes 2 used total RNA extract from *A. tumefaciens* C58C1 harbouring pYL101C::*virG-N54D* as template. Each lane labelled with a, b, and c represent negative control, non-template control and standard reaction of RT-PCR, respectively.

4.4.3 Verification for *Agrobacterium* transformants harbouring the Constructed Vector System

When the constructions of the miniaturized pYL102 and pYL101C::*virG-N54D* were completed, the vectors were electroporated into *A. tumefaciens* C58C1. For verifying the transformants, plasmids were extracted to check for the presence of pYL102 and pGWB2::*e35S-sfGFP* whereas colony PCR was performed for pYL101C::*virG-N54D* using primer F-*virG* and R-*virG*. Figure 4.27 shows the electrophoresed gel of the extracted plasmids from the putative transformants. Purified plasmids of pYL101C::*virG-N54D*, pGWB2::*e35S-sfGFP* and pYL102 were included as reference. For *A. tumefaciens* C58C1 transformed with only pYL102 or pGWB2::*e35S-sfGFP*, bands of expected sizes were observed and they were in accordance to the reference. Therefore, it can be concluded that the *Agrobacterium* transformant carries the two different plasmids. On the other hand, bands of sizes representing pYL102 and pGWB2::*e35S-sfGFP* were

observed in the total plasmid extract of *A. tumefaciens* C58C1 transformed with pYL101C::*virG*-N54D, pGWB2::*e35S-sfGFP* and pYL102. However, band representing pYL101C::*virG*-N54D was not observed in the transformant. Therefore, colony PCR was subsequently performed to verify the presence of pYL101C::*virG*-N54D in the transformed *Agrobacterium*, as shown in Figure 4.28. Band of ~800 bp was observed in the colony PCR of purified pYL101C::*virG*-N54D and also of the total extracted plasmids from *A. tumefaciens* C58C1 harbouring the constructed vector system. The result indicated that pYL101C::*virG*-N54D was successfully transformed into *Agrobacterium* together with the other plasmids.

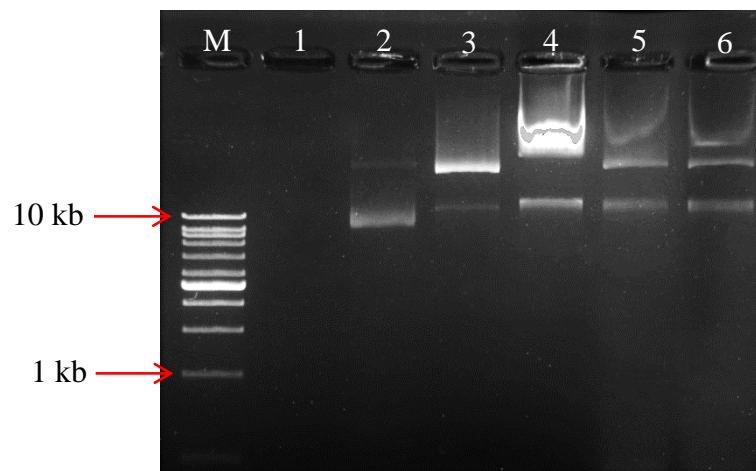


Figure 4.27: Gel electrophoresis of extracted plasmids from *A. tumefaciens* C58C1 harbouring the constructed vector system in 1.0% agarose gel at 100 V for 40 minutes. Lane M represents the 1 kb DNA ladder (Vivantis, Malaysia) whereas Lane 1 represents plasmid extract from plasmidless *A. tumefaciens* C58C1 cells (negative control). Lanes 2, 3 and 4 represent plasmids pYL101C::*virG*-N54D, pGWB2::*e35S-sfGFP* and pYL102, respectively. Lanes 5 and 6 represent the total plasmid from *A. tumefaciens* C58C1 harbouring only pYL102 and pGWB2::*e35S-sfGFP*; and *A. tumefaciens* C58C1 harbouring pYL101C::*virG*-N54D, pYL102 and pGWB2::*e35S-sfGFP*, respectively.

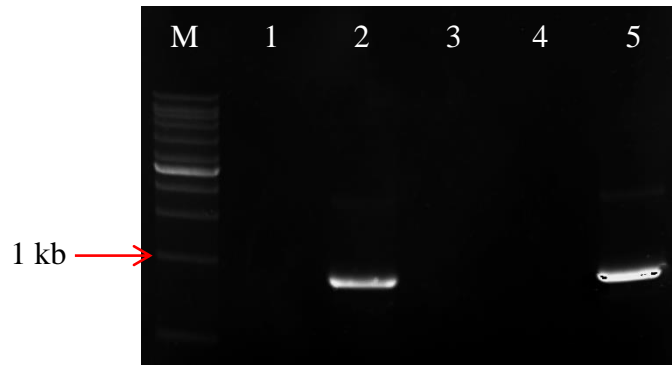


Figure 4.28: Gel electrophoresis of colony PCR on the total extracted plasmids from *A. tumefaciens* C58C1 harbouring the constructed vector system in 1.0% agarose gel at 100 V for 40 minutes. Lane M represents the 1 kb DNA ladder (Vivantis, Malaysia) whereas Lane 1 represents negative control. Lane 2 represents PCR amplicons using pYL101C::*virG*-N54D as template. Lanes 3, 4 and 5 represent PCR amplicons using the total extracted plasmids from (i) *A. tumefaciens* C58C1 harbouring only pGWB2::*e35S-sfGFP*; (ii) *A. tumefaciens* C58C1 harbouring both pYL102 and pGWB2::*e35S-sfGFP*; and (iii) *A. tumefaciens* C58C1 harbouring pYL101C::*virG*-N54D, pYL102 and pGWB2::*e35S-sfGFP*, respectively.

4.4.4 Visualization of Green Fluorescence in Infiltrated *Nicotiana benthamiana* leaves

As described in Section 3.8, *A. tumefaciens* cells harbouring different combinations of the recombinant pYL101C::*virG*-N54D, the miniaturized Ti plasmid, pYL102 and the plant reporter vector, pGWB2::*e35S-sfGFP* were used to infiltrate 6-week-old *N. benthamiana* leaves and the plants were incubated for two days. After incubation period, infiltrated leaves were plucked from the plant. Leaf disks of the infiltrated area were excised and viewed under fluorescence microscope. Figure 4.27 shows the *N. benthamiana* leaves infiltrated with bacterial cultures and Figure 4.28 depicts the microscopic images of the leaf disks taken under blue light excitation at the magnification of 400 \times . There was no green fluorescence observed in negative control, of which was infiltrated by plasmidless *A. tumefaciens* C58C1 cells; *A. tumefaciens* C58C1 harbouring

pYL101C::*virG*-N54D and pYL102; *A. tumefaciens* C58C1 harbouring pYL101C::*virG*-N54D and pGWB2::*e35S-sfGFP*; and *A. tumefaciens* C58C1 harbouring pYL102 and pGWB2::*e35S-sfGFP*, respectively. Bright green fluorescence was observed in most of the plant cells in leaf disk infiltrated by *A. tumefaciens* GV3101 harbouring pMP90 and pGWB2::*e35S-sfGFP*, which served as positive control. Bright green fluorescence was also observed in less than 50% plant cells in leaf disk infiltrated by *A. tumefaciens* C58C1 harbouring the constructed vector system, pYL101C::*sfGFP*, pYL102 and pGWB2::*e35S-sfGFP*.

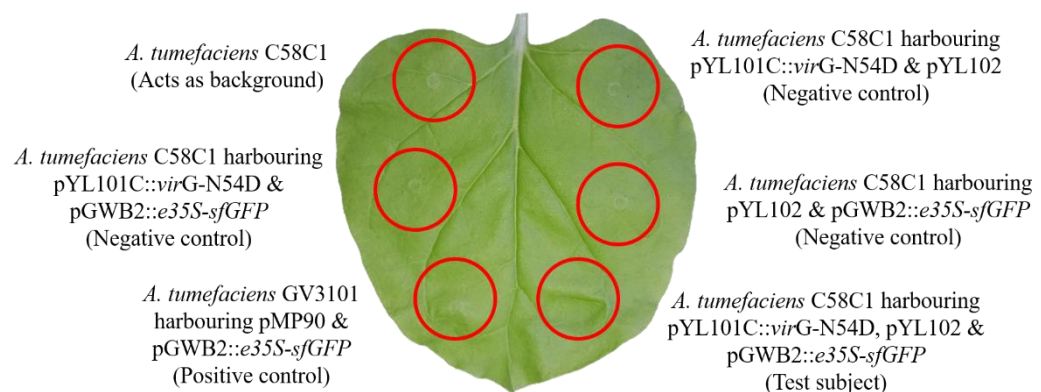


Figure 4.29: Representative image of *Nicotiana benthamiana* leaf infiltrated with various *Agrobacterium* bacterial cultures. Six spots on the leaf were agroinfiltrated and the infiltrated spots were not overlapping.

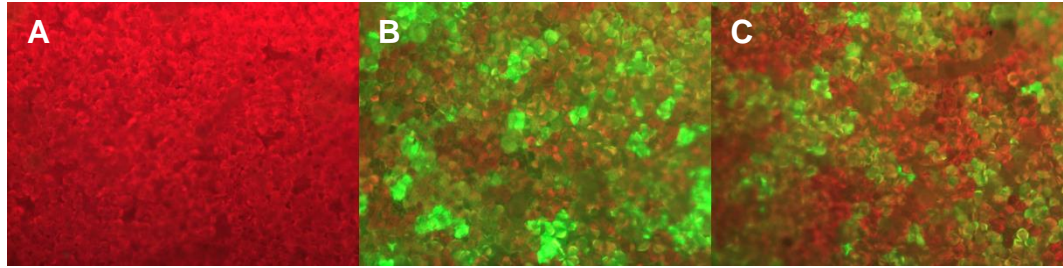


Figure 4.30: Microscopic images of *N. benthamiana* leaf disks infiltrated with *Agrobacterium* cultures under blue light excitation at magnification of 400 \times . (A) Image of leaf disks infiltrated with the negative control; (B) image of leaf disk infiltrated with the positive control (pMP90 and pGWB2::*e35S-sfGFP*); and (C) image of leaf disk infiltrated with the constructed vector system (pYL101C::*virG-N54D*, pYL102 and pGWB2::*e35S-sfGFP*).

4.4.5 Statistical Analysis of Fluorescence Intensity of the *Agrobacterium*-transformed Plant Cells

To evaluate the fluorescence intensity of the infiltrated leaves, the leaf disks were homogenized and the fluorescence intensity of the extract was measured at the excitation of 475 nm and emission of 509 nm using microplate reader. Four experimental replicates, each with technical triplicate, were carried out for the measurement of fluorescence intensity for the transformed *N. benthamiana* leaves. Average fluorescence intensity measured for the leaf extracts in four trials were shown in a bar chart of Figure 4.29. The inducer, acetosyringone was applied on *N. benthamiana* leaf during the infiltration with *A. tumefaciens* GV3101 harbouring pMP90 and pGWB2::*e35S-sfGFP* only, but not in the other four bacterial culture. As shown in the bar chart, leaves transiently transformed with *A. tumefaciens* GV3101 harbouring pMP90 and pGWB2::*e35S-sfGFP* (Bar E), which served as a positive control, showed the highest fluorescence intensity compared to the others. The level of fluorescence intensity showed in Bars A, B and C, which acted as negative controls, were relatively low or negligible. Bar

D showed the second highest fluorescence intensity, indicating that the constructed vector system which constitutes of pYL101C::*virG*-N54D, pYL102 and pGWB2::*e35S-sfGFP*, was functional in transforming plant cells.

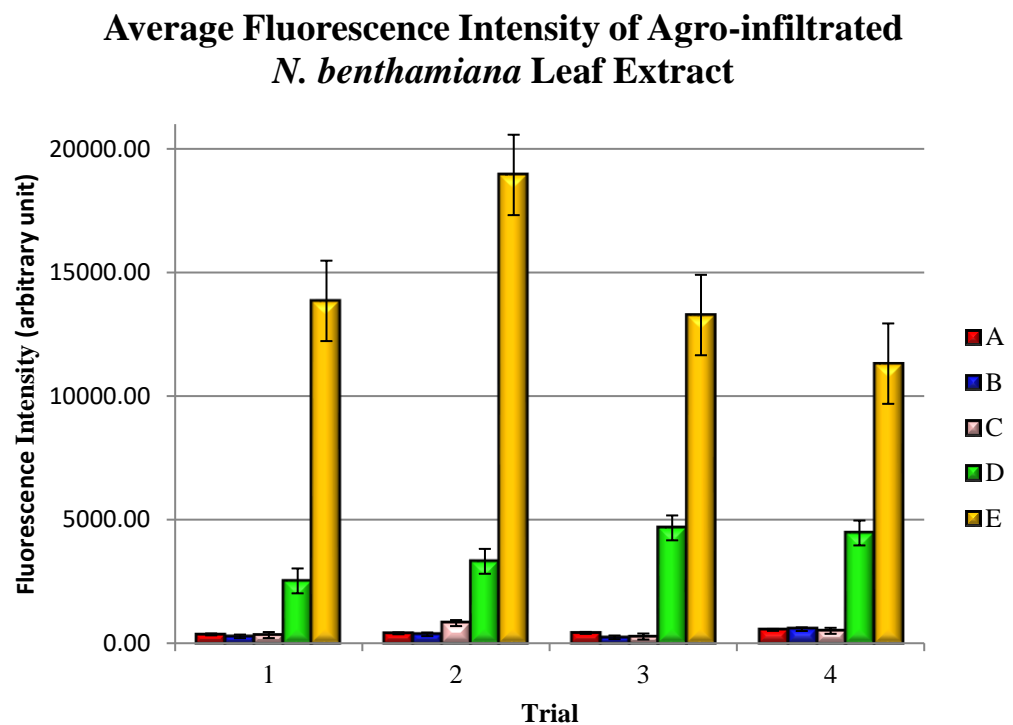


Figure 4.31: Average fluorescence intensity of *N. benthamiana* leaf extract infiltrated with different *Agrobacterium* culture. The measurement was obtained under the excitation of 475 nm and the emission of 509 nm. Bar A (red) represents leaf extracts which was infiltrated with *A. tumefaciens* C58C1 harbouring only pYL101C::*virG*-N54D and pYL102; Bar B (blue) represents leaf extracts which was infiltrated with *A. tumefaciens* C58C1 harbouring only pYL101C::*virG*-N54D and pGWB2::*e35S-sfGFP*; Bar C (pink) and Bar D (green) represent leaf extracts which was infiltrated with *A. tumefaciens* C58C1 harbouring only pYL102 and pGWB2::*e35S-sfGFP* and leaf extracts which was infiltrated with *A. tumefaciens* C58C1 harbouring pYL101C::*virG*-N54D, pYL102 and pGWB2::*e35S-sfGFP*, respectively, whereas Bar E (orange) represents leaf extracts which was infiltrated with *A. tumefaciens* GV3101 harbouring only pMP90 and pGWB2::*e35S-sfGFP*. Error bar represents the standard error from the four independent experiments (n=40).

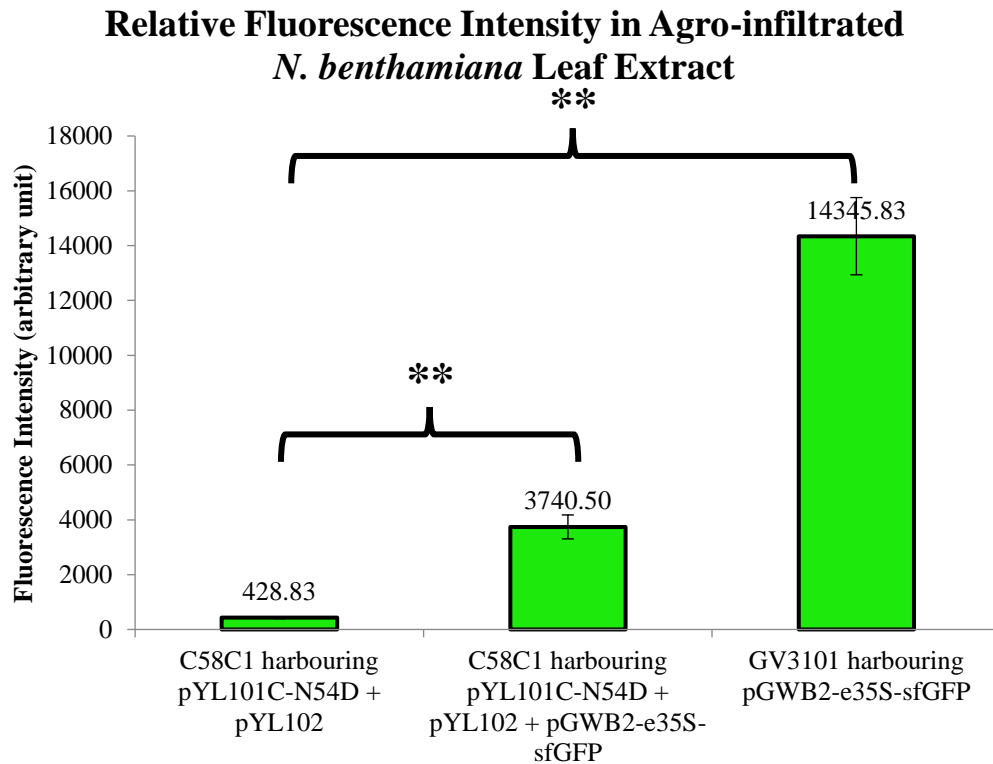


Figure 4.32: Relative fluorescence intensity of *N. benthamiana* leaf extract infiltrated with *Agrobacterium* harbouring different plasmids under blue light excitation. Leaf extract infiltrated with *A. tumefaciens* C58C1 harbouring only pYL101C::virG-N54D and pYL102 served as the mock subject and the fluorescence intensity of the positive control and the leaf extract transformed with the constructed vector system were compared against it. The asterisks indicate significant difference by T-test at $p \leq 0.01$. Error bar represents the sample mean error (n=40).

As shown in Figure 4.30, the relative fluorescence intensity of leaves infiltrated with *A. tumefaciens* harbouring the constructed vector system is about 8.7 times higher as compared to the mock-infiltrated leaves. On the other hand, the relative fluorescence intensity of positive control (*A. tumefaciens* GV3101 harbouring pMP90 and pGWB2::e35S-sfGFP) is about 3.8 times higher as compared to the constructed vector system. T-test was performed and the differences were significant at p-value less than 0.01. Therefore, the constructed vector system is proven to be functional in transforming plant cells.

CHAPTER 5

DISCUSSION

5.1 Construction of Broad Host Range Expression Vector, pYL101C

Golden Gate cloning approach was adopted to construct the BHR expression vector, pYL101C, which is made up of six separate fragments. This cloning approach permits scarless and orientated assembly of the PCR-amplified fragments by utilizing type IIS REs, namely *AarI* and *Esp3I*, to generate complementary sticky ends (Engler, Kandzia and Marillonnet, 2008). Golden Gate cloning methodology requires meticulous primer design in order to have a simultaneous orderly assembly of the fragments, despite leaving no additional RE sites in the resultant plasmid pYL101C. The sticky ends generated by RE digestions must be complementary to the sticky ends of the neighbouring fragments to facilitate a directional cloning of the fragments. Each fragment was flanked by the recognition sites of *AarI* or *Esp3I*, which recognize the sequences of 5'-CACCTGC-3' and 5'-CGTCTC-3' respectively, and cleave the DNA strand downstream of the recognition site. The recognition site for type IIs RE usually lies few bases upstream of the cleavage site, allowing the scarless cloning of the construct as the recognition site would be removed after the Golden Gate assembly (Bath *et al.*, 2002). Therefore, the primers were designed in a way that all the recognition sites for RE were at the 5'-end of the primers for easy removal after digestion. As shown in Figure 4.9, expression vector pYL101C contains two origins of replication (*ori*), namely ColE1 and pBBR1. The former allows

the expression vector to be maintained at high copy number within host cell to comply with the purposes of increasing the DNA yield and boosting the expression level of desired proteins (Camps, 2010), leading to easy genetic manipulation in *E. coli*, the model cell. The latter equips the vector with the ability to be replicated and maintained at medium high copy number within a diverse of Gram-negative bacteria. The pBBR1 ori in pYL101C was derived from pBHR1, a derivative of BHR plasmid pBBR122 (MoBiTec, 2010), of which is capable to transform at least 28 Gram-negative bacteria. The broad-host-ranged oriV resided within plasmid pBHR1 is compatible with ColE1 ori as well as commonly used IncP, IncQ and IncW group plasmids. Having both ColE1 and pBBR1 ori, pYL101C can serve multitudinous purposes as a cloning vector and a shuttle vector. Besides, pYL101C also carries the *aacCI* gene, which encodes a gentamycin acetyltransferase that confers resistance to gentamycin (Gm^R). The Gm^R selectable marker was chosen to avoid incompatibility with other vectors when it is used as a helper plasmid to the binary vector system for *Agrobacterium*-mediated transformation, where most of the available binary vectors confer kanamycin and/or hygromycin resistance.

As an expression vector, pYL101C consists of a strong constitutive promoter, P_{INTc} , one of the strongest promoter combinations and is functional in a wide range of bacteria, particularly in Gram-negative bacteria. P_{INTc} is the promoter combination of $P_{cS} + P_2$, which was originated from *K. pneumoniae*. Its promoter strength is the strongest among the promoter combinations of class I integron promoters, and is capable of driving the expression of numerous downstream genes at high level (Papagiannitsis, Tzouveleakis and Miriagou, 2009). A multiple cloning site (MCS) is located downstream of the promoter,

comprising of several common RE recognition sequences, i.e. *NotI*, *XbaI*, *Sall*, *SpeI* and *PmeI*, allowing facile cloning of gene(s)-of-interest. The expression of inserted gene(s) is placed under the control of the strong constitutive P_{INTc} and also the *T7* transcriptional terminator, which was located downstream of the MCS. The constitutive expression system of pYL101C permits the activation of transcription and translation of the desired genes without the need of external molecules as inducers and also permits the growth rate of the cell and the protein synthesis rate to be balanced at an intermediate level, saving the time lost during the lag phase (Geisel, 2011).

However, if the gene is expressed continuously without regulation, it may cause burden to the host. Constitutive expression system could be lethal to the host cell if the expressed protein is cytotoxic. Therefore, an inducible promoter is often used in a heterologous gene expression system. The IPTG-inducible *laq* promoter-repressor expression system is one of the most commonly used inducible expression system. In this system, gene expression is driven by a constitutive promoter, typically either the *lac* or T7 promoter, where the promoter activity is repressed by the binding of the *lacI* repressor to a *lac* operator, which is located downstream or within the *lac* or T7 promoter. Gene expression is turned “on” in the presence of an inducer, such as IPTG (Calos, 1978). A *lacI* repressor, typically driven by a *laqI^q* promoter, which is 10 times stronger than the wild type *lacI* promoter, is often used to repress background expression driven by the *lac* or T7 promoter. In pYL101C, a *laqI^q-lacI* repressor gene cassette is found in the vector backbone. This allows the plasmid to be modified into an IPTG-inducible expression system in the future.

Apart from *T7* terminator found downstream of MCS, *rrnB* T1 and T2 terminators were included in pYL101C downstream of the ColE1 replicon. As described in Section 4.1.1, the ColE1-Gm^R PCR fragment was amplified from the pDONR221 vector (Invitrogen) together with these terminators. The *rrnB* T1 and T2 terminators were proven to be efficient in terminating gene expression by Orosz *et al.* (1991). These termination regions play a protecting role on the inserted gene(s) in pDONR221 from expression driven by the vector-encoded promoters. As such, they were included in pYL101C, upstream of *P_{INTc}*, to eliminate undesirable effect from other promoters on the constitutive *P_{INTc}*.

5.2 BHR Reporter Vector, pYL101C::*sfGFP*

In order to verify the functionality of pYL101C, the superfolder green fluorescence protein (*sfGFP*) gene was cloned into pYL101C empty vector and the resultant plasmid, pYL101C::*sfGFP* was used to transform several Gram-negative bacteria, including two strains of *A. tumefaciens*. In this study, *sfGFP* gene was selected as reporter gene because its expression can be monitored via non-invasive method and the visualization does not require any substrate. The *sfGFP* protein is well-known for its brightness, improved folding ability and enhanced folding kinetics, even when fused to poorly-folded proteins, rendering it a higher tolerance towards chemical denaturants. As mentioned in Section 2.6.1, the fluorescence of *sfGFP* is directly proportional to the total expression of fusion protein (Cotlet *et al.*, 2006), making it an eligible candidate to investigate real-time gene expression.

In this study, five Gram-negative bacteria, as mentioned in Section 4.2.2, were transformed with the recombinant pYL101C::*sfGFP*. Electroporation transformation method was adopted in introducing pYL101C::*sfGFP* into the bacterial cells due to its relatively high efficiency rate in the uptake of plasmid DNA by the electro-competent cells. As described previously, the BHR1 replicon resided within pYL101C::*sfGFP* enables the plasmid to be replicated maintained stably with the transformed Gram-negative bacteria. Here, the host range of the BHR1 replicon was validated in *E. coli* and *A. tumefaciens*, including two different strains of C58 and LBA4404. These two bacterial strains were chosen for host range test because they have different chromosomal background of C58 and Ach5, respectively. Both of them are widely used in *Agrobacterium*-mediated transformation and the positive outcome of the host range test on these two distinct *A. tumefaciens* strains indicates that pYL101C is plausible to be used as binary vector for *Agrobacterium*-mediated transformation.

Furthermore, the list of bacterial hosts for BHR1 replicon has been expanded by including *K. pneumoniae* and two *Pantoea* sp., namely *P. ananatis* and *P. dispersa*. *K. pneumoniae* is a human pathogen that can cause serious lung infection and could lead to lethal effect whereas *Pantoea* sp. are isolated as rice pathogen that responsible for leaf blight in paddy plant in Sekinchan, Malaysia (Toh, Loh and Wong, 2019). This might shine light onto the pathogenicity-related studies regarding these pathogens. For instance, pYL101C::*sfGFP* can be used to monitor the infection pathway of *Pantoea* sp. on rice plants and thus aids in elucidating its molecular mechanism of pathogenicity and its respective counteractions. On the other hand, the strong constitutive *P_{INTc}*, which can be functional in a wide range of Gram-negative bacteria, drives the expression of

the cloned *sfGFP* gene at high level, resulting in the bright fluorescence in the transformed bacteria. The high level of heterologous gene expression afforded by the constitutive P_{INTc} in *Agrobacterium* makes pYL101C a potential expression vector to be adopted and utilized as a helper plasmid, apart from serving as a reporter vector to provide real-time observation and localization of the pathogenic bacteria.

5.3 Construction of Miniaturized Ti Plasmid, pYL102

The wild-type Ti plasmid of *Agrobacterium* has the size of ~ 200 kb and becomes a great obstacle in genetic manipulation of this phytopathogen (Christie and Gordon, 2014). Researchers had put in a vast effort to develop binary vector systems where the T-DNA region and the virulence gene clusters are carried on two independent plasmids, thereby simplifying the molecular cloning of the transgene and the transformation processes. The pCAMBIA vector series is well established and widely used for *Agrobacterium*-mediated transformation due to some favourable features, such as moderate copy number per cell and adequate MCS for genetic manipulation in *E. coli*. The vector series is also equipped with the 35S promoter for *in planta* expression purpose together with the GUS (β -glucuronidase) reporter gene for screening purpose.

In this study, plasmid pCAMBIA5105 was used as the basis of pYL101 construction as we aimed to construct a smaller helper Ti plasmid, which contains only the essential virulence gene clusters required for the type IV secretion system (T4SS) and T-DNA integration (Wise and Binns, 2016). Restriction enzyme *MauBI* was chosen for the removal T-DNA region from the

pCAMBIA5105 and it cleaves two restriction sites, which flank the transgene expression cassette and LB repeat of the T-DNA region. The *Mau*BI-digested plasmid was allowed to self-ligate and re-circularize to form the intermediate plasmid, pYL102-P1 with the size of ~37.8 kb. Intact and re-circularized pCAMBIA5105 were eliminated via *Sbf*I digestion prior to transformation of competent *E. coli* cells.

To further reduce the size of the plasmid, the redundant *virG* gene and non-essential Neo/Kan^R selectable marker gene were excluded by long PCR amplification. The functions of *virA* and *virG* genes are replaced by *virG*-N54D, which will be cloned and expressed from pYL101C. The Neo/Kan^R gene also needs to be removed because it conflicts with the Kan^R selectable marker carried by most binary vectors. The subsequent step towards the construction of pYL102 was simplified by adopting the versatile homologous recombination strategy. The three PCR-amplified fragments were flanked by their respective homologous sequences of 15 bp. Based on the overlapping 15-bp homologous sequences, the three fragments would recombine in the pre-determined order, generating the recombined plasmid pYL102 (~30.2 kb) using the NEBuilder® HiFi DNA Assembly Cloning Kit. This cloning strategy saved the time spent on RE digestion and DNA ligation, which may take more than one day.

For verifying the constructed pYL102-P1 and pYL102, restriction enzyme analysis was performed on these plasmids. Due to the large size of the plasmids, the entire plasmids were not sequenced. Instead, plasmid pCAMBIA5105, pYL102-P1 and pYL102 were digested with *Eco*RI and their resultant restriction band patterns were compared. The restriction band patterns obtained corresponded with the expected removal DNA sequences of

pCAMBIA5105 that were achieved through the *Mau*BI digestion and reassembly fragments via *in vitro* homologous recombination. Thus, the functionality of pYL102 as a helper Ti plasmid needs to be verified *in planta* to test it in a binary vector system.

5.4 Molecular Cloning of Key Virulence Gene, *virG*-N54D into pYL101C

As described in Section 2.2.4, the expression of *virG*-N54D gave a positive impact in enhancing *Agrobacterium*-mediated stable transformation efficiency (Van der Fits *et al.*, 2000). Therefore, the *virG*-N54D gene was amplified by PCR and cloned into the *Bsa*I and *Sal*I restriction sites in the MCS of pYL101C vector, giving rise to pYL101C::*virG*-N54D. The *virG*-N54D insert was verified by colony PCR and DNA sequencing. The recombinant pYL101C::*virG*-N54D was used to transform *A. tumefaciens* and the transformant was verified by colony PCR. The expression of *virG*-N54D was verified by reverse transcription PCR (RT-PCR), in which the negative control and non-template control were included in RT-PCR to eliminate false positive result.

In the *Mau*BI-digestion that generated pYL102-P1, the *virA* gene was removed together with the T-DNA region removal. The lack of *virA* and *virG* genes in pYL102 is complemented by the expression of *VirG*-N54D encoded in pYL101C::*virG*-N54D. *VirG*-N54D, which is constitutively expressed under the strong P_{INTc} , serves as an auto-activator transcriptional regulator for the activation of other virulence genes.

5.5 Functionality of Constructed Vector System in *Agrobacterium*-mediated Plant Transformation

The *Agrobacterium*-mediated transformation method is categorized into two types, i.e. stable transformation and transient transformation. Transient transformation is preferable as it is often used to provide a rapid and efficient assay of the gene expression because it could be completed within few days. Agroinfiltration is the one of the most widely used method for transient expression and the “syringe infiltration” is the most popular methods. This method does not require any sophisticated equipment except for a needleless syringe to infiltrate *Agrobacterium* into plant leaves. A single assay and multiple assays can be conducted using this method as the leaf can be used as whole or divided into several areas, as illustrated in Figure 4.27.

In this study, different combinations of vectors were tested via syringe agroinfiltration, as described in Section 4.4.3, to study the functionality of each constructed vector. The negative controls used were either lacked of pYL101C::*virG*-N54D or pYL102 or the binary vector, pGWB2::*e35S-sfGFP*. For a success plant transformation, a binary vector that consists gene(s)-of-interest to be integrated into plant’s genome and the Ti plasmid that supplies all the essential virulence proteins must be co-exist. In the vector system constructed in this study, the pYL101C::*virG*-N54D is essential for the transformation to work because it supplies the key virulence protein, VirG-N54D, which is required for the activation of other virulence genes which are resided on pYL102. Therefore, the transformation is only successful if both pYL101C::*virG*-N54D and pYL102 are present in the *Agrobacterium* cells, as depicted in Section 4.4.3.

Statistical analysis was performed to evaluate the fluorescence intensity of the infiltrated *N. benthamiana* leaves and the p-value obtained was less than 0.01, indicating the differences in average fluorescence intensity among the infiltrated leaves were significant. In short, the constructed vector system, comprised of pYL101C::*virG*-N54D and pYL102, is capable to facilitate the integration of T-DNA from pGWB2::*e35S-sfGFP* into the genome of *N. benthamiana* leaf cells. The constitutive expression of *virG*-N54D is expected to solve the bottleneck of low expression of virulence genes. Equipped with the pYL101C::*virG*-N54D for expression of *virG*-N54D and a smaller helper Ti plasmid pYL102 for the expression of other virulence genes, *Agrobacterium*-mediated plant transformation efficiency is estimated to be increased and this vector system may be utilized to boost the transformation efficiency in plant transformation, especially in recalcitrant plants. However, the fluorescence intensity of leaf cells transformed with *Agrobacterium* harbouring the constructed vector system did not reflect in higher transformation efficiency manner as compared to that of the positive control.

5.6 Future Prospective

Undoubtedly, the ultimate goal of boosting *Agrobacterium*-mediated transformation efficiency has not been fully achieved in this study. Numerous improvements can be made on the prototype vectors, pYL101C and pYL102, to meet this goal.

For the BHR expression vector, pYL101C, the constitutive expression system driven by the P_{INTc} could be modified into an IPTG-inducible expression

system. Compared to that of a constitutive expression system, an inducible expression system provides a regulatable control on the gene expression by the use of the inducer, whereby *virG-N54D* gene expression may be switched on or off for optimizing plant transformation. The presence of *lacI* operon in pYL101C will make it easier for engineering the inducible version of pYL101C in the future. Furthermore, the host range of the pBBR1 replicon can be further tested in a wider range of Gram-negative bacteria, expanding the use of this BHR expression vector for multitudinous purposes, especially in pathogenicity-related studies.

As for the miniaturized helper Ti plasmid pYL102, DNA sequencing of the entire plasmid sequence could be obtained in near future. This may eliminate any potential hidden problem such as random mutations and gene disruptions that may affect future work on the plasmid engineering and improvement on the functionality of the miniaturized helper Ti plasmid pYL102. Investigations into the IPTG inducer concentration to be used need to be optimized to activate *virG-N54D* expression for boosting plant transformation efficiency.

CHAPTER 6

CONCLUSION

This project aimed to construct two plasmid vectors with the ultimate purpose for enhancing the efficiency of *Agrobacterium*-mediated transformation. Firstly, a broad host range bacterial expression vector, designated as pYL101C, was successfully constructed for expression key regulatory virulence gene, *virG*-N54D. The ease of utilizing Golden Gate cloning approach for construct-making was demonstrated in the construction of the BHR pYL101C. Plasmid pYL101C contains all the essential features of a prokaryotic expression vector, including two origins of replication, namely ColE1 and pBBR1 ori, a strong constitutive integron promoter (P_{INTc}) for heterologous gene expression together with a strong transcriptional terminator downstream of the multiple cloning site (MCS) and a gentamycin resistance gene (Gm^R) as a selectable marker. Equipped with the broad-host-ranged pBBR1 ori and P_{INTs} -driven gene expression cassette, the cloned *sfGFP* reporter gene was successfully expressed in a few Gram-negative bacteria, indicating these features are functional. The constructed pYL101C can serve multitudinous purposes in molecular biology, for instance, the key regulatory virulence gene, *virG*-N54D, was cloned and constitutively expressed for *Agrobacterium*-mediated plant transformation.

In the second part of this study, a miniaturized helper Ti plasmid, pYL102 was successfully constructed using the plasmid pCAMBIA5105 as the backbone, where the plasmid size was reduced by ~40%. Restriction enzyme

digestion and homologous recombination approach were used to construct pYL102. The smaller plasmid size of pYL102 may contribute an enhancement in the *Agrobacterium*-mediated plant transformation efficiency. For verifying the functionality of plasmids pYL102 and pYL101C::*virG*-N54D, the binary vector, pGWB2::*e35S-sfGFP* was transferred to the *Agrobacterium* transformant cells carrying the two constructed plasmids. The resultant *Agrobacterium* transformant was able to transform plants, as indicated by sfGFP expression in the agroinfiltrated *N. benthamiana* leaves. However, the sfGFP fluorescence was lesser than that of the positive control, indicating the plant transformation efficiency was not enhanced. This may be caused by the constitutive promoter system of pYL101C::*virG*-N54D.

In summary, two helper plasmids (pYL101C::*virG*-N54D and pYL102) were successfully constructed in this study for *Agrobacterium*-mediated transformation. The BHR plasmid pYL101C can also be used for heterologous expression in Gram-negative bacteria. In the future, the constitutive promoter system could be improved and altered into inducible system to allow the optimization of the key regulatory virulence gene *virG*-N54D for enhancing plant transformation efficiency. In addition, the smaller size of the helper Ti plasmid pYL102 can facilitate future plasmid engineering for continuation improvement in *Agrobacterium*-mediated plant transformation.

REFERENCES

- Anand, A., Bass, S. H., Wu, E., Wang, N., McBride, K. E., Annaluru, N., Miller, M., Hua, M. And Jones, T. J., 2018. An improved ternary vector system for *Agrobacterium*-mediated rapid maize transformation. *Plant Molecular Biology*, 97, pp. 187-200.
- Anjanappa, R. B. and Gruissem, W., 2021. Current progress and challenges in crop genetic transformation. *Journal of Plant Physiology*, 261, doi: 10.1016/j.jplph.2021.153411.
- Arpino, J. A. J., Rizkallah, P. J. and Jones, D. D., 2012. Crystal structure of enhanced green fluorescent protein to 1.35 Å resolution reveals alternative conformations of Glu222. *PLoS One*, 7(10), e47132.
- Bath, A. J., Milsom, S. E., Gormley, N. A. and Halford, S. E., 2002. Many type IIs restriction endonucleases interact with two recognition sites before cleaving DNA. *The Journal of Biological Chemistry*, 277(6), pp. 4024-4033.
- Brondyk, W. H., 2009. Selecting an appropriate method for expressing a recombinant protein. *Methods in Enzymology*, 463, pp. 131-147.
- Brown, T. A., 2006. *Gene cloning & DNA analysis: an introduction*. 5th ed. Singapore: Blackwell Publishing.
- Calos, M. P., 1978. DNA sequence for a low-level promoter of the *lac* repressor gene and an “up” promoter mutation. *Nature*, 274, pp. 762-765.

- Camps, M., 2010. Modulation of ColE1-like plasmid replication for recombinant gene expression. *Recent Patents on DNA & Gene Sequences*, 4(1), pp. 58-73.
- Chen, Y. C. and Winans, S. C., 1991. Controlled expression of the transcriptional activator gene *virG* in *Agrobacterium tumefaciens* by using the *Escherichia coli* lac promoter. *Journal of Bacteriology*, 173, pp. 1139-1144.
- Christie, P. J. and Gordon, J. E., 2014. The *Agrobacterium* Ti plasmids. *Microbiology Spectrum Journal*, 2(6), pp. 1-29.
- Christie, P. J., Whitaker, N. and González-Rivera, C., 2014. Mechanism and structure of the bacterial type IV secretion system. *Biochimica et Biophysica Acta*, 1843(8), pp. 1578-1591.
- Cotlet, M., Goodwin, P. M., Waldo, G. S. and Werner, J. H., 2006. A comparison of the fluorescence dynamics of single molecules of a green fluorescent protein: one- versus two-photon excitation. *ChemPhysChem*, 7(1), pp. 250-260.
- Dalal, J., Yalamanchili, R., Hovary, C. L., Ji, M., Rodriguez-Welsh, M., Aslett, D., Ganapathy, S., Gruden, A., Sederoff, H. and Qu, R., 2015. A novel gateway-compatible binary vector series (PC-GW) for flexible cloning of multiple genes for genetic transformation of plants. *Plasmid*, 81, pp. 55-62.
- De Cleene, M. and De Ley, J., 1976. The host range of crown gall. *Botanical Review*, 42(4), pp. 389-466.
- Debnath, M., Prasad, G. B. and Bisen, P. S., 2010. Reporter genes. In *Molecular Diagnostics: Promises and Possibilities*. Springer, Dordrecht, pp. 71-84.

Dinh, T. and Bernhardt, T. G., 2011. Using superfolder green fluorescent protein for periplasmic protein localization studies. *Journal of Bacteriology*, 193(18), pp. 4984-4987.

Ellis, H. M., Yu, D., DiTzio, T. And Court, D. L., 2001. High efficiency mutagenesis, repair, and engineering of chromosomal DNA using single-stranded oligonucleotides. *PNAS*, 98(12), pp. 6742-6746.

Engler, C. and Marillonnet, S., 2014. Golden Gate cloning. *Methods in Molecular Biology (Clifton, N.J.)*, 1116, pp. 119-131.

Engler, C., Kandzia, R. and Marillonnet, S., 2008. A one pot, one step, precision cloning method with high throughput capability. *PLoS One*, 3(11), e3647.

Fraley, R. T., Rogers, S. G., Horsch, R. B. and Gelvin, S. B., 1986. Genetic transformation in higher plants. *Critical Reviews in Plant Sciences*, 4(1), pp. 1-46.

Fuad, F. A. A., Ismail, I., Sidik, N. M., Zain, C. R. C. M. and Abdullah, R., 2008. Super binary vector system enhanced transformation frequency and expression level of polyhydroxyvalerate gene in oil palm immature embryo. *Asian Journal of Plant Sciences*, 7(6), pp. 526-535.

Gao, R. Mukhopadhyay, A., Fang, F. and Lynn, D. G., 2006. Constitutive activation of two component response regulators: characterization of VirG activation in *Agrobacterium tumefaciens*. *Journal of Bacteriology*, 188(14), pp. 5204-5211.

Gearing, M., 2015. *Plasmids 101: Golden Gate cloning*. [blog] 15 May, 2014. Available at: < <https://blog.addgene.org/plasmids-101-golden-gate-cloning>> [Accessed on 5 August, 2021].

Geisel, N., 2011. Constitutive versus responsive gene expression strategies for growth in changing environments. *PLoS One*, 6(11), e27033.

Gelvin, S. B., 2003. *Agrobacterium*-mediated plant transformation: the biology behind the “gene-jockeying” tool. *Microbiology and Molecular Biology Review*, 67(1), pp. 16-37.

Goklke, J. and Deeken, R., 2014. Plant responses to *Agrobacterium tumefaciens* and crown gall development. *Frontiers in Plant Science*, 5(155), pp. 1-11.

Goodsell, D., 2014. *GFP-like Proteins*. [online] Available at: <<https://pdb101.rcsb.org/motm/174>> [Accessed 16 May, 2020].

Hellens, R., Mullineaux, P. and Klee, H., 2000. Technical focus: a guide to *Agrobacterium* binary Ti vectors. *Trends in Plant Science*, 5(10), pp. 446-451.

Hoekema, A., de Pater, B. S., Fellingner, A. J., Hooykaas, P. J. J. And Schilperoort, R. A., 1984. The limited host range of an *Agrobacterium tumefaciens* strain extended by a cytokinin gene from a wide host range T-region. *The European Molecular Biology Organization Journal*, 3(13), pp. 3043-3047.

Hoekema, A., Hirsch, P. R., Hooykaas, P. J. J., Schilperoort, R. A., 1983. A binary plant vector strategy based on separation of *vir*- and T-region of the *Agrobacterium tumefaciens* Ti-plasmid. *Nature*, 303(5913), pp. 178-180.

Hwang, H. H., Yu, M. And Lai, E. M., 2017. *Agrobacterium*-mediated plant transformation: biology and applications. *American Society of Plant Biologists: The Arabidopsis Book*. e0186, doi: 10.1199/tab.0186.

International Service for the Acquisition of the Agri-biotech Applications, 2021. *ISAAA Brief 55-2019-Executive Summary: Biotech Crops Drive Socio-Economic Development and Sustainable Environment in the New Frontier*. Available at: <<https://www.isaaa.org/>> [Accessed on 23 August, 2021].

Jacobus, A. P. and Gross, J., 2015. Optimal cloning of PCR fragments by homologous recombination in *Escherichia coli*. *PLoS One*, 10(3), e0119221.

Jung, Y. C., Gu, Y., Wu, D. And Jin, S., 2004. Mutants of *Agrobacterium tumefaciens* *virG* gene that activate transcription of *vir* promoter in *Escherichia coli*. *Current Microbiology*, 49(5), pp. 334-340.

Keshavareddy, G., Kumar, A. R. V. and Ramu, S. V., 2018. Methods of plant transformation – a review. *International Journal of Current Microbiology and Applied Sciences*, 7(7), pp. 2656-2668.

Kiyokawa, K., Yamamoto, S., Sakuma, K., Tanaka, K., Moriguchi, K. and Suzuki, K., 2009. Construction of disarmed Ti plasmids transferable between *Escherichia coli* and *Agrobacterium* species. *Applied and Environmental Microbiology*, 75(5), pp. 1845-1851.

Knauf, V. C., Panagopoulos, C. G. And Nester, E. W., 1982. Genetic factors controlling the host range of *Agrobacterium tumefaciens*. *Phytopathology*, 72, pp. 1545-1549.

- Komari, T., Hiei, Y., Saito, Y., Murai, N. and Kumashiro, T., 1996. Vectors carrying two separate T-DNAs for co-transformation of higher plants mediated by *Agrobacterium tumefaciens* and segregation of transformants free from selection markers. *The Plant Journal*, 10(1), pp. 165-174.
- Komari, T., Ishida, Y. and Hiei, Y., 2004. Plant transformation technology: *Agrobacterium*-mediated transformation. doi: 10.1002/0470869143.kc014.
- Komori, T., Imayama, T., Kato, N., Ishidam, Y., Ueki, J. And Komari, T., 2007. Current status of binary vectors and superbinary vectors. *Plant Physiology*, 145, pp. 1155-1160.
- Krishnamohan, A., Balaji, V. and Veluthambi, K., 2001. Efficient *vir* gene induction in *Agrobacterium tumefaciens* requires *virA*, *virG*, and *vir* box from the same Ti plasmid. *Journal of Bacteriology*, 183(13), pp. 4079-4089.
- Leclercq, J., Szablocs, T., Martin, F. and Montoro, P., 2015. Development of a new pCAMBIA binary vector using Gateway® technology. *Plasmid*, 81, pp. 50-54.
- Lee, K., Dudley, M. W., Hess, K. M., Lynn, D. G., Joerger, R. D. and Binns, A. N., 1992. Mechanis, of activation of *Agrobacterium* virulence genes: identification of phenol-binding proteins. *Proceeding of the National Academy of Sciences of the United States of America*, 89(18), pp. 8666-8670.
- Lee, L. Y. and Gelvin, S. B., 2008. T-DNA binary vectors and system. *Plant Physiology*, 146(2), pp. 325-332.

Lee, S., Su, G., Lasserre, E., Aghazadeh, M. A. And Murai, N., 2012. Small high-yielding binary Ti vectors pLSU with co-directional replicons for *Agrobacterium tumefaciens*-mediated transformation of higher plants. *Plant Science: An International Journal of Experimental Plant Biology*, 187, pp. 49-58.

Lewis, J.C., Feltus, A., Ensor, C. M., Ramanathan, S. and Daunert, S., 1998. Peer reviewed: applications of reporter genes. *Analytical Chemistry*, 70(17), pp. 579A-585A.

Li, S., Chen, L., Peng, X., Wang, C., Qin, B., Tan, D., Han, C., Yang, H., Ren, X., Liu, F., Xu, C. and Zhou, X., 2018. Overview of the reporter genes and reporter mouse models. *Animal Models and Experimental Medicine*, 1(1), pp. 29-35.

Li, S., Cong, Y., Liu, Y., Wang, T., Shuai, Q., Chen, N., Gai, J. And Li, Y., 2017. Optimization of *Agrobacterium*-mediated transformation in soybean. *Frontiers in Plant Science*, 8(246), doi: 10.3389/fpls.2017.00246.

Loenen, W. A. M., Dryden, D. T. F., Raleigh, E., A., Wilson, G. G. and Murray, N. E., 2014. Highlights of the DNA cutters: a short history of the restriction enzymes. *Nucleic Acids Research*, 42(1), pp. 3-19.

Loper, J. E. and Kado, C. I., 1979. Host range conferred by the virulence-specifying plasmid of *Agrobacterium tumefaciens*. *Journal of Bacteriology*, 139(2), pp. 591-596.

Marillonnet, S. and Grützner, R., 2020. Synthetic DNA assembly using Golden Gate cloning and the hierarchical modular cloning pipeline. *Current Protocols in Molecular Biology*, 130(1), e115.

McCullen, C. A. and Binns, A. N., 2006. *Agrobacterium tumefaciens* and plant cell interactions and activities required for interkingdom macromolecules transfer. *Annual Review of Cell and Development Biology*, 22, pp. 101-127.

MoBiTec, 2017. *Broad host range vectors pBBR122 and pBHR1*. MoBiTec GmbH, Germany.

Mohammadhassan, R., Kshefi, B. and Delcheh, K. S., 2014. *Agrobacterium*-based vectors: a review. *International Journal of Farming and Allied Sciences*, 3(9), pp. 1002-1008.

Murai, N., 2013. Review: Plant binary vectors of Ti plasmid in *Agrobacterium tumefaciens* with a broad host-range replicon of pRK2, pRi, pSa or pVS1. *American Journal of Plant Sciences*, 4, pp. 932-939.

Narayanan, K. and Chen, Q., 2011. Bacterial artificial chromosome mutagenesis using recombineering. *Journal of Biomedicine and Biotechnology*, 2011, pp. 1-10, doi: 10.1155/2011/971296.

Narayanan, K., Sim, E. U. H., Ravin, N. V and Lee, C. W., 2009. Recombination between linear double-stranded DNA substrates *in vivo*. *Analytical Biochemistry*, 387(1), pp. 139-141.

National Human Genome Research Institute, 2014. *Homologous Recombination*. Available at: < <https://www.genome.gov/genetics-glossary/homologous-recombination> > [Accessed on 4th, December, 2021].

Nester, E. W., 2015. *Agrobacterium*: nature's genetic engineer. *Frontiers in Plant Science*, 5(730), doi: 10.3389/fpls.2014.00730.

Nora, L. C., Westmann, C. A., Martins-Santana, L., de Fátima Alves, L., Monteiro, L. M., O., Guazzaroni, M. and Silva-Rocha, R., 2018. The art of vector engineering: towards the construction of next-generation genetic tools. *Microbial Biotechnology*, 12, pp. 125-147.

Novick, R. P., 1987. Plasmid Incompatibility. *Microbiological Reviews*, 51(4), pp. 381-395.

OpenWetWare, 2007. *Isopropanol precipitation for PCR purification*. [online] Available at: <https://openwetware.org/wiki/Isopropanol_Precipitation_for_PCR_Purification> [Accessed on 16 May, 2020].

Orosz, A., Boros, I. and Venetianer, P., 1991. Analysis of the complex transcription termination region of the *Escherichia coli* *rrnB* gene. *The European Journal of Biochemistry*, 201(3), pp. 653-659.

Otten, L., Burr, T. and Szegedi, E., 2008. *Agrobacterium*: a disease-causing bacterium. In Tzfira T. and Citovsky, V. (eds), *Agrobacterium: from biology to biotechnology*. Springer, New York, USA, pp. 1-46.

Özyiğit, İ. İ., 2012. *Agrobacterium tumefaciens* and its use in plant biotechnology. In Ashraf, M., Öztürk, M., Ahmad, M. S. A. and Askoy, A. (eds), *Crop Production for Agricultural Improvement*, 1, Springer, Dordrecht, pp. 317-361.

Papagiannitsis, C. C., Tzouvelekis, L. S. and Miriagou, V., 2009. Relative strengths of the class 1 integron promoter hybrid 2 and the combinations of strong and hybrid 1 with an active P2 promoter. *Antimicrobial Agents and Chemotherapy*, 53(1), pp. 277-280.

Patrick, M., 2014. *Fluorescent Proteins 101: Green Fluorescent Protein (GFP)*. [blog] 15 May, 2014. Available at: <<https://blog.addgene.org/plasmids-101-green-fluorescent-protein-gfp>> [Accessed on 16 May, 2020].

Pédelacq, J. D. and Cabantous, S., 2019. Development and applications of superfolder and split fluorescent protein detection systems in biology. *International Journal of Molecular Sciences*, 20 (14), pp. 1-19.

Pédelacq, J. D., Cabantous, S., Tran, T., Terwilliger, T. C. and Waldo, G. S., 2006. Engineering and characterization of a superfolder green fluorescent protein. *Nature Biotechnology*, 24(1), pp. 79-88.

Phillips, T., 2008. Genetically modified organisms (GMOs): transgenic crops and recombinant DNA technology. *Nature Education*, 1(1), pp. 213.

Pingoud, A. and Jeltsch, A., 2001. Structure and function of type II restriction endonucleases. *Nucleic Acids Research*, 29(18), pp. 3705-3727.

Pingoud, A., Wilson, G. G. and Wende, W., 2014. Type II restriction endonucleases – a historical perspective and more. *Nucleic Acids Research*, 42(12), pp. 7489-7527.

Pitzschke, A. and Hirt, H., 2010 New insights into an old story: *Agrobacterium* induced tumour formation in plants by plant transformation. *Journal of European Molecular biology Organization*, 29, pp. 1021-1032.

Preston, A. and Casali, N., 2003. *E. coli plasmid vectors: methods and applications* Humana Press: Totowa, New Jersey.

Rosano, G. L. and Ceccarelli, E. A., 2014. Recombinant protein expression in *Escherichia coli*: advances and challenges. *Frontiers in Microbiology*, 5(172), doi: 10.3389/fmicb.2014.00172.

Sah, S. K., Kaur, A., Kaur, G. And Cheema, G. S., 2014. Genetic transformation of rice: problems, progress and prospects. *Journal of Rice Research*, 3(1), pp. 1-10.

Sawitzke, J. A., Thomason, L. C., Costantino, N., Bubunencko, M. Datta, S., Court, D. L., 2007. Recombineering: in vivo genetic engineering in *E. coli*, *S. enterica*, and beyond. *Methods in Enzymology*, 421, pp. 171-199.

Scott, D. J., Gunn, N. J., Yong, K. J., Wimmer, V. C., Veldhuis, N. A., Challis, L. M., Petrou, S., Bathgate, R. A. D. and Griffin, M. D. W., 2018. A novel ultra-stable, monomeric green fluorescent protein for direct volumetric imaging of whole organs using CLARITY. *Scientific Reports*, 8(1), pp. 667-681.

Simpson, R. B., Spielmann, A., Margossian, L. And McKnight, T. D., 1986. A disarmed binary vector from *Agrobacterium tumefaciens* functions in *Agrobacterium rhizogenes*. *Plant Molecular Biology*, 6, pp. 403-415.

Smith, G. R., 1987. Mechanism and control of homologous recombination in *Escherichia coli*. *Annual Reviews of Genetics*, 21, pp 179-201.

Son Y. J., Ryu, A. J., Han, N., S. and Jeong, K. J., 2016. Development of a high-copy plasmid for enhanced production of recombinant proteins in *Leuconostoc citreum*. *Microbial Cell Fact*, 15(12), doi: 10.1186/s12934-015-0400-8.

Subramoni, S., Nathoo, N., Klimov, E. and Yuan, Z., 2014. *Agrobacterium tumefaciens* responses to plant-derived signaling molecules. *Frontiers in Plant Science*, 5(322), doi: 10.3389/fpls.2014.00322.

Terpe, K. 2006. Overview of bacterial expression systems for heterologous protein production: from molecular and biochemical fundamentals to commercial systems. *Applied Microbiology and Biotechnology*, 72(2), pp. 211-222.

Toh, W. K., 2017. *Enhancement of plant transformation by expression of Cdr2 protein*. Master. Universiti Tunku Abdul Rahman, Malaysia.

Toh, W. K., Loh, P. C. And Wong, H. L., 2019. First report of leaf blight of rice caused by *Pantoea ananatis* and *Pantoea dispersa* in Malaysia. *Plant Disease*, 103(7), pp. 1764.

Tomlinson, A. D. and Fuqua, C., 2009. Mechanisms and regulation of polar surface attachment in *Agrobacterium tumefaciens*. *Current Opinion in Microbiology*, 12(6), pp. 708-714.

Torisky, R. S., Kovacs, L., Avdiushko, S., Newman, J. D., Hunt, A. G. and Collins, G. B., 1997. Development of a binary vector system for plant transformation based on the supervirulent *Agrobacterium tumefaciens* strain Chry5. *Plant Cell Reports*, 17, pp. 102-108.

Uniprot, 2020. *Taxonomy – Agrobacterium fabrum (strain C58/ ATCC 33970) (Agrobacterium tumefaciens (strain C58))*. [online] Available: <<http://www.uniprot.org/taxonomy/176299>> [Accessed on 16 May, 2020.]

Van Baarlen, P. and Szelen, R. J., 2009. Genomics of plant-associated microbes. *Microbial Biotechnology*, 2(4), pp. 406-411.

Van der Fits, L., Deakin, E. A., Hoge, J. H. C. and Memelink, J., 2000. The ternary transformation system: constitutive virG on a compatible plasmid dramatically increases *Agrobacterium*-mediated plant transformation. *Plant Molecular Biology*, 43(4), pp. 495-502.

Vollset, S. E., Goren, E., Yuan, C., Cao, J., Smith, A. E., Hsiao, T., Bisignano, C., Azhar, G. S., Castro, E., Chalek, J., Dolgert, A. J., Frank, T., Fukutaki, K., Hay, S. I., Lozano, R., Mokdad, A. H., Nandakumar, V., Pierce, M., Pletcher, M., Robalik, T., Steuben, K. M., Wunrow, H. Y., Zlavog, B. S. and Murray, C. J. L., 2020. Fertility, mortality, migration, and population scenarios for 195 countries and territories from 2017 to 2100: a forecasting analysis for the Global Burden of Disease Study. *The Lancet*, 396 (10258), pp. 1129-1306.

Wilson, G. G., Wang, H., Heiter, D. And Lunnen, K. D., 2012. Restriction enzymes in microbiology, biotechnology and biochemistry. *Revista Encuentro*, 93, pp. 19-48.

Wise, A. A. and Binns, A. N., 2016. The receiver of the *Agrobacterium tumefaciens* VirA histidine kinase forms a stable interaction with VirG to activate virulence gene expression. *Frontiers in Microbiology*, 6(1546), doi: 10.3389/fmicb.2015.01546.

Xu, R. and Li, Q. Q., 2008. Protocol: streamline cloning of genes into binary vectors in *Agrobacterium* via the Gateway® TOPO vector system. *Plant Methods*, 4(4), doi: 10.1186/1746-4811-4-4.

Zhang, Y., Muyrers, J. P. P., Testa, G. and Stewart, A. F., 2000. DNA cloning by homologous recombination in *Escherichia coli*. *Nature Biotechnology*, 18, pp.1314-1317.

Zhi, L., TeRonde, S., Meyer, S., Arling, M. L., Register, J. C., Zhao, Z. Y., Jones, T. J. And Anand, A., 2015. Effect of *Agrobacterium* strain and plasmid copy number on transformation frequency, event quality and usable event quality in an elite maize cultivar. *Plant Cell Reports*, 34(5), doi: 10.1007/s00299-014-1734-0.

Ziemienowicz, A., 2013. *Agrobacterium*-mediated plant transformation: factors, applications and recent advances. *Biocatalysis and Agricultural Biotechnology*. doi: 10.1016/j.bcab.2013.10.004.

Zou, Y. W., 2014. Green Fluorescent Protein. *Embryo Project Encyclopedia*. [online] Available at: <<https://embryo.asu.edu/pages/green-fluorescent-protein>> [Accessed on 16 May, 2020].

APPENDIX A

Table A: List of primers used in this study.

Primer	Sequence
F-ColE1	GTCACCTGCAGTCGAGGTCACTCATGGTGATTTCTCAC
R-rrnTer	GTCACCTGCTATCGGCTGAGAGTAGGGAACGCCAG
F-oriV	TGCACCTGCTATTAGGAGCTTGCTCTCCGGGCTTC
R-oriV	TGCACCTGCTGCACGTAGGAACAGCGCACTTACGG
F-pINTc	GTCGTCTCGAGCCGAATTAGACGATATAGGCGCCA
R-pINTc	GTCGTCTCGAAACTTGTATGTATACTCCTTC
F-T7ter	GTCGTCTCAGCTCACCGCTGAGCAATAACTAG
R-T7ter	GTCGTCTCATCCTCGTCCTGTGGATATCCGGA
F-lacI	GTCGTCTCATA CG ATCACGCATCTTCCCGACA
R-lacI	GTCGTCTCGCCTCGTTGTAGGTGGACCAGTTG
F-MCS	GGCTACCACCTGCAGTCTTTTGC GGCCGCTCTAGAGTCGACACTAGTGTTTA AAC
R-MCS	GGCTACCACCTGCAGTCA GC GGTTTAAACACTAGTGTCGACTCTAGAGCGG CCGC
F-col-pINTc	TCTTCCGACTGAGCCTTTCG
R-col-oriV	GGCTACGGTCTCAGCGTGCTTTGCGTTCGGTTTGC
F-sfGFP	TAGGTCTCAG GC CATGTCAAAGGAGAAGAGCTG
R-sfGFP	TT GTCGACT CTAGAGCGGCCGCTTACTTATAAAGCTCATCCATGCCG
F-virG	AAGGTCTCAG GC CCTGACGAACTGCCCATTTAG
R-virG	TT GTCGACC CTCCTGCGGCCGAGCCAGATAATTAAGAGCCAAATG
R-col-virG	CATCTTCACGACCTAAGTC
F-102-F1	TCCTCTTGATATCGCCCATTCGGTCATCAG
R-102-F1	GGTTTGAGGCAGTGAAACGCTTCGAGGTTACAG
F-102-F2	GTTTCACTGCCTCAAACCTACACTCAATATTTG
R-102-F2	GAAAACCGCCGTCAAGAAGAAGCCAGTTTCC
F-102-F3	CTTCTTGACGGCGGTTTTTCATGGCTTCTTG
R-102-F3	TGGGCGATATCAAGAGGAACAAGCATGAAACC

*The RE sites are underlined and the sticky ends generated by RE digestion are in **bold** letters.

APPENDIX B

Table B: List of restriction endonucleases (REs) used in this study.

RE	Description	Manufacturer
<i>AarI</i>	<ul style="list-style-type: none"> • Recognizes 5'-CACCTGCNNNN<u>NNNN</u>-3' • Utilized for Golden Gate cloning for pYL101C construction 	Thermo Fisher Scientific, USA
<i>BsaI</i>	<ul style="list-style-type: none"> • Recognizes 5'-GGTCTC<u>NNNNN</u>-3' • Used to digest <i>sfGFP</i> and <i>virG</i>-N54D genes to be cloned into pYL101C • Generates sticky ends that is complementary to sticky ends generated by <i>NotI</i> digestion 	Thermo Fisher Scientific, USA
<i>EcoRI</i>	<ul style="list-style-type: none"> • Recognizes 5'<u>GAATTC</u>-3' • Multiple restriction sites on pCAMBIA5105 and its derivatives, pYL102-P1 and pYL102 • Generates distinguishable digestion profiles for each of the mentioned plasmids 	Vivantis, Malaysia
<i>Esp3I</i>	<ul style="list-style-type: none"> • Recognizes 5'-CGTCTC<u>NNNNN</u>-3' • Utilized for Golden Gate cloning for pYL101C construction 	Thermo Fisher Scientific, USA
<i>KpnI</i>	<ul style="list-style-type: none"> • Recognizes 5'-GGT<u>ACC</u>-3' • Unique cutter on pYL101C • Utilized for preliminary verification of pYL101C 	Thermo Fisher Scientific, USA
<i>MauBI</i>	<ul style="list-style-type: none"> • Recognizes 5'-CG<u>CGCGCG</u>-3' • Two restriction sites on pCAMBIA5105, flanking the T-DNA region • Used to remove non-essential T-DNA region 	Thermo Fisher Scientific, USA
<i>NotI</i>	<ul style="list-style-type: none"> • Recognizes 5'-GCGG<u>CCGC</u>-3' • Present in the MCS of pYL101C • Used to linearize pYL101C for cloning 	Thermo Fisher Scientific, USA
<i>SacI</i>	<ul style="list-style-type: none"> • Recognizes 5'-G<u>AGCTC</u>-3' • Unique cutter on pYL101C • Utilized for preliminary verification of pYL101C::<i>sfGFP</i> 	Thermo Fisher Scientific, USA
<i>Sall</i>	<ul style="list-style-type: none"> • Recognizes 5'-G<u>TCGAC</u>-3' • Present in the MCS of pYL101C • Used to linearize pYL101C for cloning 	Thermo Fisher Scientific, USA
<i>SbfI</i>	<ul style="list-style-type: none"> • Recognizes 5'-CCTG<u>CAGG</u>-3' • Unique cutter on pCAMBIA5105 • Used to distinguish pCAMBIA5105 and pYL102-P1 	Thermo Fisher Scientific, USA
<i>XbaI</i>	<ul style="list-style-type: none"> • Recognizes 5'-T<u>CTAGA</u>-3' • Unique cutter on pYL101C • Utilized for preliminary verification of pYL101C::<i>sfGFP</i> 	Thermo Fisher Scientific, USA

*The underlined letters represent the sticky ends generated by the REs

APPENDIX C

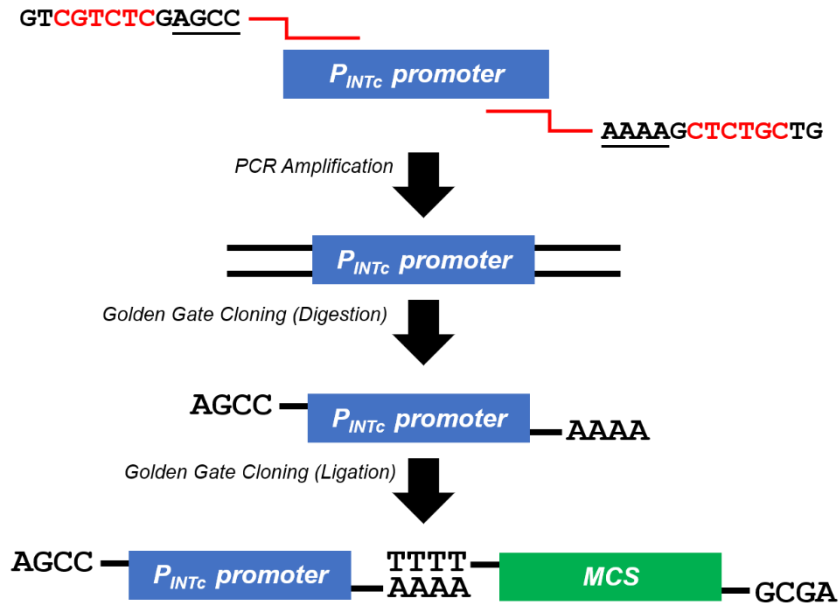


Figure C1: Schematic representation on pYL101C construction using Golden Gate cloning, starting from PCR amplification to ligation. Primers were designed carefully so that the sticky ends generated was complementary to the neighbouring fragments' sticky ends for directional cloning and the RE recognition sequences were lost after cloning (*Letters in RED represent the recognition sequence of RE and the underlined letters represent cleavage site*).

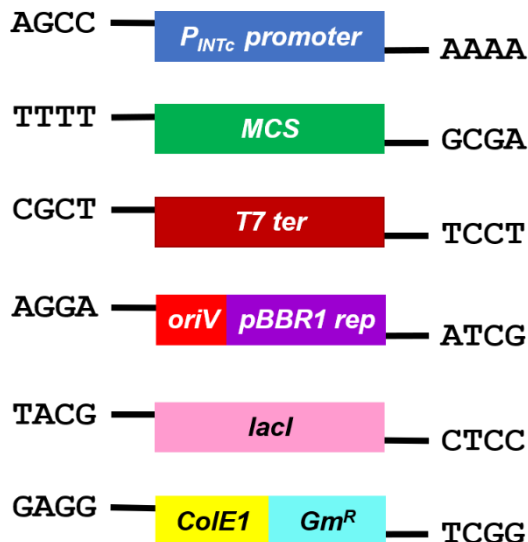


Figure C2: Schematic diagram of the six fragments to-be assembled for pYL101C after *AarI* and *Esp3I* digestion. Sticky ends generated after digestion were complementary to the sticky ends of both the neighbouring fragments, allowing the fragments to be cloned in a correct orientation.

APPENDIX D

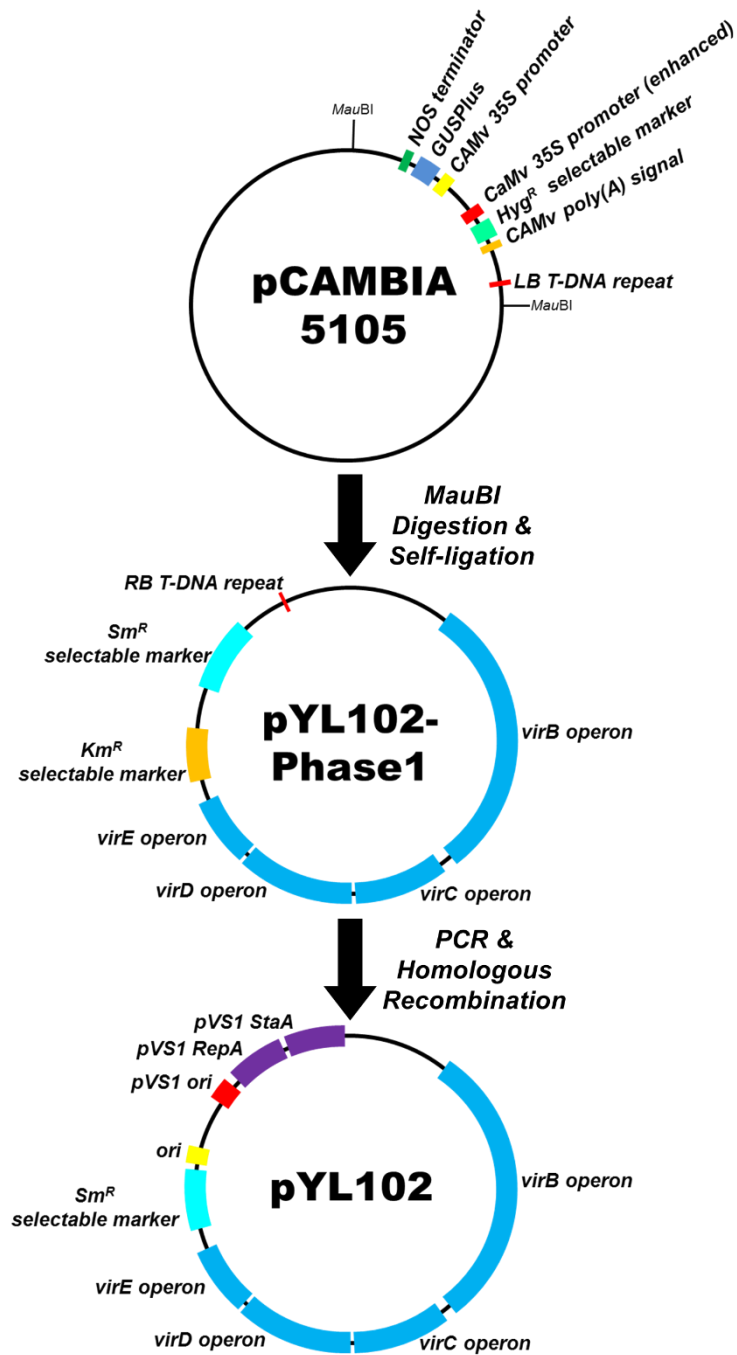


Figure D: Flowchart of pYL102 construction via RE digestion, PCR amplification and homologous recombination.

APPENDIX E

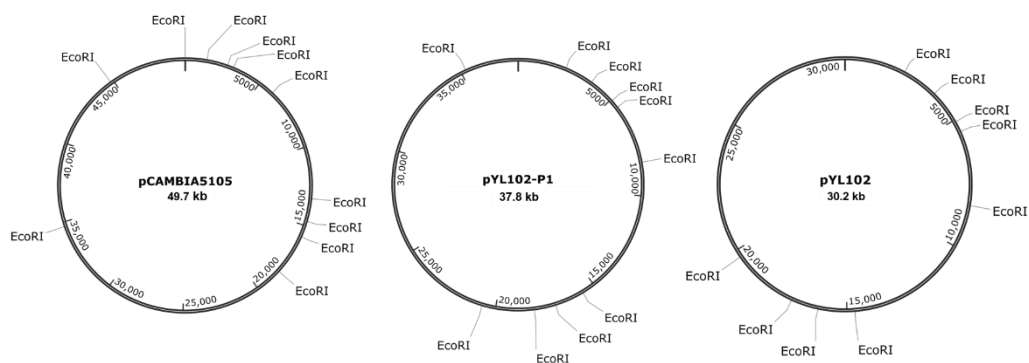


Figure E: Schematic diagrams of plasmids pCAMBIA5105, pYL102-P1 and pYL102, with *EcoRI* restriction sites labelled.

Table E: Fragment sizes of plasmids after *EcoRI* digestion.

Length of Digested Fragments in bp		
pCAMBIA5105	pYL102-P1	pYL102
412	412	412
1047	1047	1047
1311	1311	1311
1398	1398	1398
1419	1419	1419
2545	2545	2545
2884	2884	2884
4952	4952	6315
7284	7284	12832
10103	14573	
16402		

APPENDIX G

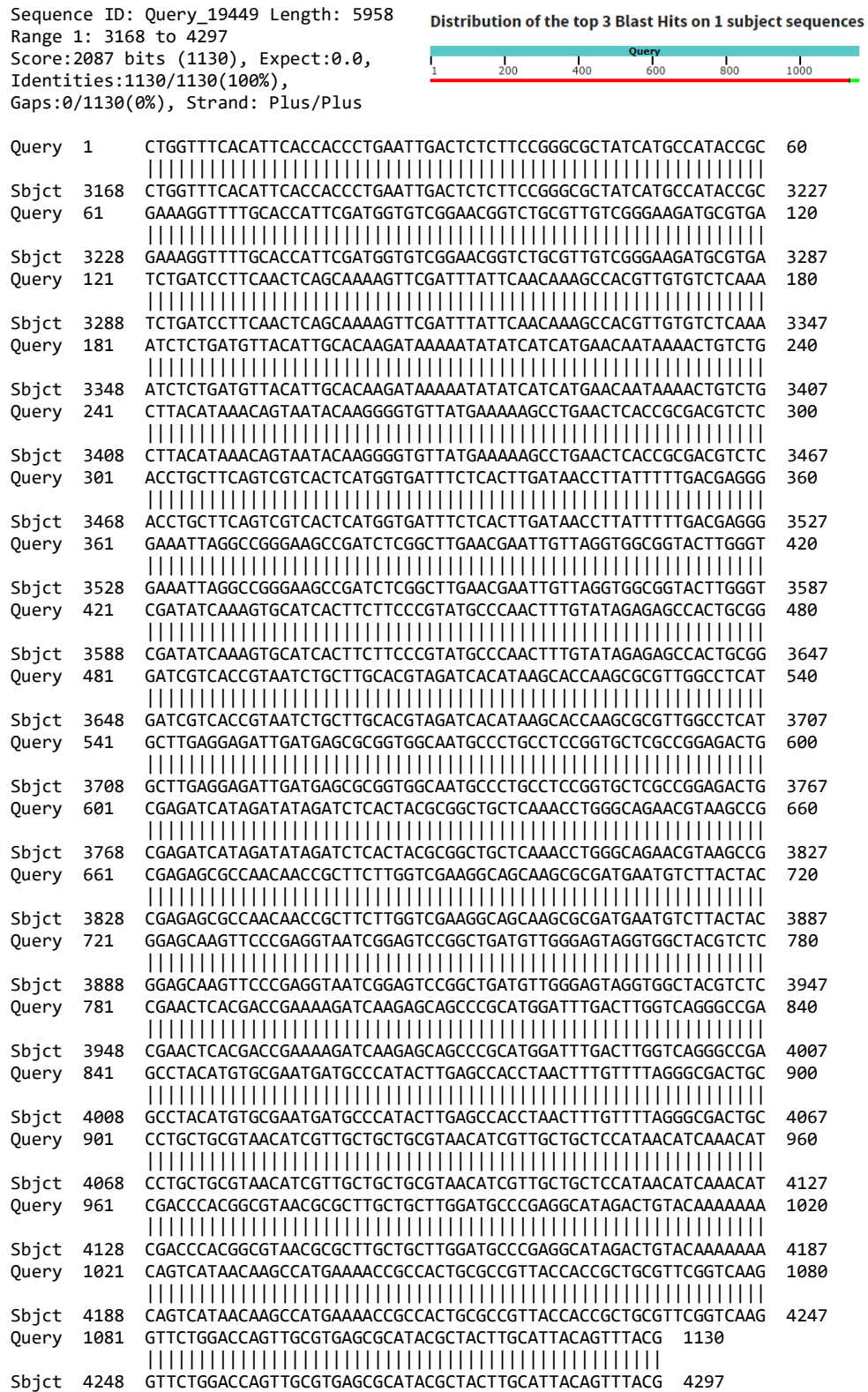


Figure G: Sequence alignment of *lacI* promoter and Gm^R region on the constructed pYL101C, showing 100% identical to the expected sequence.

APPENDIX H

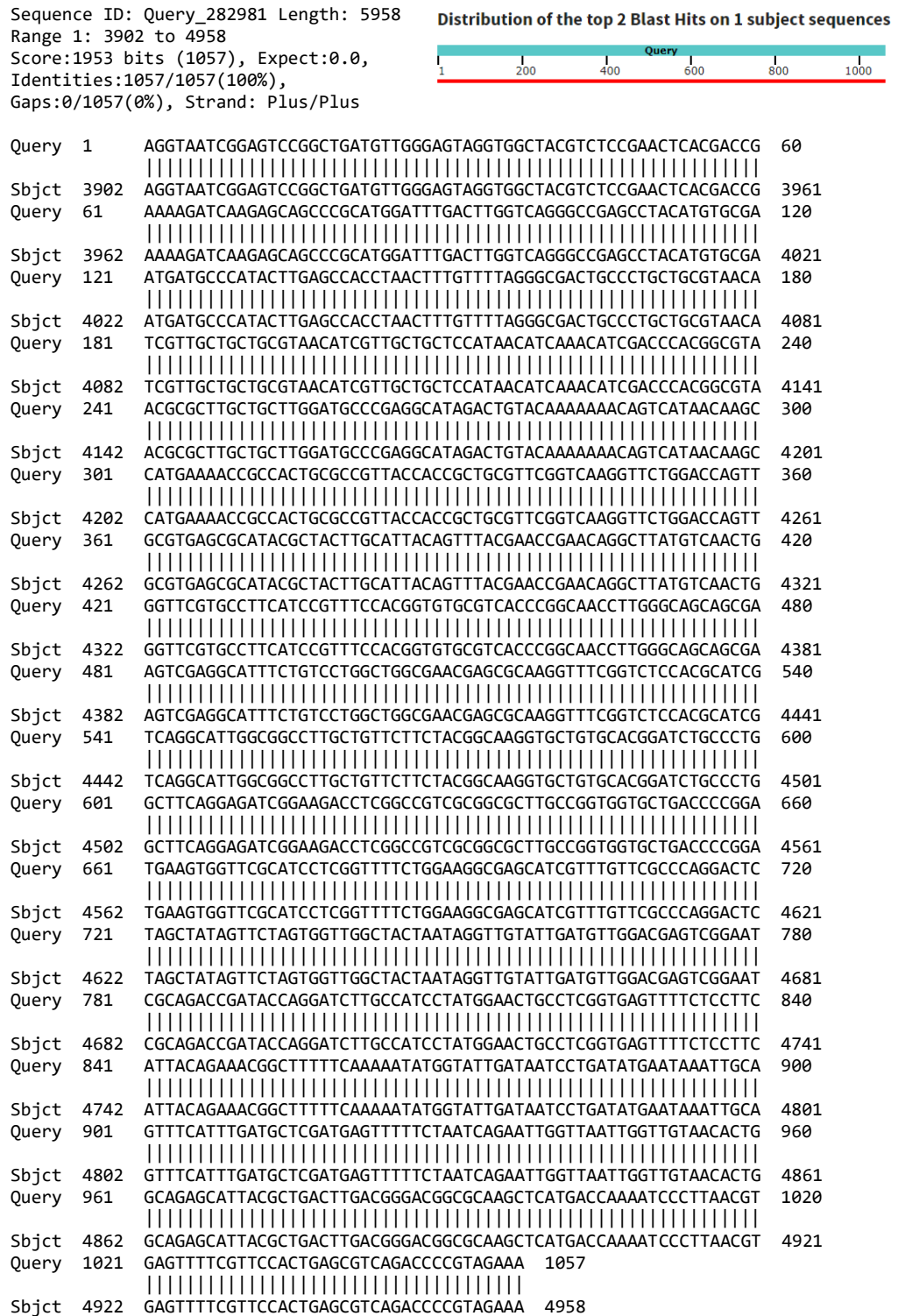


Figure H: Sequence alignment of Gm^R region on the constructed pYL101C, showing 100% identical to the expected sequence.

APPENDIX I

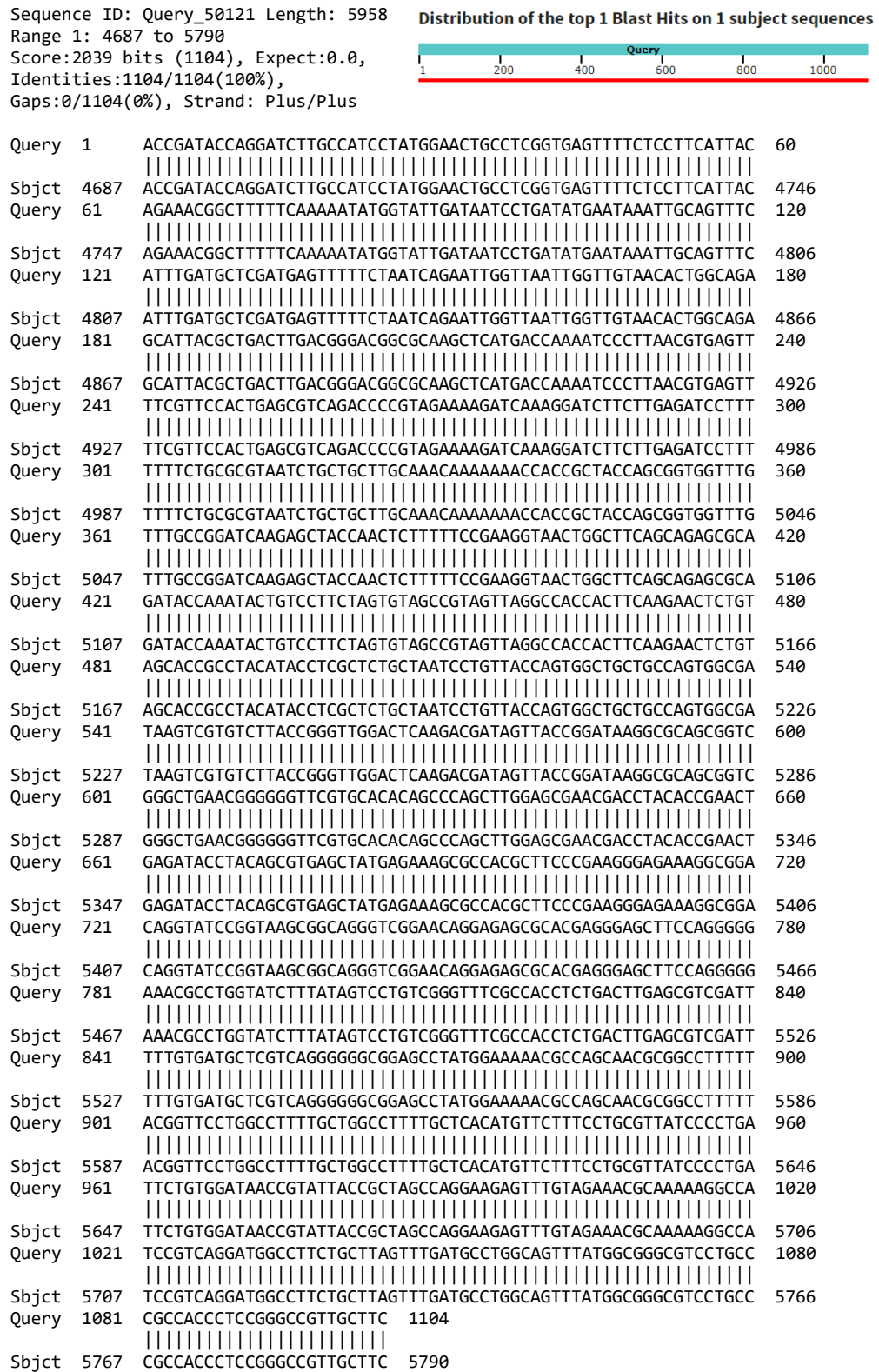


Figure I: Sequence alignment of ColE1 ori region on the constructed pYL101C, showing 100% identical to the expected sequence.

APPENDIX J

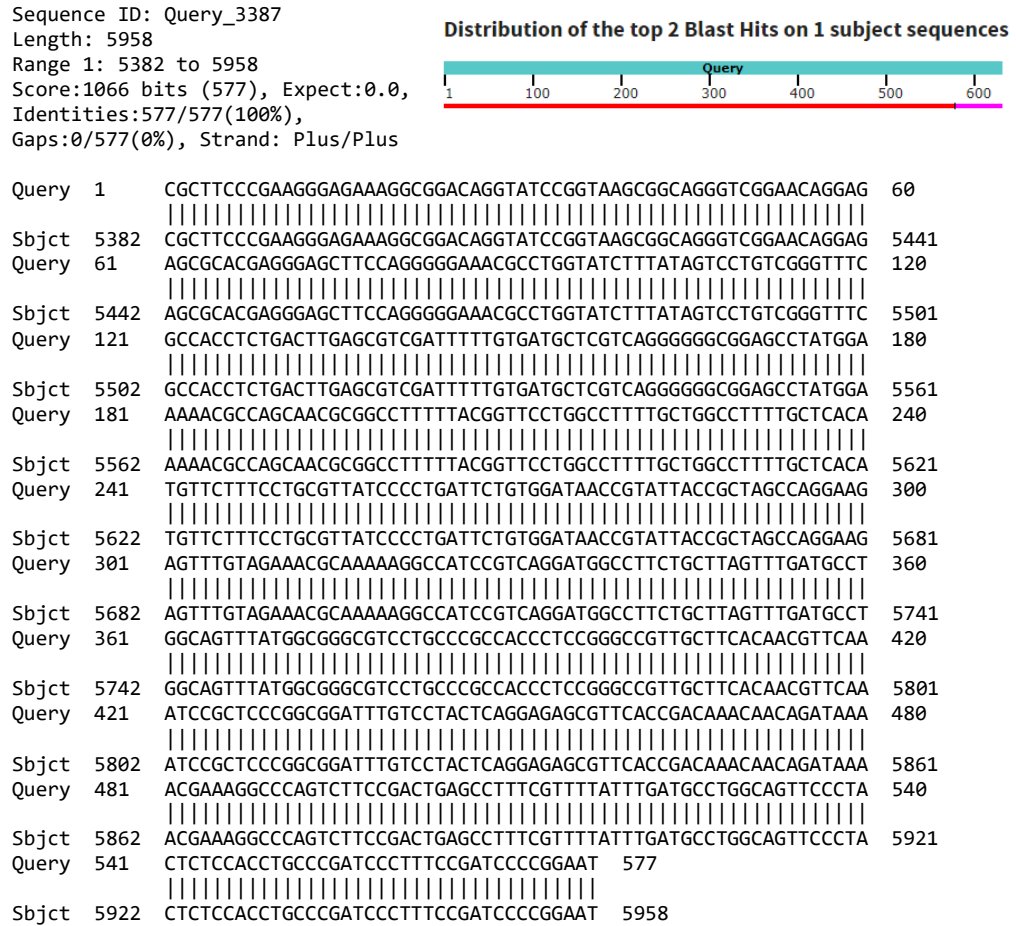


Figure J: Sequence alignment of *rrnB* terminators and P_{INTc} regions on the constructed pYL101C, showing 100% identical to the expected sequence.

APPENDIX K

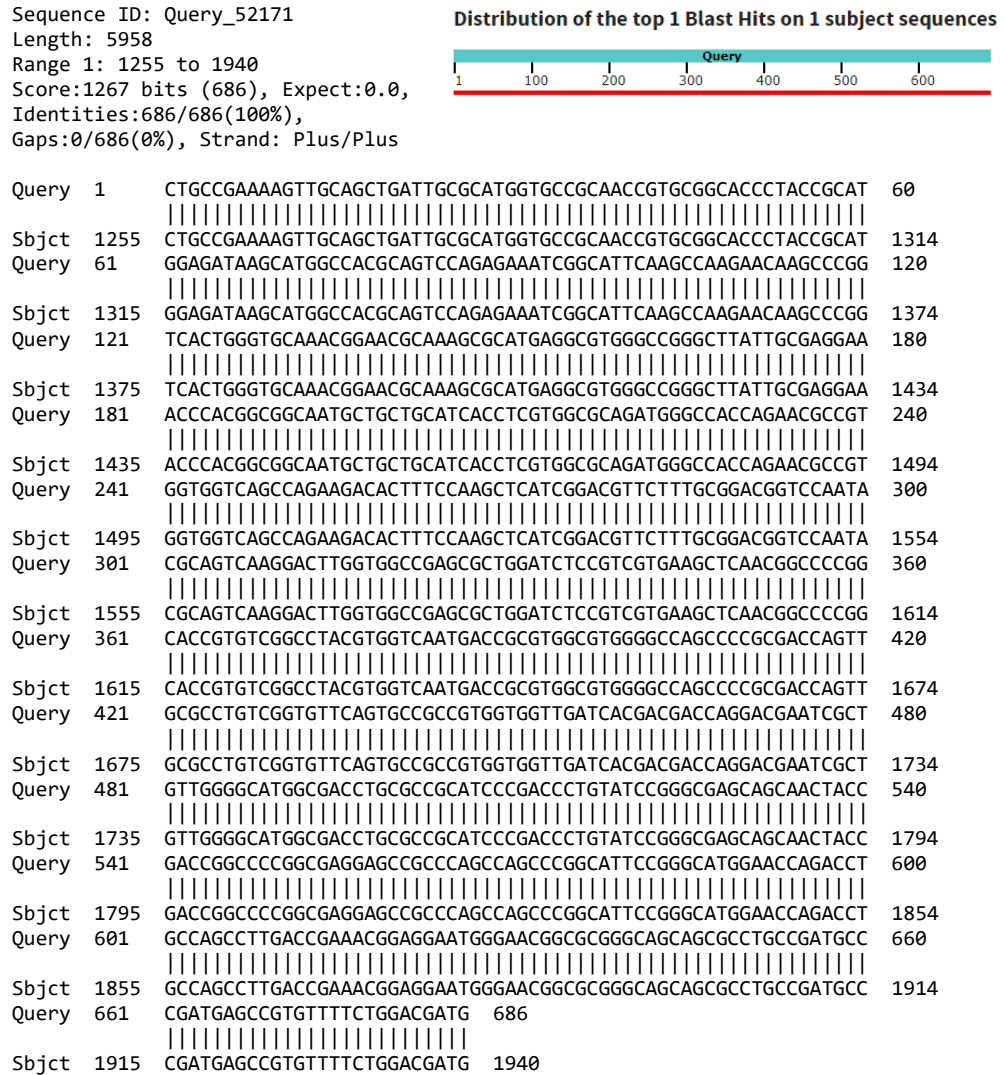


Figure K: Sequence alignment of *T7* terminators and *oriV* regions on the constructed pYL101C, showing 100% identical to the expected sequence.

APPENDIX L

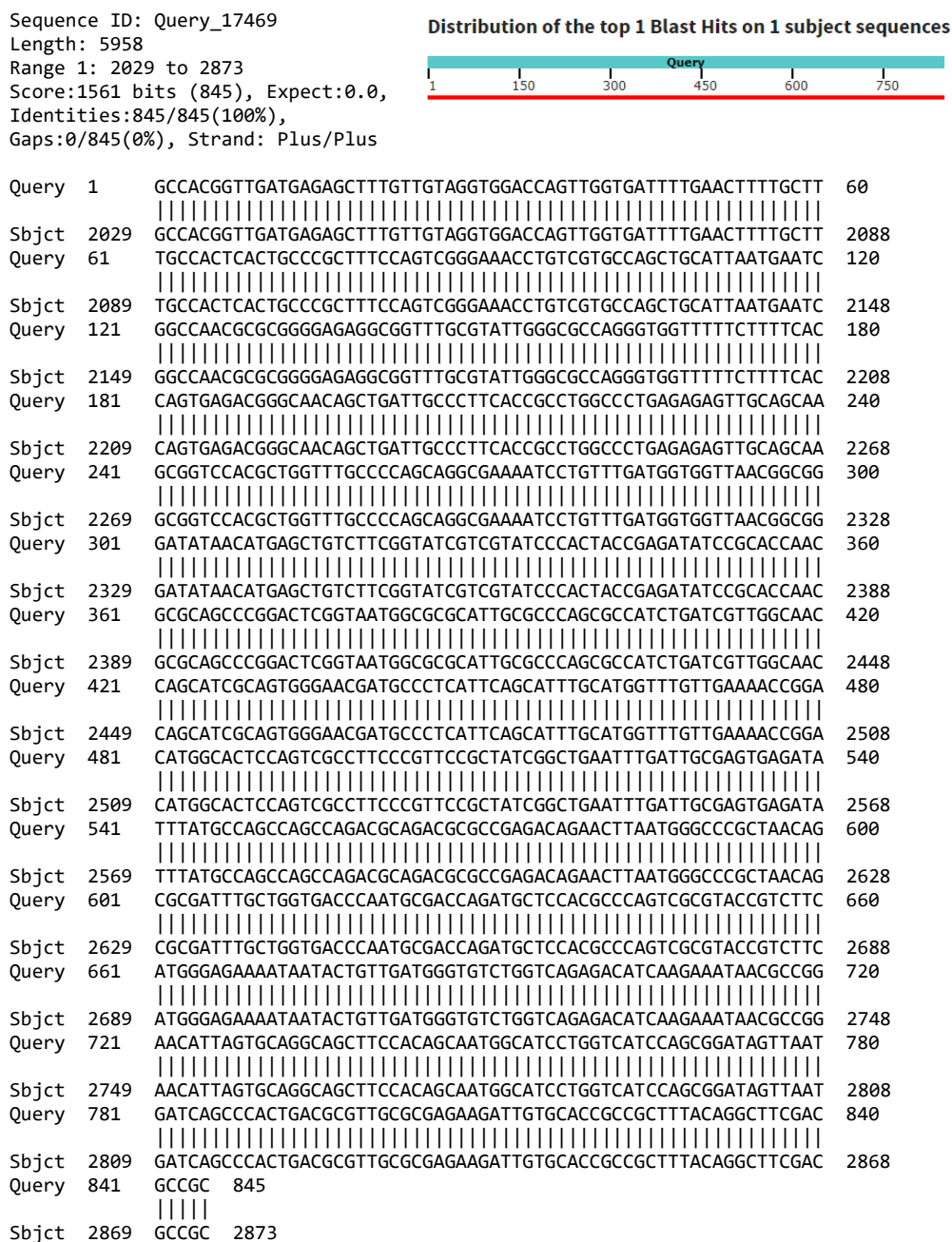


Figure L: Sequence alignment of *pBBR1 rep* and *lacI* regions on the constructed pYL101C, showing 100% identical to the expected sequence.

APPENDIX M

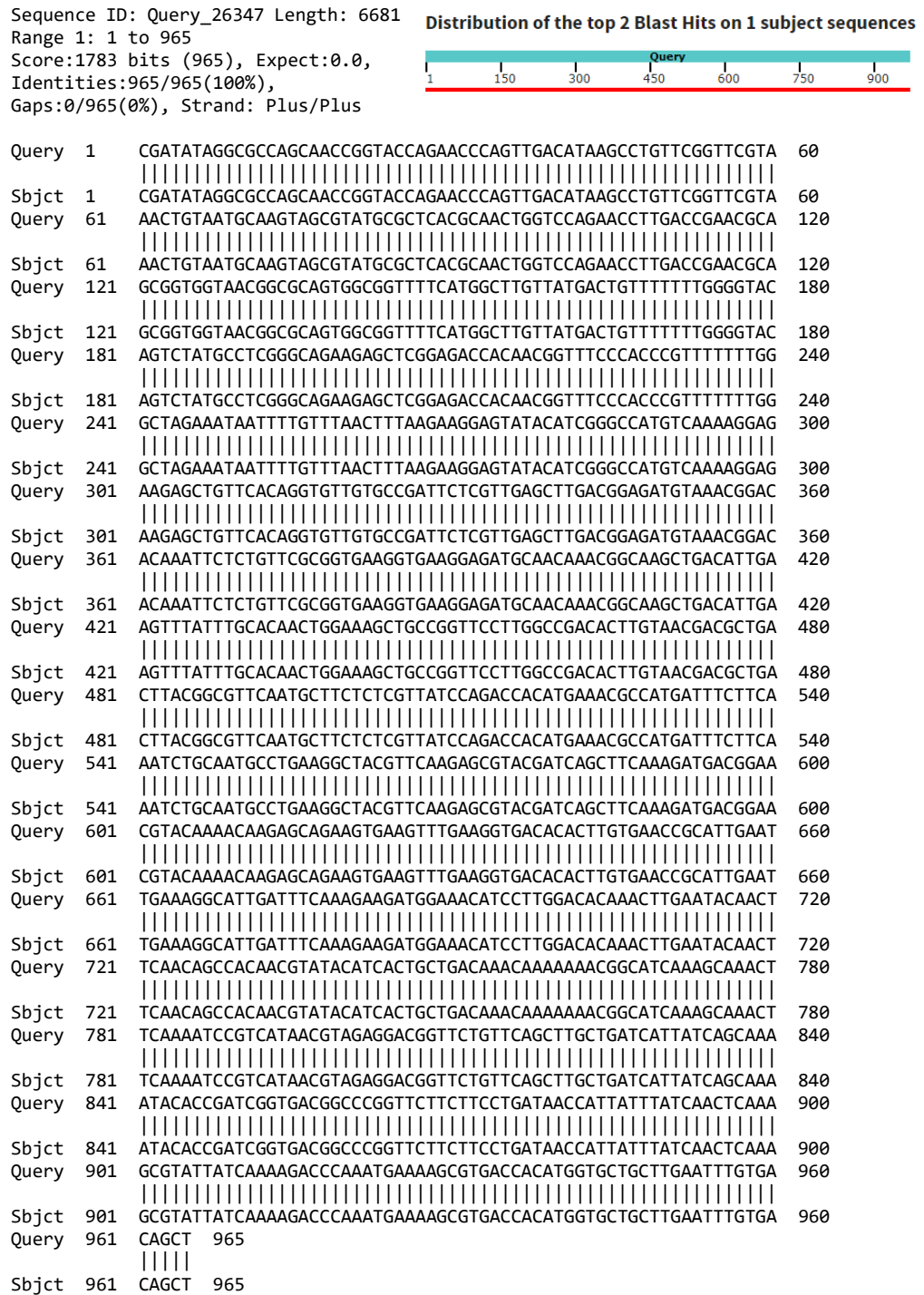


Figure M: Sequence alignment of *sfGFP* gene on the recombinant pYL101C::*sfGFP*, showing 100% identical to the expected sequence.

APPENDIX N



Figure N: Sequence alignment of *virG*-N54D gene on the recombinant pYL101C::*virG*-N54D, showing 100% identical to the expected sequence.

APPENDIX O

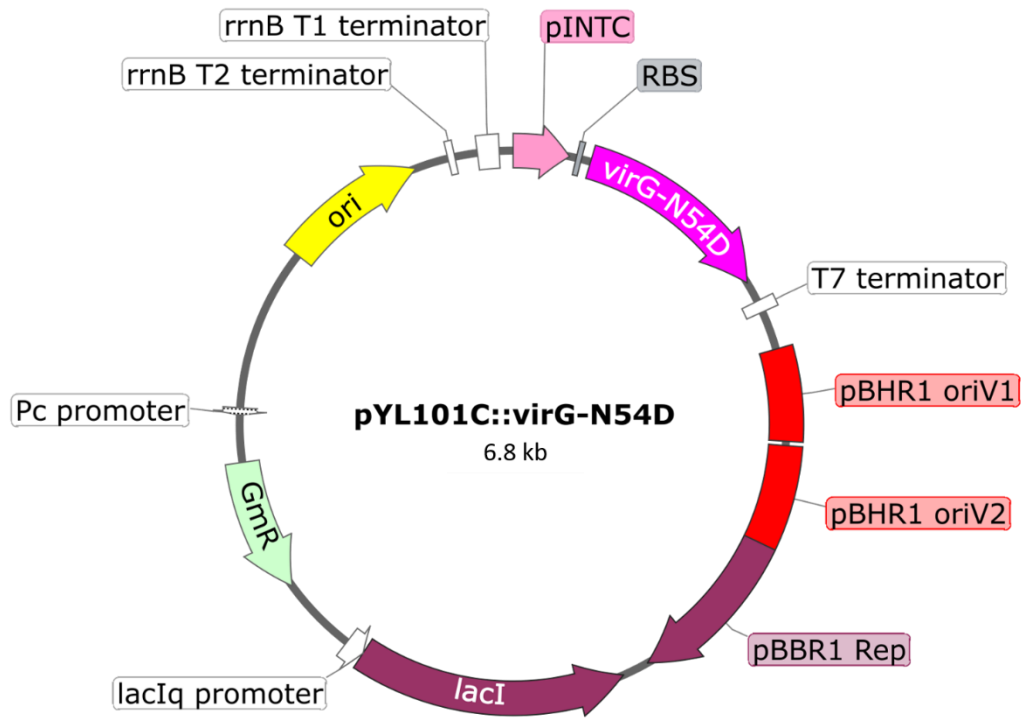


Figure O: Schematic diagram of plasmid map for the recombinant pYL101C::virG-N54D.

APPENDIX P

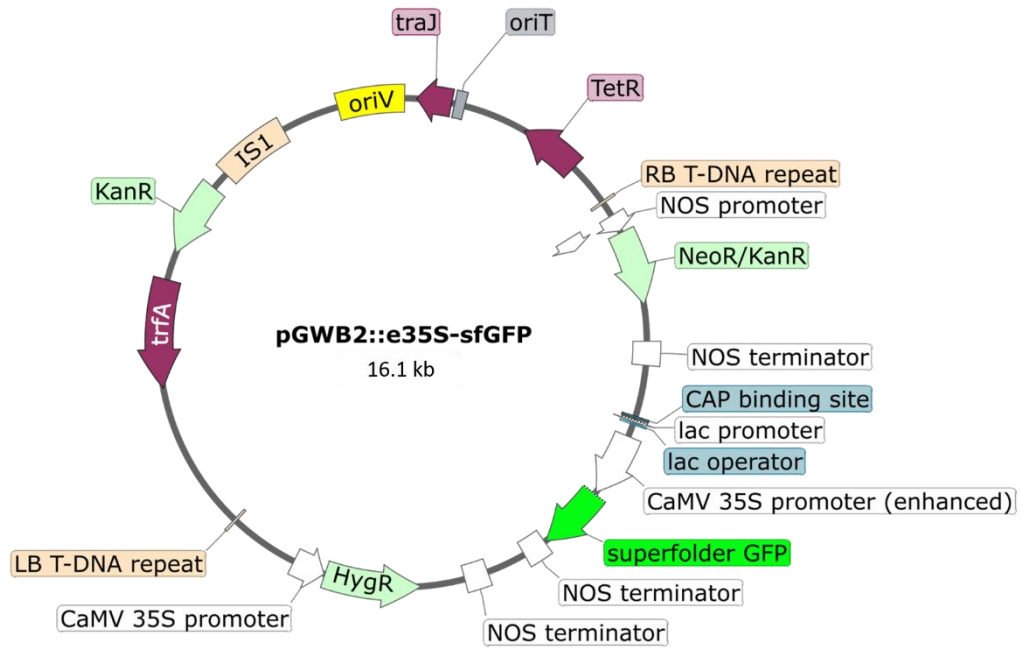


Figure P: Schematic diagram of plasmid map for the binary vector pGWB2::e35S-sfGFP.